INVESTIGATION OF GAS-GAS IMMISCIBILITY IN

MIXTURES OF CARBON TETRAFLUORIDE AND n-ALKANES

Thesis submitted for the degree of
Doctor of Philosophy in the University of London

by

A. MUKHERJEE

Department of Chemical Engineering and
 Chemical Technology,
Imperial College of Science and Technology.

January 1978

TO MY FATHER

CONTENTS

ABSTRACT

A new apparatus has been constructed and used to study gas-liquid equilibrium at high pressures in the vicinity of the critical point. The composition of the co-existing liquid and gas phases was determined using gas chromatography and critical conditions were located by observing the opalescence at the critical point through two sapphire windows mounted in the stirred equilibrium cell.

Phase equilibria measurements have been made in the following binary mixtures:-

1. $(CH_4 + n-C_7H_{16})$ at $30^{\circ}C$ over the pressure range 30-700 atm.

2. $(CF_4 + n-C_6H_{14})$ from 26-50°C over the pressure range 30-700 atm.

3. $(CF_4 + n-C_5H_{12})$ at 0°C and -2°C over the pressure range 30-700 atm.

It was found that both $(CF_4 + n-alkane)$ systems exhibit gas-gas immiscibility of the second type; the pressure and temperature co-ordinates of the point of double contact in the $(CF_4 + n-C_6H_{14})$ system are estimated to be 615 atm. and 29°C and those for $(CF_4 + n-C_5H_{12})$ system are 510 atm. and -3°C.

The experimental results have been used to test the validity of existing semi-empirical criteria for gas-gas immiscibility but none is satisfactory. The general pattern of phase behaviour of these systems has been compared with that of $(CH_4 + n-alkane)$, $(CO_2 + n-alkane)$, $(Ar + n-alkane)$ and $(H_2O + n-alkane)$ systems and it is concluded that Rowlinson and Teja's model, based on

the theory of corresponding states, is capable of giving a qualitatively correct description of the different types of behaviour found in the non-polar systems. Unfortunately, the values of the interaction parameters needed to secure agreement in the critical region are smaller than those obtained from measurements away from the critical point and this limits the usefulness of the theory to predict phase behaviour in other binary (CF_4 + n-alkane) mixtures. Nevertheless it is predicted that as the number of carbon atoms in the n-alkane increases from 1 to 7, the binary (CF_4 + n-alkane) systems should show a continuous transition from liquid-liquid, through liquid-gas to gas-gas equilibrium.

It is concluded that experimental measurement should be made on other (CF_4 + n-alkane) systems over a wide range of pressure and temperature conditions since the different types of phase behaviour expected of these systems will provide a critical test for current theories of phase equilibria.

ACKNOWLEDGEMENT

LIST OF SYMBOLS

(Minor symbols which appear in isolated places in the text are not listed)

B, C	Virial coefficients
A	Helmholtz free energy
G	Gibbs' free energy
M	Molecular weight
P	Pressure
V	Volume
T	Temperature
ε	Energy parameter in intermolecular pair potential energy function
σ	Collision diameter
I	Ionization potential
δ	Solubility parameter
μ	Chemical potential
ξ, η	Interaction parameters
x	Mole fraction (liquid phase)
y	Mole fraction (gas phase)
ϕ	Fugacity coefficient
γ	Activity coefficient

Subscripts

o	Pure component or reference state
C	Critical conditions
G	Gas phase
L	Liquid phase
12	1-2 interaction
1, 2	Components 1 and 2

CHAPTER 1

INTRODUCTION

The increasing use of high pressure in industry has led to many separation processes such as distillation and absorption being carried out under pressure and there is a need for a better understanding of liquid-vapor phase equilibrium under these conditions. Furthermore, phase equilibria at high pressure are of importance in geological exploration such as the drilling and the recovery of oil and natural gas.

While the technical importance of high pressure phase equilibria studies has been recognised for a long time, a quantitative approach to the problem has only been possible in recent years. The difficulties encountered in a theoretical approach are quite complex; at high pressure it is very difficult to calculate the effects of pressure on the thermodynamic properties of both phases. Moreover under high pressure conditions, one or more of the components is likely to be supercritical. Phase equilibria in this critical region are characterized by large deviations from ideality which give rise to unusual phenomena such as retrograde condensation, barotropic inversion and gas-gas immiscibility. Since no completely satisfactory method has yet been devised for prediction of phase equilibria near critical conditions, accurate data can be obtained only by experiment.

Mixtures of simple fluorocarbons and hydrocarbons are of special interest since they have large values of excess functions and therefore often show liquid-liquid immiscibility with upper critical solution temperatures.

Although mixtures of fluorocarbons and hydrocarbons have been studied by various authors at atmospheric conditions, only very recently have these mixtures been investigated under high pressure conditions in the vicinity of critical point. Sideras [1] was probably the first to investigate the vapor-liquid phase behaviour of binary mixtures of these components in the region of critical point. He studied carbon tetrafluoride-n-heptane at temperatures of $50^{\circ}C$ and $100^{\circ}C$ over the pressure range 24 to 976 atm. The shape of isothermal pressure - composition curves indicate that the system exhibits gas-gas immiscibility. The work described in this thesis was undertaken as part of a systematic study to see whether other (fluorocarbon + hydrocarbon) mixtures behave in the same way. In particular the objectives of the present investigation were:-

i)   To compare the liquid-vapor phase behaviour of the
      (fluorocarbon + hydrocarbon) systems with that of
      the corresponding binary hydrocarbon system.

ii)   To show whether the principle of corresponding states
      can be used to predict the phase behaviour of these
      systems and hence obtain a better understanding of the
      nature of the attractive forces between the unlike
      molecules.

With this conception in mind an apparatus was designed to study the phase equilibria of the binary systems:

i)   (Methane + n-heptane) at $30^{\circ}C$ in the pressure range
      of 30 to 250 atm.

ii)   (Carbon tetrafluoride + n-hexane) at $26^{\circ}-50^{\circ}C$ in the
      pressure range of 30 to 700 atm.   and

iii) (Carbon tetrafluoride + n-pentane) at 0° and -2^OC

   in the pressure range of 30 to 700 atm.

The equilibrium cell, designed for this purpose, was

provided with two sapphire windows in order to observe

the gas-liquid interface. Both the gas and liquid phases

were analyzed by gas chromatography.

CHAPTER 2

PHASE EQUILIBRIA OF FLUID MIXTURES AT HIGH PRESSURE

1. Characteristic Behaviour of a Liquid and Gas

The equilibrium diagram for a binary mixture can be represented graphically (see Figure 2.1) as a pair of surfaces (P, T, x) and (P, T, y) drawn in pressure, temperature and composition space where x and y are compositions in the liquid and vapor phase respectively. These surfaces are known as bubble point and dew point surfaces respectively. Lines AC_1 and BC_2 represent the vapor pressure curves for the pure components A and B respectively and terminate at the critical points C_1 and C_2. The bubble point surface and the dew point surface join along the dashed line C_1CC_2 which represents the locus of the critical points of mixtures at different compositions. Thus the point, C, represents the critical point of a mixture of composition x. For many purposes it is more convenient to consider the two dimensional projections of the bubble and dew point surfaces as shown in Figure 2.2.

The characteristic behaviour of a liquid and gas in equilibrium may be modified by a number of unusual phenomena which occur in the neighbourhood of the critical curve.

a) Retrograde condensation

This phenomenon is a direct consequence of the rounded nature of the projection of the dew point and bubble point curves in the pressure - temperature coordinates. Figure 2.3 shows the (P, T) loop of a binary fluid mixture of constant composition, made up of two boundary curves - one for the
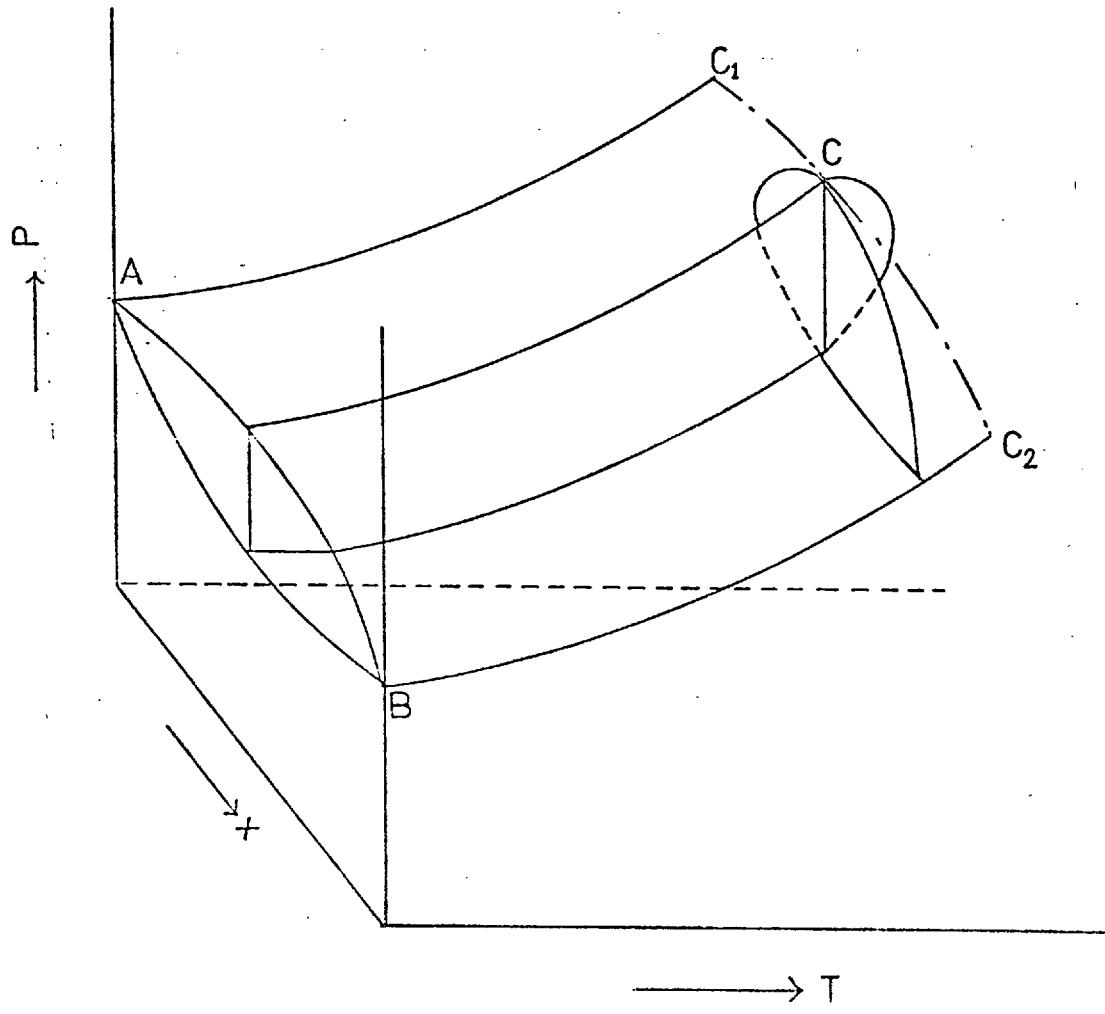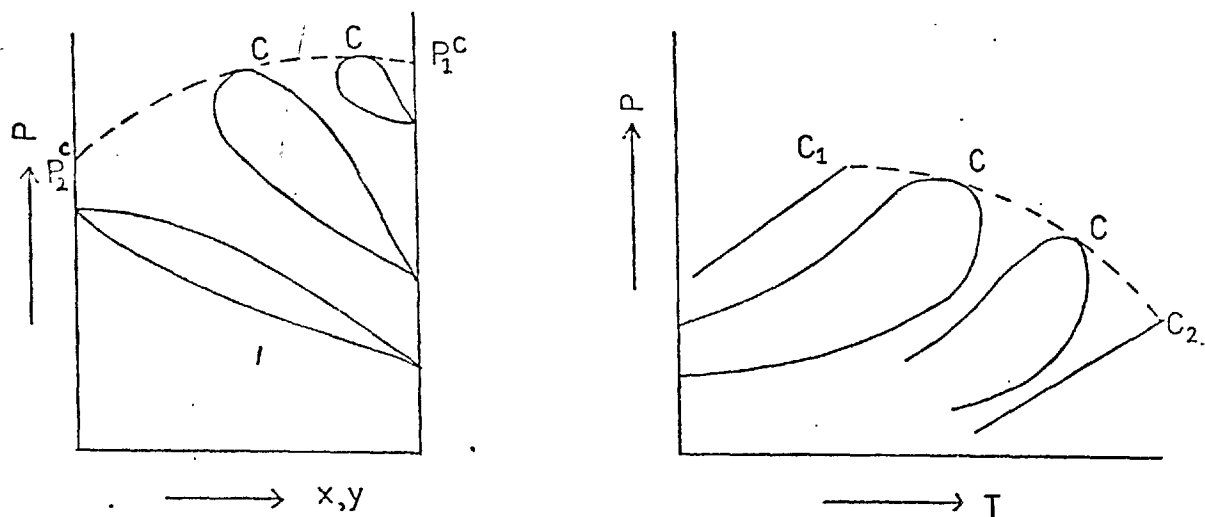
FIGURE 2.1: P-T-x SURFACE

FIGURE 2.2   P-x & P-T PROJECTIONS OF FIG. 2.1
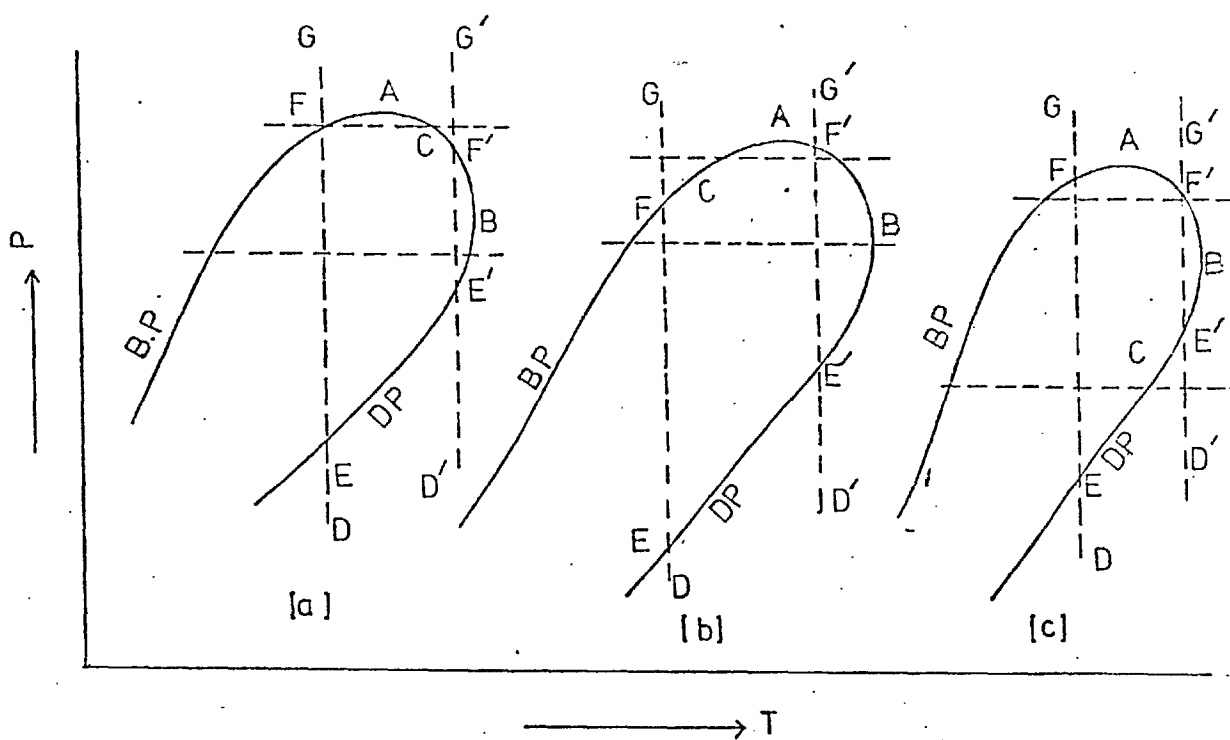
FIGURE 2.3:   RETROGRADE CONDENSATION

liquid (bubble point curve) and one for the vapor (dew
point curve), which meet at the critical point C. It is
interesting to note that the critical point C is neither
the point of maximum pressure A (which is called
cricondenbar) nor that of maximum temperature B (called
cricondentherm). If a mixture is compressed isothermally
at a temperature below C (as shown in Figure 2.3(a)),
normal condensation occurs i.e. the liquid phase first
formed at the dew point E continues to increase until the
whole system is liquid at the bubble point F. However,
if a mixture whose composition lies between that of C and B
(as shown in Figure 2.3(a)) is isothermally compressed,
a line of increasing pressure (D'G') cuts the (p, T) loop
at two dew points. At E' the first drop of liquid is
formed and with increasing compression the amount of liquid
first increases then decreases until it finally disappears
at the second dew point F'. Further compression will not
produce any phase separation. This evaporation of a liquid
by the isothermal increase of pressure is called retrograde
condensation. However the critical point need not
necessarily lie between A and B but can lie outside these
points as shown in Figures 2.3(b) and 2.3(c). Isotherms
that pass through two dew points (Figures 2.3(a) and 2.3(b))
are said to exhibit retrograde condensation of the first
kind whereas isotherms that pass through two bubble points
(Figure 2.3(c)) are said to exhibit retrograde condensation
of the second kind.

Similar phenomena have been observed when a mixture
is heated or cooled under isobaric conditions. In this case
the composition of the mixture will lie between that of
the critical point C and the cricondenbar point A (as shown

in Figure 2.3(a)). The type of retrograde condensation depends on the relative position of C and A. The path of the process is such that it cuts the bubble point or dew point curve at two points.

b)   Barotropic_phenomenon

When a gas of high molar mass is mixed with a liquid of low molar mass a situation may arise due to the relative compressibility of the two phases in which the liquid phase has a lower density than the gas phase. Under these circumstances, the phases invert so that the gas phase sinks to the bottom of the container. This phenomenon is known as barotropic inversion.

2.   Gas-Gas Equilibrium

Before considering this phenomenon in detail, it is worthwhile to review briefly how the term gas-gas equilibrium came into use and to show that the behaviour it describes in an extension of ordinary gas-liquid and liquid-liquid equilibria.

Gas-gas equilibria can be best understood by plotting the locus of critical points of mixtures on a pressure - temperature plane. The resulting P-T diagrams can be classified into three groups:-

i)   Mixtures formed from two components whose gas-liquid critical temperatures are not too dissimilar. In such mixtures the intermolecular forces are similar and the critical locus is a continuous curve between the critical points of the two pure components as shown in Figure 2.4.

ii)   Mixtures of two components with very different gas-liquid critical temperatures. In these mixtures there is no continuous critical line joining the critical points of the pure components.

iii) Very complex mixtures exhibiting such phenomenon as low temperature lower critical solution temperatures.

Figure 2.4 shows the (P,T) projection of a simple binary mixture in which the critical locus passes through a maximum pressure. The greater the difference of size and intermolecular energy of the molecules of the two pure components, the higher is the maximum.

If the two components are very different or if the intermolecular force between the two components is very small, the liquid phase separates into two immiscible phases. Under these circumstances, a three phase line,
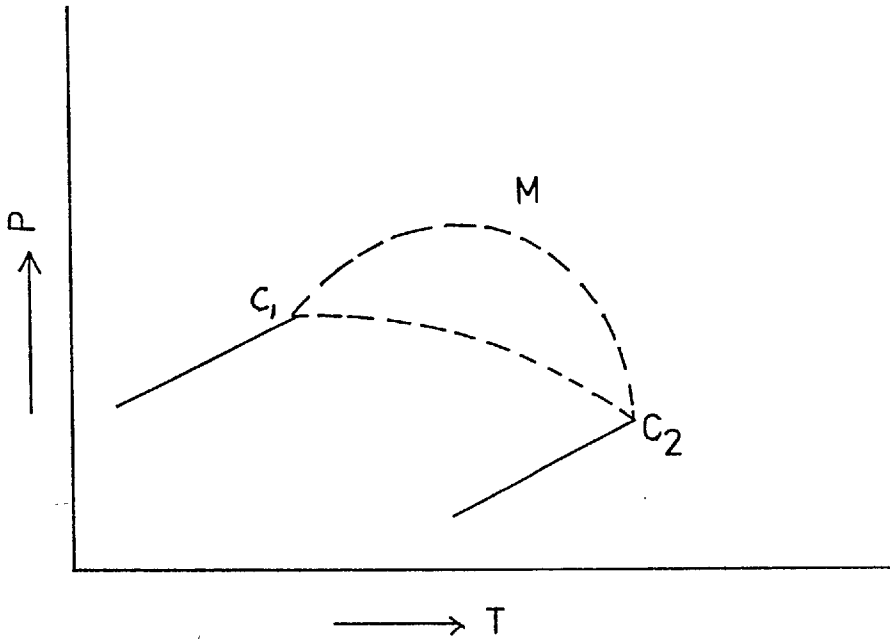
FIGURE 2.4   CRITICAL LOCUS OF SIMILAR MOLECULES
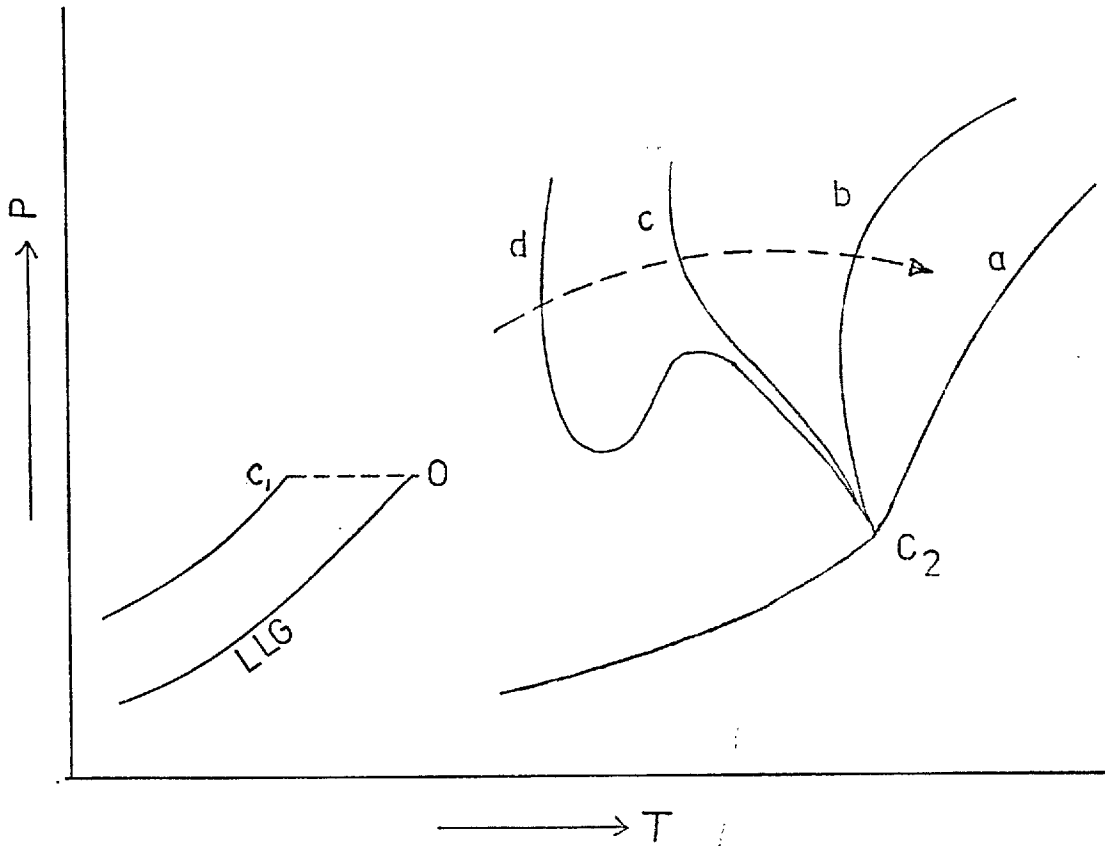
FIGURE 2.5   CRITICAL LOCUS OF DISSIMILAR MOLECULES

along which two liquid phases and a gas phase are in
equilibrium, exists in the critical region. This is
represented in Figure 2.5. The three phase line (LLG)
ends at a critical end point O where the liquid phase
rich in Component 1 becomes identical with the gas phase.
The critical line starting from C_2 rises to higher pressures
as the proportion of Component 1 increases. Rowlinson [2]
has pointed out that as the disparity between the two
components increases (i.e. the intermolecular force between
the two molecules decreases) the critical curve moves to
higher temperatures (as shown by the arrow in Figure 2.5).
When it has moved sufficiently far for part or all of it to
lie above the gas liquid critical point of both components,
(curves a and b in Figure 2.5) the region of so called
gas-gas immiscibility is reached. Rowlinson [3] points
out that this phenomenon is a rule rather than exception for
systems with weak intermolecular forces between unlike
molecules.

This phenomenon was predicted theoretically by van der
Waal [4] and Kamerlingh-Onnes and Keeson [5] around the
beginning of this century but it was not confirmed
experimentally by Krichevskii and his colleagues [6]
until 1940. Krichevskii's early experiments were
reproduced by Lindroos and Dodge [7]. Tsiklis [8,9] pointed
out that the following two types of equilibria are possible.

i) On leaving the critical point of the less volatile
    component (C_2) the critical curve rises monotonically
    so that dP_c/dT_c is always positive (curve a in Figure 2.5).
    This behaviour is known as gas-gas immiscibility of
    the first type. A typical example is the He-Xe system
    shown in Figures 2.6(a) and 2.6(b) which was investigated
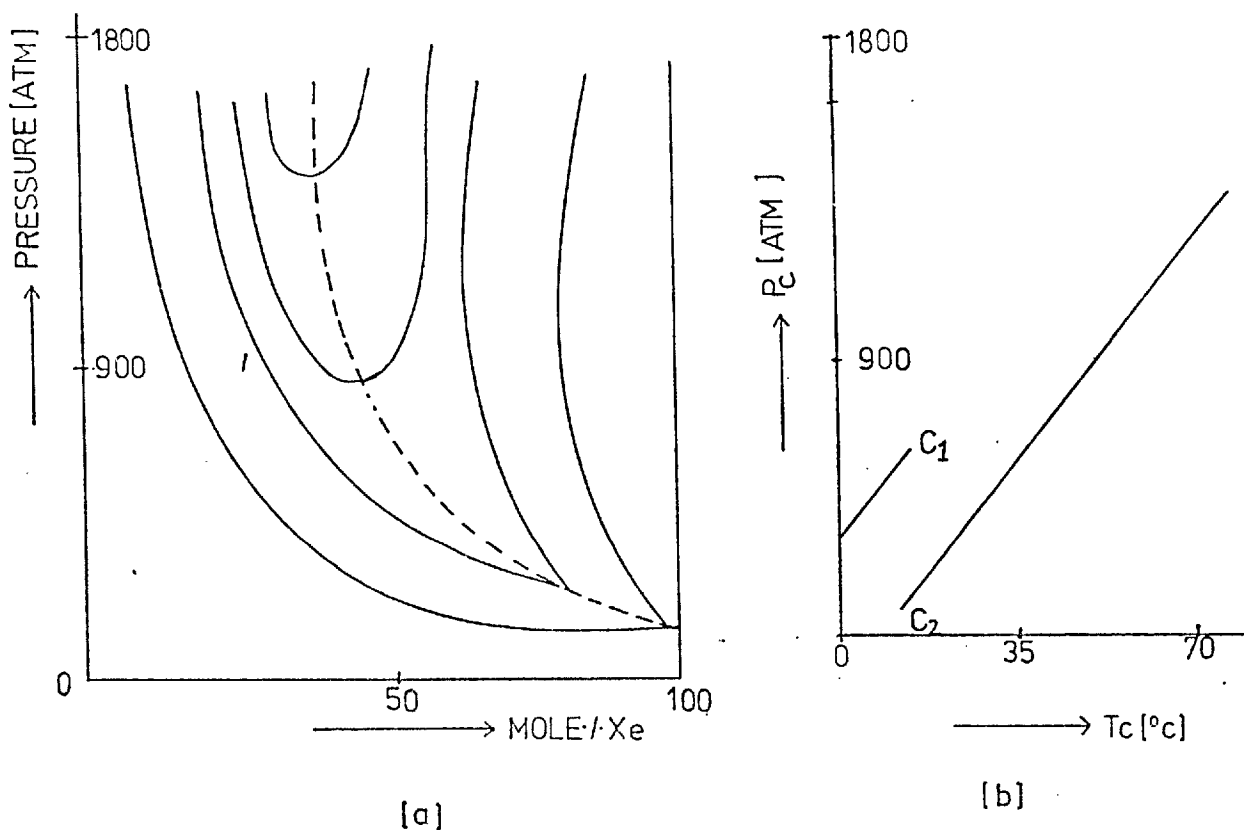
FIGURE 2.6: G-G IMMISCIBILITY OF FIRST TYPE [He-Xe]
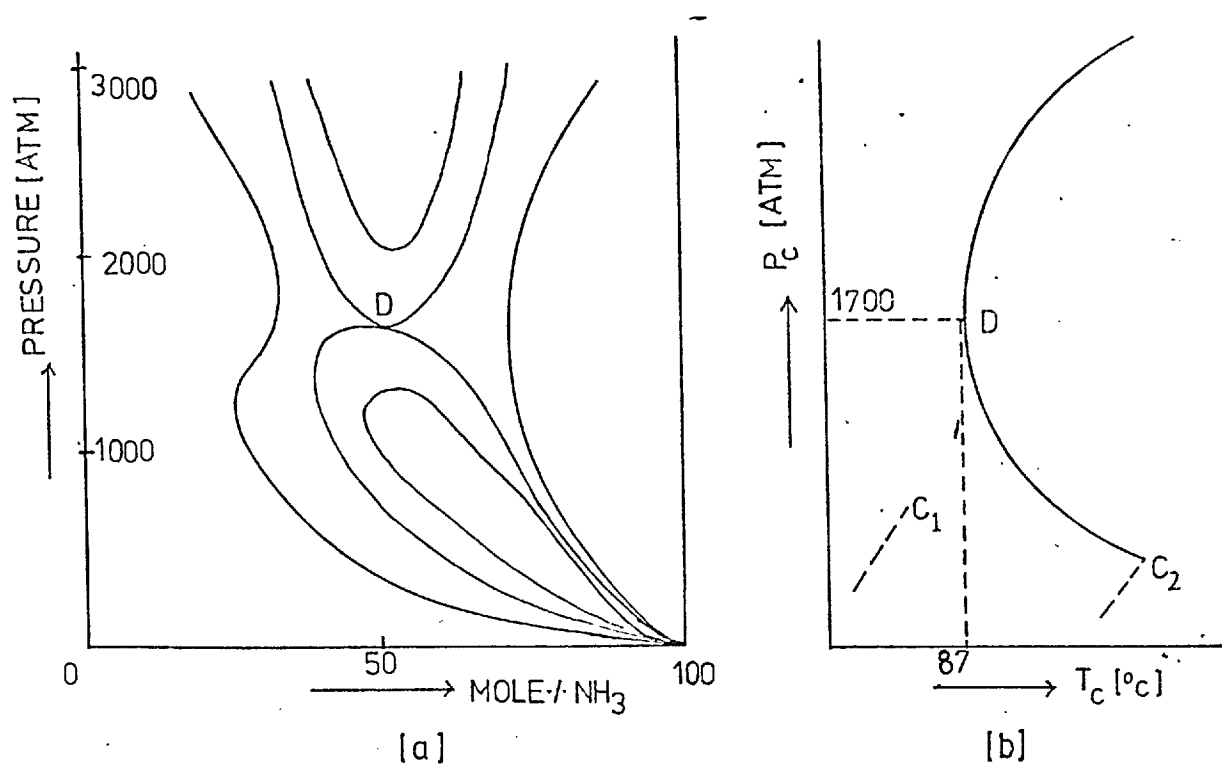
FIGURE 2.7: G-G IMMISCIBILITY OF SECOND TYPE [N₂ - NH₃]

by De Swaan Arons and Diepen [10].

ii) The critical line leaves C_2 with a negative slope $(\frac{dP_c}{dT_c} < 0)$, passes through a minimum in temperature and then takes on a positive slope at higher pressures as shown in Figure 2.7. Systems behaving in this manner are said to exhibit gas-gas immiscibility of the second type [6]. The point D, corresponding to the minimum temperature in the critical curve, is the point where liquid-gas and gas-gas equilibrium curves touch. van der Waal defined this point as the point of double contact. Above this temperature the pressure-composition loops (as shown in Figure 2.7(a)) divide into gas-liquid and gas-gas equilibrium curves. It is also interesting to note that pressure-composition loops at temperatures below D possess an unusual slope which Rowlinson [3] defines "waisted". This implies that the solubility of the gas in liquid component passes through a maximum with increasing pressure.

·Many authors [8, 10, 11] have maintained that the critical locus must reverse its course eventually and return to the critical point of the more volatile component (C_1 in Figures 2.6(b) and 2.7(b)). Rowlinson [3] points out that this cannot be so. This conclusion has been reinforced by the experimental evidence presented by Streett [12] which suggests that gas-gas immiscibility may persist to very high temperature and pressure, perhaps even to the limits at which atomic and molecular structure begin to break down.

The term gas-gas equilibrium has been criticized by various authors [13, 14, 15] who suggest that the phases should be termed liquids because their densities are

comparable to those of ordinary liquids. However, Gordon [16]
points out that this is not true for low pressure systems
and considers that it is reasonable to refer to the
supercritical phases as gases and describe their behaviour
as gas phase immiscibility. In the opinion of the author,
the term "FLUID-FLUID EQUILIBRIUM", proposed by Lindroos
and Dodge [7] is preferable to either term but the use of
gas-gas equilibrium will be retained in view of its wide
acceptance.

3. Theoretical Treatment of Gas-Gas Equilibria

Various procedures have been put forward to predict gas-gas equilibria in binary mixtures, which are based on the properties of pure components and take account of the interaction between the two molecules. The methods proposed can be divided into several categories:-

i)   Solubility parameter approach

ii) Correlation function treatment

iii) Approach based on equation of state

iv) Approach based on conformal solution theory

v)   Approach based on lattice gas model   and

vi) Corresponding states treatment

Solubility parameter approach

Hildebrand's solubility parameter (D) was used by Kreglewski [17] to predict gas-gas immiscibility. He suggested that the greater the difference in D^2 values of the pure components, the more probable will be the existence of gas-gas immiscibility in their binary mixtures. According to Hildebrand the solubility parameter is given by

$$D^2 = \frac{\bar{E}}{\bar{V}} \quad \text{where} \quad \bar{E} = \text{energy of vaporization per mole}$$
$$\bar{V} = \text{molar volume}$$

Making use of Von Dranen's [17] hypothesis that $\bar{E} = \frac{3RT_c}{2}$ at the critical point

$$D^2 = \frac{3}{2} \frac{RT_c}{V_c}$$

However, Kreglewski's criterion is not always obeyed. For example, for the NH_3-H_2 system the difference in the value of D^2 is greater than that for the NH_3-N_2 system, but gas-gas immiscibility is not found in NH_3-H_2 system. Moreover this criterion is not applicable to fluorocarbon-hydrocarbon systems; for example the difference in the D^2

value of 43.6 atm. for the $(CF_4 + n-C_7H_{16})$ system is much less than that for the $(NH_3 + N_2)$ system but gas-gas immiscibility is found in the former.

Kreglewski's criterion was modified by Kaplan [18] in the following way. The components are arranged in a table in order of increasing D^2 values towards the right and towards the bottom, the systems formed by the intersecting horizontal rows and vertical columns can be predicted to exhibit the gas-gas immiscibility on the basis of experimental findings and the rule that in a series of systems containing one compound in common, the greater the D^2 difference between the components, the greater the probability that gas-gas equilibrium will occur. The following example illustrates the use of this procedure:-

	He	H_2	C_8H_{18}	C_6H_{14}	N_2
D^2	(11.3)	(63.2)	(143)	(170)	(173)
He				y^E	y
H_2			N	N^E	N
C_8H_{18}		N		N	N
C_6H_{14}	y^E	N^E	N		N^E
N_2	y	N	N	N^E	

(y - yes, n - no, suffix E - experimentally verified)
Since H_2-n-C_6H_{14} ($\Delta D^2 = 107$ atm.) does not show gas-gas equilibrium experimentally, H_2-n-C_8H_{18} ($\Delta D^2 = 80$ atm.) is predicted not to exhibit this type of behaviour. Similarly since He-n-C_6H_{14} ($\Delta D^2 = 159$ atm.) shows gas-gas equilibrium, He-N_2 is predicted to do the same.

One drawback of this technique is that it fails to predict what type of gas-gas equilibrium will occur. Although this limitation has been partly overcome by by recent modifications [19], the method does not predict

the experimentally observed gas-gas immiscibility in
He-fluorocarbon and fluorocarbon-hydrocarbon systems [20].
Hence its usefulness is restricted.

Correlation function treatment

From an approximate correlation function treatment
using the so called two index distribution functions,
Rott [21] developed a criterion for the prediction of gas
-gas immiscibility of the first type. According to this
theory, the criterion for exhibiting immiscibility of
the first type is expressed by a parameter β given by

$$\beta = \frac{3.31 \frac{\varepsilon}{k} \sigma^4}{Tr_0^4} \qquad (2.1)$$

where r_0 is the radius corresponding to molecular volume
$(v = \frac{4}{3}\pi r_0^3)$,

ε and σ are the parameters of L-J potential,

k is the Boltzman constant

and T the temperature.

For a binary system values of T and r_0 for the less
volatile component were inserted in the denominator of
equation (2.1) and values of ε and σ for the more volatile
component in the numerator. If the resulting value of β is
greater than that of the pure less volatile component at
the critical point, then the system should exhibit gas-gas
immiscibility of the first type.

This criterion is not very reliable, especially for
systems containing polar components. For example, the
systems $n-C_4H_{10}-H_2O$ and $C_6H_6-H_2O$ were both predicted to
show gas-gas immiscibility of the first type where-as both
these systems exhibit gas-gas immiscibility of the second
type [22] [23]. On the other hand, the Ar-H_2O system
exhibits immiscibility of the first type [24] which is not

predicted. However, this approach has been quite
successful in predicting gas-gas immiscibility in binary
mixtures containing helium.

Approach based on equations of state

The possibility of phases co-existing is determined
by the form of the surface representing either the
Helmhotz's free energy A, as a function of volume,
temperature and composition or the Gibbs free energy F
as a function of pressure, temperature and composition.
Limited miscibility arises when the surface representing A
as a function of v, T and x or G as a function of P, T
and x contains a fold along the v or P axis, a so called
longitudinal fold. Such a fold can appear only if
$(\frac{\delta^2 A}{\delta x^2})_{v,T}$ or $(\frac{\delta^2 G}{\delta x^2})_{P,T}$ is negative. In general the Helmhotz
free energy, A, is calculated as a function of v, T and x
as it is easier to obtain the values of density as a
function of temperature.

This criterion was used by Tempkin [25] to predict
gas-gas immiscibility in a wide variety of binary
mixtures. His predictions were based on van der Waal's
equation of state for a binary mixture

$$(p + \frac{a}{\bar{V}^2}) \ (\bar{V} - b) = RT$$

with the usual assumptions: $a = a_1 (1 - x)^2 + 2a_{12} x (1 - x) + a_2 x^2$

$$b = b_1 (1 - x)^2 + 2b_{12} x (1 - x) + b_2 x^2$$

where $a_{12} = (a_1 a_2)^{\frac{1}{2}}$

$b_{12} = \frac{1}{2}(b_1 + b_2)$

From this equation of state, the condition $(\frac{\delta^2 A}{\delta x^2})_{v,T} < 0$
was calculated for binary mixtures at or above the critical
temperature of the less volatile component and the
following criteria were established for gas-gas immiscibility:-

$$b_1 \geq 0.42 b_2 \qquad\qquad (2.2)$$

$$a_1 < 0.053 a_2 \qquad\qquad (2.3)$$

Schneider [15] has pointed out that these criteria
are a strong indication that gas-gas immiscibility is
more a consequence of the difference in intermolecular
force between the two molecules rather than a difference
in size. De Swaan Arons and Diepen [10] used this criterion
to predict gas gas immiscibility for the He-Xe system
and found that their experimental results agreed well with
the prediction.

Essentially the same method and mixing rules were
used by Van Konynenburg and Scott [26] to calculate phase
equilibria and the critical locus for a wide variety of
binary mixtures.

Van der Waal's equation of state is not applicable
at high pressures and hence the criteria expressed by
equations (2.2) and (2.3) can only be regarded as
approximations. Thus it is not surprising that gas-gas
immiscibility in $CF_4-n-C_7H_{16}$ system [20] does not conform
to the criteria proposed by Tempkin [25]. On the other
hand, Scott [26] was able to explain the phase behaviour
of a wide variety of binary fluid mixtures using van der
Waal's equation of state.

The theoretical analysis can be improved considerably
if one of the equations of state applicable at high
density is used to calculate the free energy. However,
the approach becomes more complicated because of the
complexity of the equation and the large number of
constants required by, say, the B.W.R. equation.

Peter and Wenzel [27] and very recently Schneider [28]
used Redlich-Kwong's equation of state:-

$$P = \frac{RT}{V-b} - \frac{a}{\sqrt{T}V(V + b)}$$

with the following mixing rules:

$$a = a_{11}x_1^2 + 2a_{12}x_1x_2 + a_{22}x_2^2$$

$$b = b_{11}x_1^2 + 2b_{12}x_1x_2 + b_{22}x_2^2$$

where $a_{12} = (1 - \eta) \sqrt{a_{11}a_{22}}$ and $b_{12} = (1 - \xi)\frac{1}{2} (b_{11} + b_{22})$

(η and ξ being adjustable parameters)

to calculate phase equilibria and critical phenomena

in a wide variety of binary fluid mixtures under high

pressure conditions. The Helmhotz free energy A was

calculated from the equation of state and the subsequent

equations were solved to predict the isothermal P-x

diagrms. The critical conditions:

$$\frac{1}{A_{vv}} (A_{vv}A_{xx} - A_{vx}^2) = 0$$

$$\frac{1}{A_{vv}^2} (A_{xxx}A_{vv}^2 - 3A_{vxx}A_{vx}A_{vv} + 3A_{vvx}A_{vx}^2 - A_{vvv}A_{xx}A_{vx}) = 0$$

where $A_{vv} = (\frac{\delta^2 A}{\delta v^2})$, $A_{vxx} = (\frac{\delta^3 A}{\delta v \delta x^2})$ and so on

were solved to find   the critical locus of these

binary mixtures. It was found that by varying the values

of η and ξ, azeotropes, liquid-liquid and gas-gas

immiscibility could be represented reasonably well.

This method has been successfully applied to a

wide variety of binary mixtures e.g. (CH_4 + hydrocarbons),

(Fluorocarbon + hydrocarbon), rare gas mixtures, etc.

The method can also be applied to mixtures of strongly

polar compounds e.g. (H_2O + C_2H_5OH) with surprising

accuracy. However the method fails for mixtures of

non-polar with strongly polar compounds.

Schafer [29] used $\overset{The}{\wedge}$ virial equation of state:-

$$P\bar{V} = RT + BP + CP^2$$

where the second virial coefficient B and the third

virial coefficient C for the mixture were calculated
from the following mixing rules:

$$B = x_1^2 B_{11} + 2x_1 x_2 B_{12} + x_2^2 B_{22}$$

$$C = x_1^3 C_{111} + 3x_1^2 x_2 C_{112} + 3x_1 x_2^2 C_{122} + x_2^3 C_{222}$$

where the cross terms B_{12}, C_{112}, C_{122} etc. are properties
of the mixture and cannot be determined from those of the
pure substances. The Gibbs free energy was calculated
from this equation of state as a function of P, T and x
and the following criterion was established for the phase
separation to occur:

$$\frac{18|\delta|RT}{\alpha^2} < 3 - 2\left(\frac{\beta}{\delta} + 1\right) - 2\left\{\left(\frac{\beta}{\delta} + 1\right)^2 - 3\left(\frac{\beta}{\delta} + 1\right)\right\}^{\frac{1}{2}} \qquad (2.4)$$

where $\alpha = B_{11} + B_{22} - 2B_{12}$

$\beta = \frac{1}{2}(C_{111} - C_{112}) + (C_{111} + C_{222} - 2C_{112})$

$\delta = \frac{1}{2}(C_{111} - 3C_{112} + 3C_{122} - C_{222})$

Both sides of inequality (2.4) contain functions of the
virial coefficients and temperature. Large negative values
of α show the limited miscibility characteristic of
mixtures in which one component has a dipole moment.
Schafer has applied this criterion to standard systems
such as N_2-NH_3 and CH_4-NH_3. However it has not been
used for the majority of systems and much remains to be
done to make it a widely acceptable method of prediction.
The author points out that additional virial coefficients
must be introduced at higher pressures.

Approach based on conformal solution theory (CST)

The basis of conformal solution theory is that
compounds having the same form of intermolecular potential
and differing only in the magnitude of their LJ parameters
(ε and α), have excess thermodynamic properties of mixing
governed by these parametric differences. In this theory,

the thermodynamic property of a system is expanded

in the form of a Taylor's series about the same property

for a hypothetical reference compound.

Conformal solution theory has been recently used by.

Tan, Luks and Kozak [30] to predict gas-gas immiscibility

in rare gas mixtures. Their approach was as follows:-

Specifically the excess free energy in the second order

CST can be represented by:-

$$\Delta G^E/x_1 x_2 RT = \Omega \qquad (2.5)$$

where

$$\Omega = \Lambda_1^* \left(\frac{\sigma_1 - \sigma_2}{\sigma_r}\right)^2 + 2\Lambda_2^* \frac{(\sigma_1 - \sigma_2)(\varepsilon_1 - \varepsilon_2)}{\sigma_r \varepsilon_r} + \Lambda_3^* \left(\frac{\varepsilon_1 - \varepsilon_2}{\varepsilon_r}\right)^2$$

$$(2.6)$$

In equations (2.5) and (2.6), x_1 and x_2 are mole fractions

of the components 1 and 2, and ε and σ are the L-J

parameters. These parameters can be used to define a

reduced temperature $\theta = \frac{\varepsilon_r}{kT} = \frac{1}{T^*}$ and a reduced density,

$y = \frac{1}{6}\pi \rho_r^3 = \frac{1}{6}\pi n^*$ where the subscript r refers to the

reference substance. The coefficients (Λ_i) are state

functions of the reduced variables (T^*, n^*).

Using the condition for material stability in

conjunction with equation (2.5) it has been shown that

at the critical temperature:

$$\Omega = 2 \text{ for } x_1 = x_2 = 0.5 \qquad (2.7)$$

Hence, to determine the critical temperature of phase

separation using conformal solution theory, the value of Ω

is computed as a function of n^* at constant T^* using

equations (2.5) and (2.6). The critical point is given by

the intersection of this curve with the straight line

representing equation (2.7).

The major problem in the conformal solution theory

is the choice of a suitable reference substance. However, this approach has been used to predict the critical locus in He-Xe system using Xe as a reference substance [30]. The predicted values agree well with the experimental results obtained by De Swaan Arons and Diepen [10].

An interesting feature of Tan's work is that on the basis of the conformal solution theory, a criterion has been developed which permits the prediction and classification of the different types of gas-gas equilibria known to occur in binary mixtures of rare gases.

If a larger molecule is taken as the reference substance in all systems, equation (2.6) may be written in the form:

$$\Omega = \Lambda_1{}^* (\xi^{-1} - 1)^2 + 2\Lambda_2{}^* (\xi^{-1} - 1)(\eta^{-1} - 1) + \Lambda_3{}^* (\eta^{-1} - 1)^2$$

(2.8)

where $\xi = \sigma_2/\sigma_1$ (2.9)

$\eta = \varepsilon_2/\varepsilon_1$ (2.10)

An ordering of the values of ξ for the various systems known to exhibit gas-gas immiscibility reveals that ξ can be used to characterize the type of gas-gas equilibrium.

The gas-gas immiscibility is of the first type if $\xi > 1.50$, of the second type if $\xi < 1.41$ and of the intermediate type if $1.41 < \xi < 1.50$. These criteria are very similar to those proposed by Temkin [25] namely that $b_{11} \gtrsim 0.42 b_{22}$ for systems exhibiting immiscibility of the first type, where $b (= \frac{2}{3}\pi\sigma^3)$ is the van der Waal's parameter. In terms of ξ, Temkin predicts immiscibility of the first type when $\xi \gtrsim 1.34$.

Similarly ordering of the values of η for different systems indicates that for immiscibility of the first type $\eta > 30.0$, for that of the second type $\eta < 20.0$ and for that of the intermediate type $20.0 < \eta < 30.0$.

The approach based on conformal solution theory has been used only for mixtures containing one or more rare gases and has not been tested for mixtures containing polar components (e.g. NH_3, H_2O etc.) many of which exhibit gas-gas immiscibility. However, it has been recently reported by Kay and his colleagues [31] that the theory can be used satisfactorily to determine the composition dependence of critical temperature and pressure (T_c, P_c) for a wide variety of (fluorocarbon + n-alkane) mixtures.

Approach based on lattice gas model

Guggenheim [32] has developed a lattice theory for a two component system to explain the critical behaviour of binary mixtures. In this model the following assumptions are made:-

a)   The motion of the molecules reduces to oscillations about equilibrium positions and that each molecule occupies a lattice point. This is a questionable approximation for liquids but X-ray analysis has shown that the mutual arrangement of neighbouring molecules in liquids is much like that in a solid. However the main difference between liquids and solids is that whereas the number of nearest neighbours has a well defined value in crystals only average values can be ascribed to liquids.

b)   The homogeneous mixture will split into two phases if there is an increase in free energy.

A disadvantage of this model is that the particle density is assumed to be equal in the two co-existing phases and hence it cannot be used to describe vapor-liquid equilibria. On the other hand, it has been used widely for

studying the critical properties of pure substances.

Trappeniers, Schouten and Ten Seldam [33] have used the two_component_lattice_gas_model to predict gas-gas immiscibility in binary mixtures. The model developed is, in fact, based on the theory of regular solutions for a ternary system in which the molecules of one of the components (holes) have no interaction with either similar or dissimilar molecules.

Consider a system consisting of N_1 molecules of Component 1, N_2 molecules of Component 2 on the points of a lattice and N_0 vacant lattice sites. The total number of lattice points N is then: $N = N_1 + N_2 + N_0$. It is assumed that the interaction energy between molecules which are not nearest neighbours can be neglected.

W_1 and W_2 are defined as the energies required to remove a molecule of species 1 and 2 from their respective lattices and an interchange energy 2W is the energy required to effect an exchange of molecules 1 and 2 between their respective lattices.

Using the so called zeroth approximation i.e. random mixing of Components 1 and 2 and the vacant sites, the configurational free energy of a system of N lattice points is given as:-

$$F_c = -N_1W_1 - N_2W_2 + Nx_0x_1W_1 + Nx_0x_2W_2 + Nx_1x_2W$$
$$+ NkT(x_1\ln x_1 + x_2\ln x_2 + x_0\ln x_0) \qquad (2.9)$$

where $x_1 = \dfrac{N_1}{N}$, $x_2 = \dfrac{N_2}{N}$, $x_0 = \dfrac{N_0}{N}$

The following procedure was used to find a numerical solution for the co-ordinates of the critical point.

The equation of the spinodal curve can be written as:-

$$fx_1x_1 fx_2x_2 - fx_1^2x_2 = 0 \qquad (2.10)$$

(where $fx_1x_2 = \dfrac{\delta^2 f}{\delta x_1 \delta x_2}$) which is the locus of the points on the isothermal f-v-x surface where the curvature changes sign. This curve is the border line between the metastable and unstable states of a system.

The condition for an extremum of pressure on the spinodal curve which corresponds to a critical point, results in:-

$$fx_1x_1x_2 fx_1x_2 fx_2x_2 + 3fx_1x_1x_2 fx_1{}^2x_2 - 3fx_1x_2x_2 fx_1x_2 fx_1x_1$$
$$+ fx_2x_2x_2 fx_1{}^2x_1 = 0 \qquad (2.11)$$

Equations (2.9), (2.10) and (2.11) have been solved by numerical methods for several combinations of energy parameters W_1, W_2 and W in equation (2.9). The mole fractions (x_1 and x_2) at the critical temperature were calculated from equations (2.10) and (2.11). The critical pressure was calculated from the equation:-

$$Pv_0 = -kT \ln x_0 - (x_1 W_1 + x_2 W_2)(x_1 + x_2) + x_1 x_2 W \qquad \text{or,}$$

$$P^* = -T^* \ln x_0 - (x_1 + x_2\tfrac{W_2}{W_1})(x_1 + x_2) + x_1 x_2\tfrac{W}{W_1} \qquad (2.12)$$

where $P^* = \dfrac{Pv}{W_1}$ and $T^* = \dfrac{kT}{W_1}$

In this way pressure-composition diagrams can be drawn for a wide variety of binary mixtures with several combinations of energy parameters W_1, W_2 and W. The results of these calculations show that gas-gas immiscibility of the first type occurs if $W = W_1 + W_2$ and that of the second type when $W > (W_2 - W_1)$ and $W > W_1$. Normal behaviour in which the system does not exhibit gas-gas immiscibility occurs when $-(W_2 - W_1) < W < (W_2 - W_1)$ and $W < W_1$. Although the model looks promising it has been tested only for rare mixtures (e.g. Ne + kr) and much remains to be done to extend it so that it can be used to predict phase equilibria in binary mixtures of all types.

Approach based on the principle of corresponding states

This has the strongest theoretical bases. This has been discussed in detail in Chapter 3.

4.   Review of Gas-Gas Equilibrium Data

a)   General

Gas-gas equilibrium is a high pressure extension of ordinary gas-liquid and liquid-liquid equilibria and the cause of immiscibility is the relative weakness of the intermolecular force between the two molecules. Hence it is to be expected that immiscibility will be exhibited by binary systems consisting of molecules of very different characteristics.

The systems which have been shown experimentally to exhibit gas-gas immiscibility are listed in Tables 1 and 2.

Numerous investigations [46] during recent years have shown that there is a continuous transition between gas-liquid, liquid-liquid and gas-gas equilibria. This transition can be demonstrated for mixtures of hydrocarbons with substances of very different polarity e.g. CH_4, CO_2, water and for mixtures of Helium with other condensed gases [47].

Hydrocarbon-CO$_2$ system

Figure 2.8 shows the critical curves of some binary mixtures of CO_2 with n-alkanes from methane to hexadecane [15]. Whereas the critical curves of ethane-CO_2 to undecane-CO_2 are represented by continuous lines between the critical points of pure components, the critical curve of CO_2-n-$C_{16}H_{34}$ has a very complicated shape. Starting from the critical point of the pure hydrocarbon the curve runs through a pressure maximum and then through a pressure and temperature minimum and finally rises steeply to higher temperatures and pressures. Schneider [15] points out that as the mutual solubility of CO_2 and the higher hydrocarbons ($>C_{16}$) decreases, the critical curve taken on the shape of the broken line in Figure 2.8. Hence the system will exhibit gas-gas immiscibility.

Table 1

SYSTEMS EXHIBITING GAS-GAS IMMISCIBILITY OF THE
FIRST TYPE

System	Temp. (^{O}C) (Temp. range of investigation)	P_{max} (atm.) (Max. pressure of the investigation)	Ref.
He-Ammonia	125-175	10,000	(34)
He-CO_2	25-100	10,000	(34)
He-Ethylene	25-150	10,000	(35)
He-Propane	100-150	7,000	(8, 13)*
He-Benzene	300	1,000	"
He-Methanol	245	3,000	"
He-Sulphurdioxide	175-200	7,000	"
He-n-Hexane	245	3,000	"
He-Xenon	5-65	2,000	(10)
He-Acetylene	36	64	(8)
He-Ethane	32	51	(8)
He-Dinitrogen-monoxide	37	74	(8)
He-Freon 12	25-122	330	(36)
He-Freon 22	100	330	"
He-Freon 114B_2	216-223	330	"
Ar-H_2O	270-440	3,000	(24)

* Review papers which contain references to experimental
  work.

Table 2

SYSTEMS EXHIBITING GAS-GAS EQUILIBRIA OF THE
SECOND TYPE

System	Temp. (^{O}C) (Temp. range of invest- igation)	P_{max} (atm.) (Max. pressure of the investigation)	Ref.
Ammonia-N_2	90-175	16,000	(6)
Ammonia-CH_4	45-100	10,000	(8,13)*
Ammonia-Argon	70-140	10,000	"
Ammonia-N_2-H_2	90-120	5,500	"
Ammonia-N_2-Methane	55-110	5,500	"
SO_2-N_2	35-40	9,000	"
He-N_2	-196 to -151	830	(37)
He-Ar	-182 to -126	650	(38)
Ne-kr	-110 to -63	1,800	(39)
CO_2-n-C_{16}	20-100	1,500	(40)
H_2O-N_2	300-350	6,000	(41)
H_2O-CO_2	250-350	3,500	(42)
H_2O-C_2H_6	200-400	3,700	(22)
H_2O-n-Butane	355-364	1,100	(22)
H_2O-n-Petane	340-352	620	(43)
H_2O-2-Methylpentane	330-355	500	(43)
H_2O-n-Heptane	350-355	550	(43)
H_2O-Propylene	323-350	2,500	(24)
H_2O-Cyclohexane	130-363	200	(44)
H_2O-Benzene	200-357	200	(45)
	287-300	735	(43)
H_2O-Toluene	305-310	455	(43)
	310-360	2,000	(23)
H_2O-O-Xylene	310-380	2,000	(23)
H_2O-Ethylbenzene	310-380	2,000	(23)
H_2O-n-Propylbenzene	320-400	2,000	"
H_2O-1,3,5-Trimethyl benzene	"	2,000	"

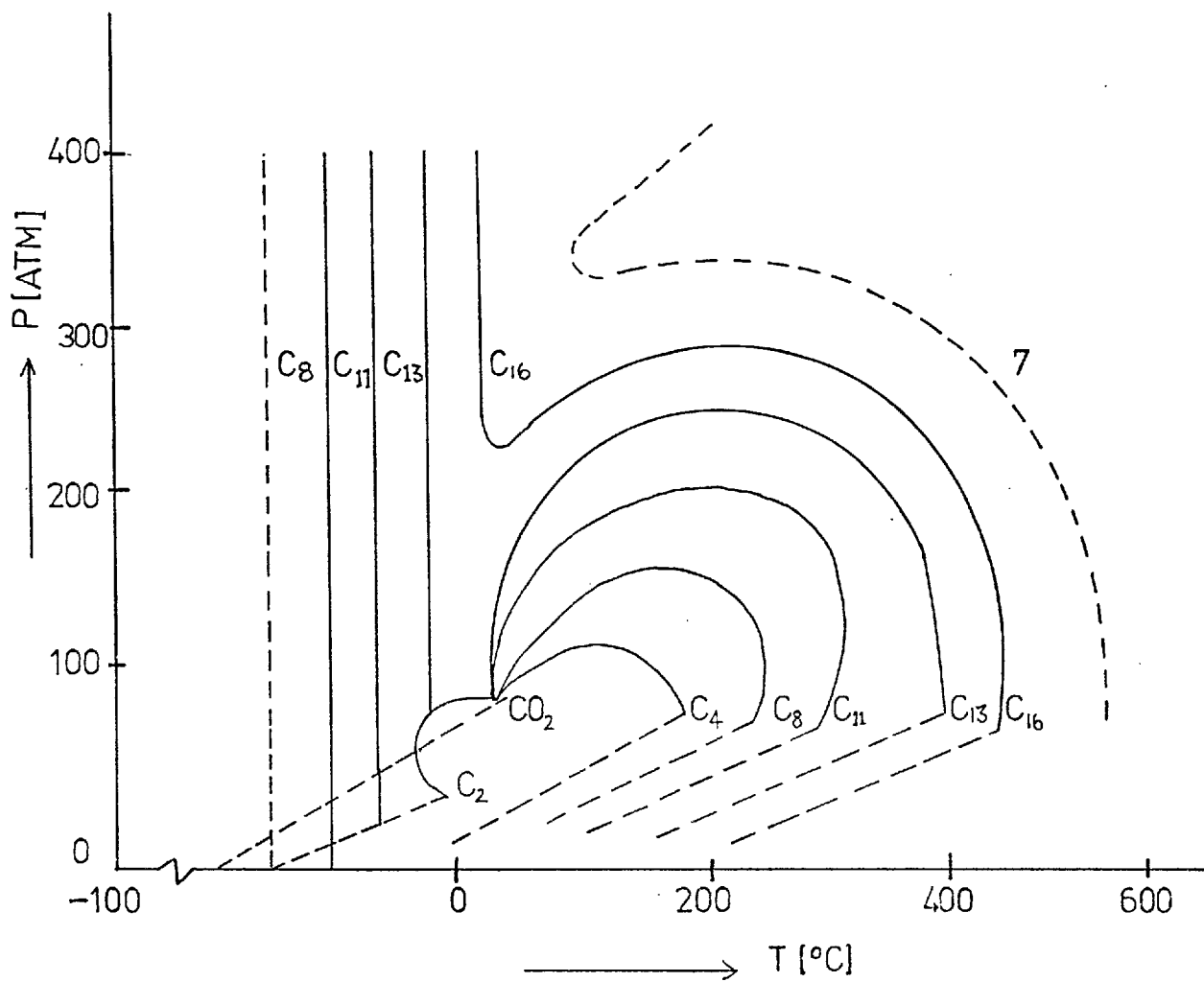* Review papers which contain references to experimental
  work.

FIGURE 2.8: CRITICAL CURVES FOR CO_2-N-ALKANE MIXTURES

Mixtures containing one or more rare gases

Gas-gas immiscibility has been observed in binary mixtures containing inert gases, especially in binary Helium mixtures. As a result of the work of Diepen [10], Trapenniers [48] and Streett [38], the characteristic behaviour of the mixtures of rare gases with Helium are known. Figure 2.9 shows parts of the critical curves for binary He-mixtures, according to a compilation by Streett [38].

It is evident from Figure 2.9 that there is a continuous transition between the second and first types of gas-gas immiscibility; the He-methane system being of an intermediate type. It has been shown recently by Trappeniers and Schouten [48] that the critical curve of Ne-Ar resembles that of He-Ar system and the system Ne-kr exhibits gas-gas equilibrium of the second type. These investigations show that gas-gas equilibrium is not restricted to systems containing He or a polar component, as might appear from Tables 1 and 2.

Recently Streett [12] attempted to define the high pressure limits of gas-gas immiscibility by studying mixtures of He-H_2, He-N_2, He-Ar, He-CH_4, Ne-Ar and Ne-CH_4 up to very high reduced pressures. Experimental evidence suggests that for Ne-Ar and He-Ar systems gas-gas immiscibility terminates at a critical end point formed by an intersection of the critical line with the three phase region (S + G_1 + G_2) whereas for He-H_2, He-N_2, He-CH_4 and Ne-CH_4 systems gas-gas immiscibility exists up to very high reduced temperatures and pressures and may persist to pressures sufficiently high for the electronic structure of the constituents to break down.
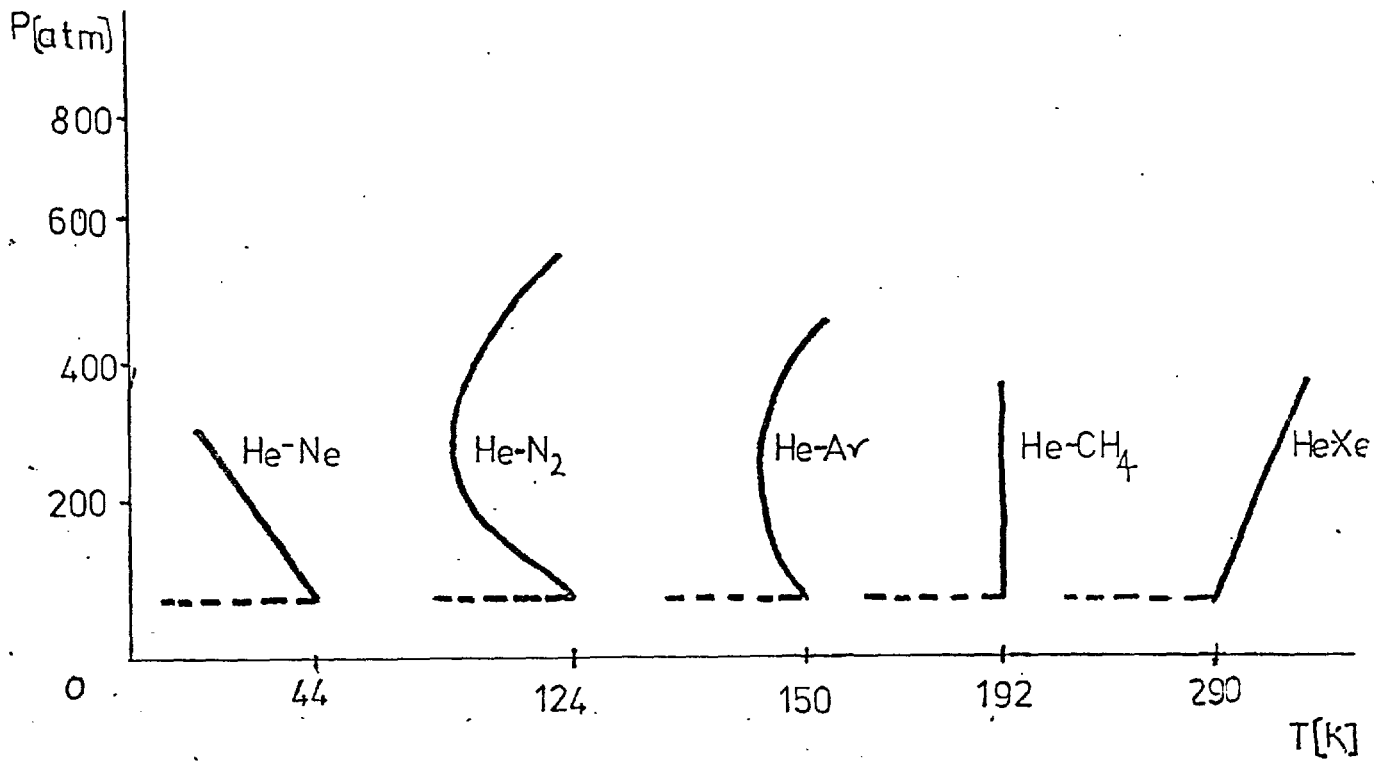
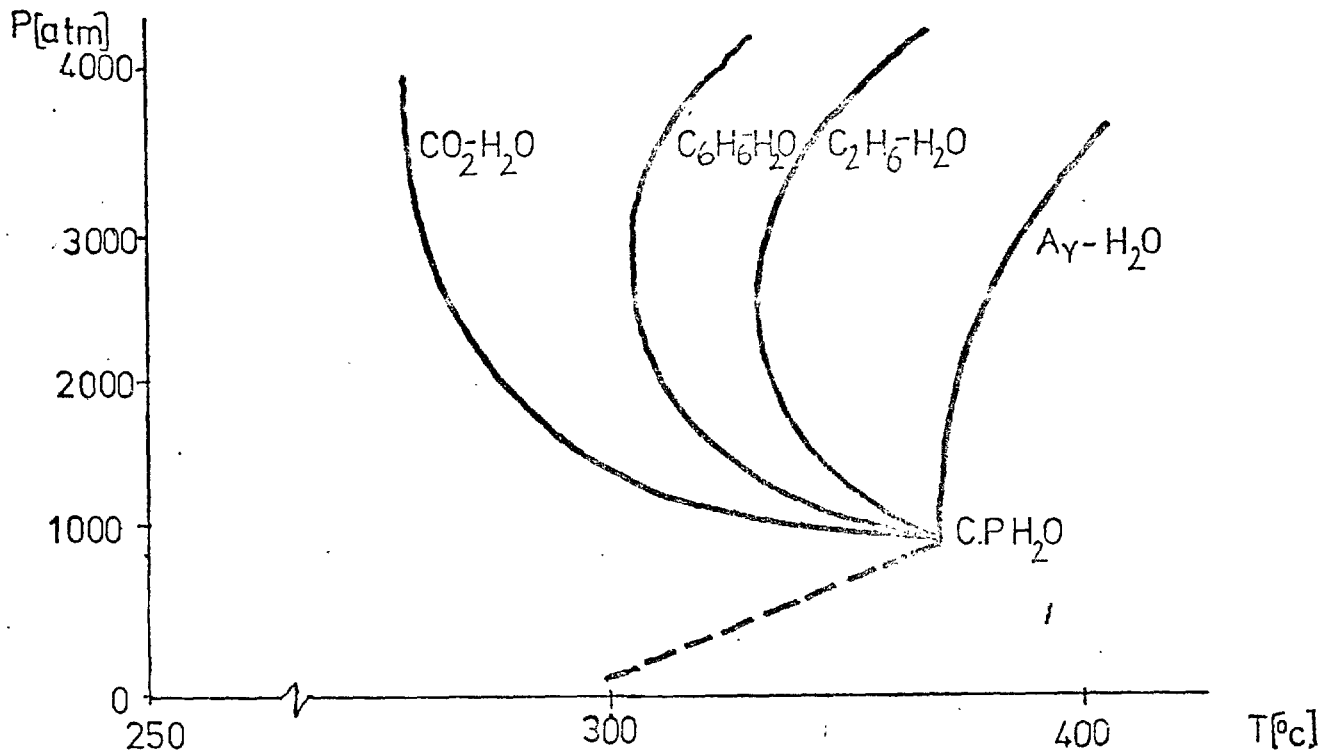FIGURE 2.9: CRITICAL LOCUS OF MIXTURE OF RARE GASES

FIGURE 2.10: CRITICAL LOCUS OF HYDROCARBON–WATER SYSTEMS

Hydrocarbon-water_systems

Because of their industrial importance, hydrocarbon-water systems have been studied extensively [49].

Measurements of the solubility of hydrocarbons in water have been extended in recent years to ranges of temperature and pressure where the hydrocarbon and water are miscible in all proportions. The critical locii of a series of binary hydrocarbon-water systems are given in Figure 2.10.

It may be noted from Figure 2.10 that most of the critical curves have the same shape and show a temperature minimum and a steep ascent to higher temperature and pressure i.e. gas-gas immiscibility of the second type. The only exception is the $Ar-H_2O$ system which exhibits gas-gas equilibrium of the first type.

Hydrocarbon-methane_system

Liquid hydrocarbons of approximately the same size are, in general, completely miscible in all proportions and as a result the critical locii of their mixtures take the form of continuous curves between the critical points of the pure components.

It has been shown by Davenport and Rowlinson [50] that liquid CH_4 is completely miscible with n-alkanes having 6 to 8 carbon atoms only below a definite temperature. Similar phenomena have also been found for binary mixtures of ethane with $C_{30}-C_{36}$ hydrocarbons [51].

The continuous transition between the various types of phase behaviour exhibited by a wide variety of methane-hydrocarbon systems is illustrated in Figure 2.11.

Critical curve 3 in Figure 2.11(d) corresponds to the methyl cyclopentane-CH_4 system. This curve starts at the
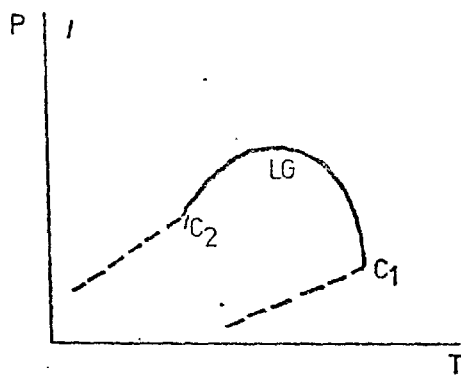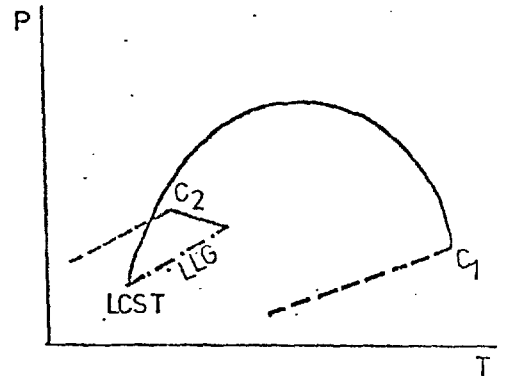
a) Type found for $(CH_4 + C_3H_8)$ b) Type found for $(CH_4+n-C_6H_{14})$

c) Type found for $(CH_4+1-hexene)$ d) Curve 3: CH_4+methylcyclo-
                                                  pentane
                                            Curve 2: CH_4+toluene

FIGURE 2.11:

critical point of methyl cyclopentane, runs successively

through a pressure maximum and a pressure minimum and ends

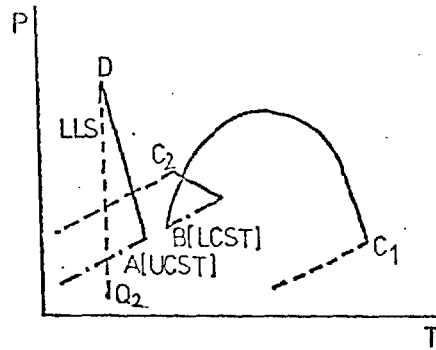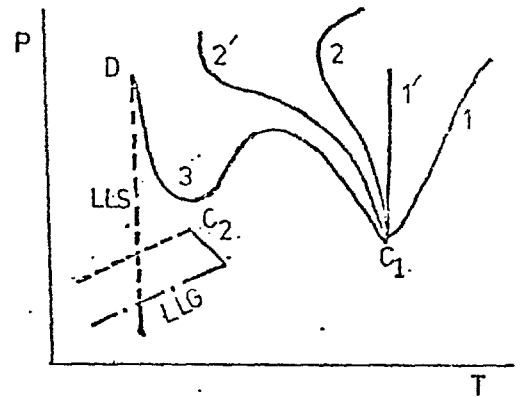at the critical end point D on a three phase line, where

solid Component 1 and two liquid phases are in equilibrium.

With increasing mutual solubility, the critical curve 3

in Figure 2.11(d) is displaced to lower pressures and may

cut the three phase LLG line twice. Such is the behaviour

shown by the CH_4-1-hexane system in Figure 2.11(c) where

point A represents the UCST and the point B represents

the LCST [52].

The critical curves of binary CH_4-hydrocarbon systems

with lower mutual solubility than that indicated by curve 3

in Figure 2.11(d) would be displaced to higher temperatures

and should show gas-gas immiscibility at high temperatures.

As yet this has not been experimentally verified.

Miscellaneous Binary Systems

In order to study the polarity effect on the critical

phase behaviour of binary fluid systems, the critical

temperatures of binary mixtures of CO_2, C_2H_6, C_2H_4, $n-C_6H_{14}$

or $1-C_6H_{12}$ with a second component of very different

polarity e.g. methanol, 2-hexanol etc. were determined as a

function of pressure up to 1000 atm. [53].

Table 3 shows the binary systems studied and Figure 2.12

shows the experimental results.

The critical P(T) curves (as shown in Figure 2.12)

exhibit a whole pattern of different transition types

between liquid-gas, liquid-liquid and gas-gas equilibria

These results verify the previous hypotlesis that there is

a continuous transition between liquid-gas, liquid-liquid

and gas-gas critical phenomena in binary fluid mixtures

at high pressure. The same continuity has also been

Table_3

Component_1	Component_2	
C_2H_6	Nitromethane	[f] *
	Methanol	[e]
	N,N-Dimethylformamide (DMFA)	
	2,5-Hexanediol	[g]
	N-Methylacetamide (NMAA)	[h]
C_2H_4	Nitromethane	[j]
	DMFA	[i]
	2,5-Hexanediol	[l]
	NMAA	[k]
CO_2	2-Hexanol	[c]
	2-Octanol	[b],[d]
	2,5-Hexanediol	[a]
Hexane	DMFA	[n]
	2,5-Hexanediol	[p]
1-Hexene	DMFA	[m]
	2,5-Hexanediol	[o]

*
REFER TO FIGURE 2.12

38
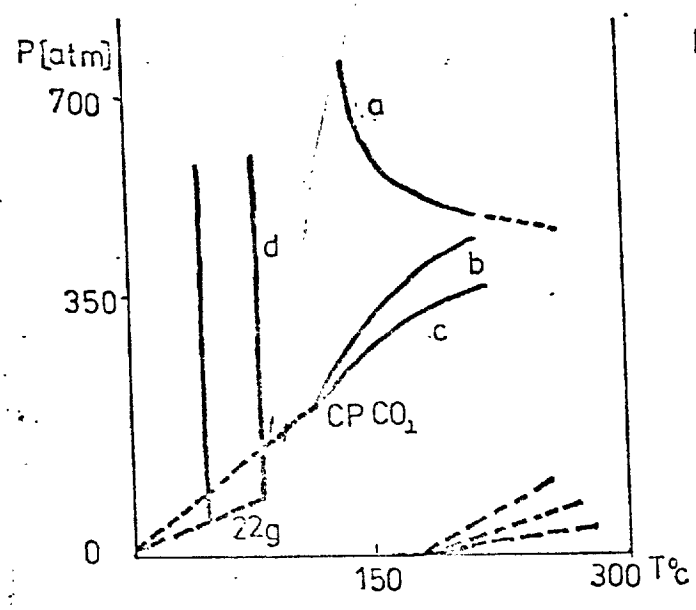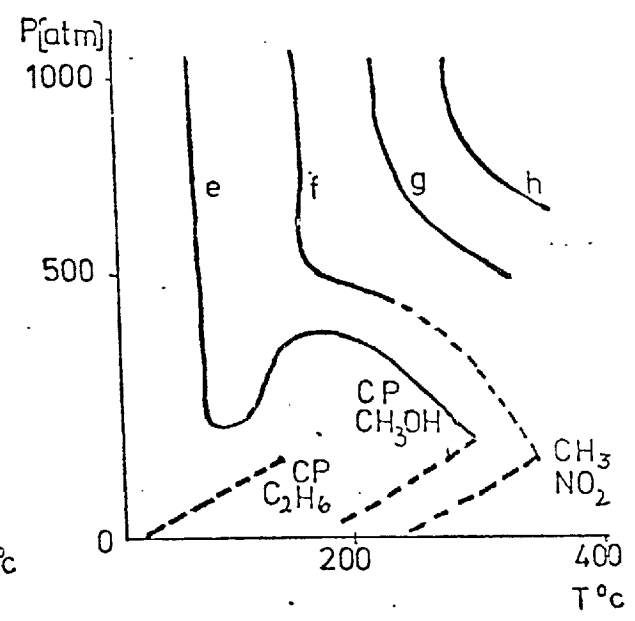
CO$_2$ BINARIES

C$_2$H$_6$ BINARIES
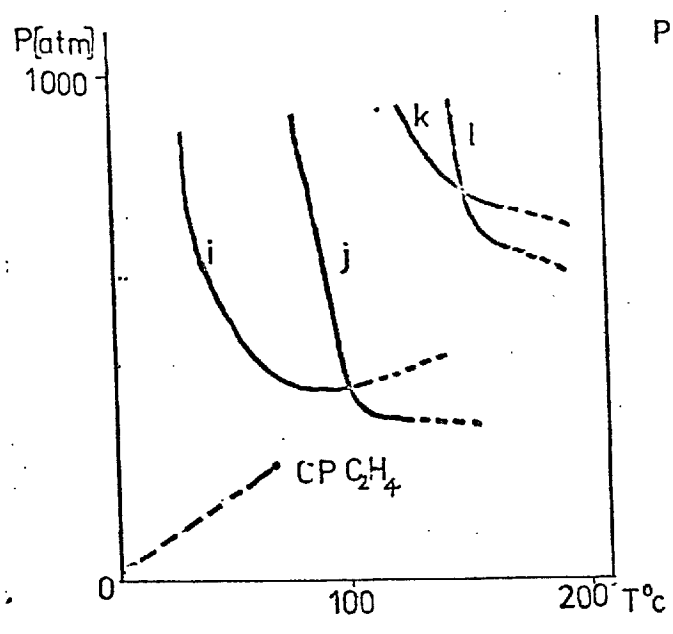
C$_2$H$_4$ BINARIES
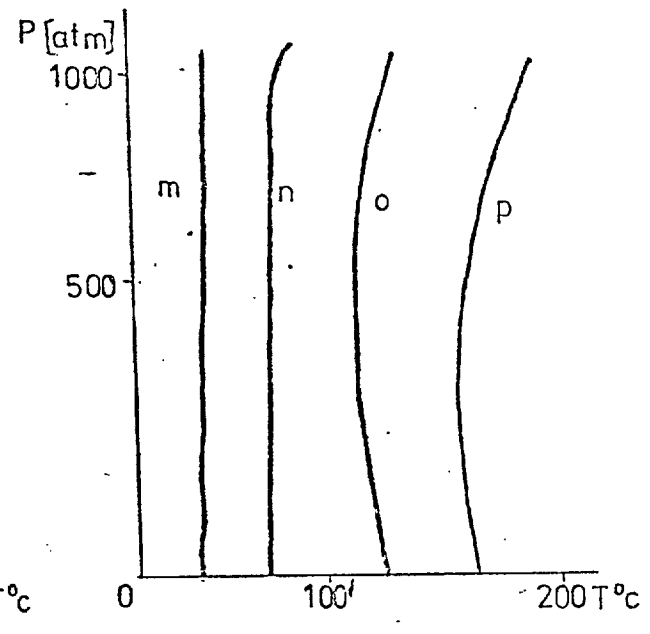
C$_6$H$_{14}$ & 1-C$_6$H$_{12}$ BINARIES

FIGURE 2.12: CRITICAL P(T) CURVES

demonstrated by computer calculations made recently by Deiters and Schneider [28].

b) Mixtures Containing Fluorocarbons

Binary mixtures of aliphatic fluorocarbon-hydrocarbon are characterized by large positive deviations from ideality leading, in most cases, to liquid-liquid immiscibility even at room temperature.

These mixtures have been investigated extensively and the experimental data have been reviewed by Scott [54] and Rowlinson [3]. Scott and his colleagues [55] have discussed the anomalous behaviour of fluorocarbon-hydrocarbon mixtures and they point out that the immiscibility must be attributed to the failure of geometric mean law for 1-2 interaction i.e.

$$\varepsilon_{FH} < (\varepsilon_{FF}\varepsilon_{HH})^{\frac{1}{2}}$$ (symbol FH means fluorocarbon-hydrocarbon interation)

Various theories have been put forward to account for the failure of geometric mean assumption. Reed [56] emphasizes that this is caused by the difference in ionization potentials and the collision diameters between the two components. Using London's theory of dispersion forces and Lennard-Jones model for the intermolecular potential, Hudson and McCoubrey [57] showed that the characteristic energy of interaction is given by the equation

$$\varepsilon_{12} = \frac{(2(I_1 I_2)^{\frac{1}{2}})}{(I_1 + I_2)} \left\{2^6 \frac{\sigma_1^3 \sigma_2^3}{(\sigma_1 + \sigma_2)^6}\right\} (\varepsilon_1 \varepsilon_2)^{\frac{1}{2}}$$

where I_1 and I_2 are the ionization potentials and σ_1 and σ_2 are the collision diameters of the two pure components.

However, the large positive deviations from ideality found in aliphatic systems are not present in aromatic systems.

It has been found recently by Swinton [58] that aromatic fluorocarbon-aromatic hydrocarbon mixtures are characterized by large negative deviations from ideality. The two components form complexes in both the liquid and solid states and these complexes apparently persist up to the gas-liquid critical temperature. By working with various aromatic and alicyclic fluorocarbons it was shown by Swinton [59] that the strength of the unlike molecular interactions in the various classes of mixture were in the order (alicyclic fluorocarbon + alicyclic hydrocarbon)< (aromatic fluorocarbon + alicyclic hydrocarbon)<(aromatic fluorocarbon + aromatic hydrocarbon). The major factor governing the strength of the unlike interaction was thought to be the relative shapes of the component molecules [59]. Rowlinson [3] points out that there is firm evidence of strong forces between these molecules but as yet there is little or no direct spectroscopic evidence of this.

Although a large number of fluorocarbon-hydrocarbon mixtures have been studied at atmospheric pressure, it was only recently that the measurements were extended to high pressure. In Table 4 those He-fluorocarbon mixtures which have been studied for gas-gas immiscibility are listed.

It is interesting to note that many of the systems (listed in Table 4) do not exhibit gas-gas immiscibility although they might have been expected to do so according to the criterion proposed by Tempkin [25]. These observations led Tsiklis [64] to conclude that the polarity of C-F bond and the small size fluorine atoms prevents the occurrence of gas-gas immiscibility in these mixtures. As the number of fluorine atoms is decreased by the substitution of chlorine, bromine or hydrogen atoms, immiscibility occurs.

Table 4

System	Temp. (°C) (Temp. range of investigation)	P_{max} (atm.) (Maximum pressure of the investigation)	Occurrence of Gas-Gas Equilibrium	Ref.
He-Freon 11 (CCl_3F)	–	–	Yes	Hypothesis
He-Freon 12 (CCl_2F_2)	25-122	330	Yes	(36)
He-Freon 13 ($CClF_3$)	–	–	No	(60)
He-Freon 14 (CF_4)	–	–	No	Hypothesis
He-Freon 21 ($CHCl_2F$)	–	–	Yes	"
He-Freon 22 ($CHClF_2$)	100	330	Yes	(61)
He-Freon 23 (CHF_3)	–	–	No	(60)
He-Freon 13B1 ($CBrF_3$)	20-71	270	No	(62)
He-Freon 111 (C_2Cl_5F)	–	–	Yes	Hypothesis
He-Freon 112 ($C_2Cl_4F_2$)	–	–	Yes	"
He-Freon 113 ($C_2Cl_3F_3$)	205-225	250	Yes	(62)
He-Freon 114 ($C_2Cl_2F_4$)	20-156	200	Yes	(62)
He-Freon 115 (C_2ClF_5)	70-84	250	No	(62)
He-Freon 113B2 ($C_2ClBr_2F_3$)	250-290	500	Yes	(62)
He-Freon 114B2 ($C_2Br_2F_4$)	216-223	330	Yes	(61)
He-Difluoroethylene ($CH_2=CF_2$)	–	–	No	(60)
He-Sulphurhexafluoride (SF_6)	–	–	No	(63)

Recently Kay and his colleagues [31] have measured the critical temperature and pressure at different compositions for each of the binary mixtures formed by:-

i) C_3H_8 with C_3F_8, C_6F_{14}, C_6H_5F

ii) C_6H_{14} with C_6F_{14}, C_6H_5F

iii) Perfluorocyclobutane with pentene-1

iv) C_7F_{16} with C_2H_6 through C_9H_{20} .

v)   Perfluoromethylcyclohexane with aliphatic hydrocarbon

The composition dependences of critical temperature and pressure calculated by means of a modified theory of conformal solutions were in satisfactory agreement with the experimental results.

Very recently Schneider and his colleagues [65] have studied liquid-liquid phase equilibria in a series of binary and ternary fluorocarbon mixtures. All these binary and ternary mixtures show upper critical solution temperatures (UCST) that rise with increasing pressure. Table 5 shows a compilation of the work done in Germany.

According to the experimental observation of Jockers [68] both the systems (C_6H_5F + H_2O) and ($1,4-C_6H_4F_2$ + H_2O) show gas-gas immiscibility in the similar range of pressure and temperature. Their results have been shown in Figures 2.13 and 2.14. However the work could not be extended to other fluorobenzenes because these are very unstable in water.

Mendonca [20] has studied (carbon tetrafluoride + n-heptane) system in the temperature range 50-90°C and has shown that the system exhibits gas-gas equilibrium of the second type, the point of double contact being approximately 57°C and 700 atm. The distinguishing feature of this work

Table 5

LIQUID-LIQUID PHASE EQUILIBRIA AND CRITICAL
PHENOMENA IN FLUID MIXTURES

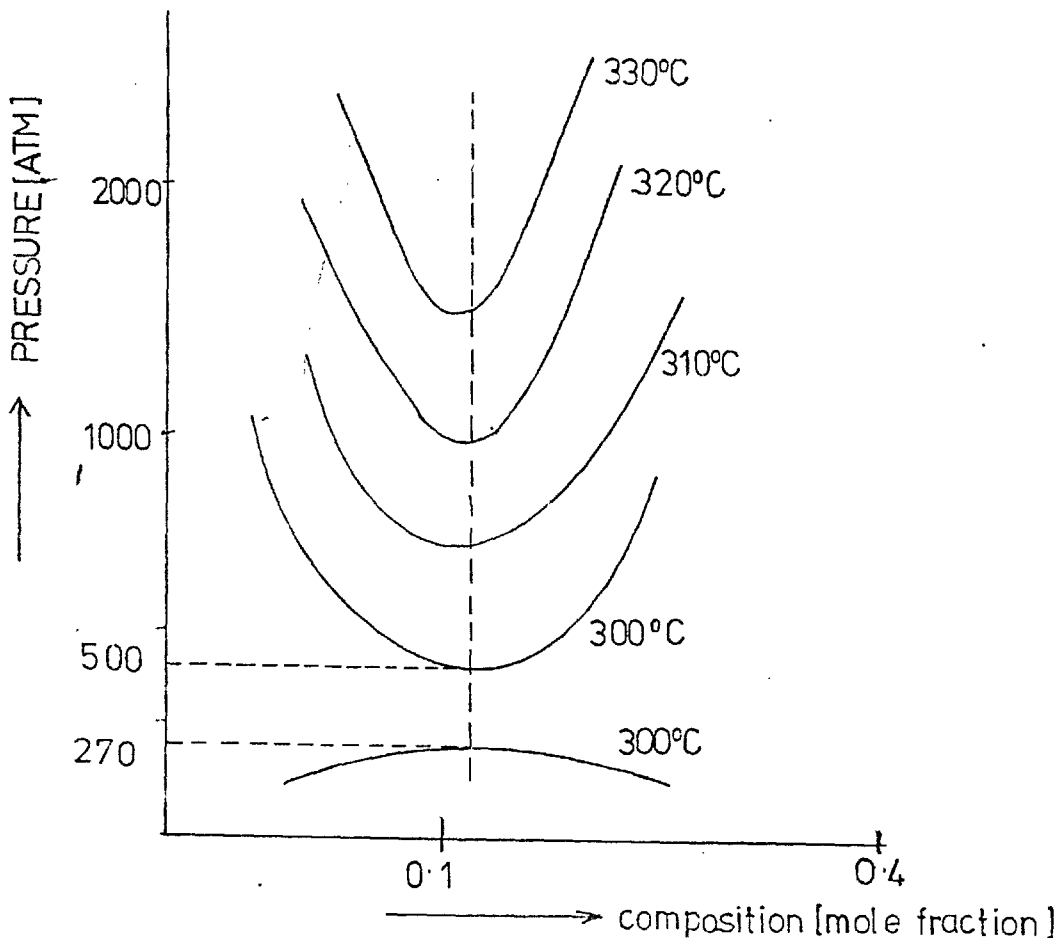| System	Pressure and Temp. Range	Ref.
$CHF_3-C_2H_6$	20 atm.$<P<$1700 atm. $-123^{O}C<T<-54^{O}C$	(65)
CHF_3-CF_4	200 atm.$<P<$1245 atm. $-155^{O}C<T<-139^{O}C$	(65)
$CF_4-C_2H_6$	33 atm.$<P<$1650 atm. $-132^{O}C<T<-89^{O}C$	(65)
CF_4-CH_4	100 atm.$<P<$1600 atm. $-187^{O}C<T<-153^{O}C$	(67)
$C_2H_6-CF_4-CHF_3$	200 atm.$<P<$1400 atm. $-150^{O}C<T<-70^{O}C$	(66)
CH_4-CHF_3	$P\leq$1900 atm. $-118^{O}C<T<-95^{O}C$	(67)
$C_6H_5F-H_2O$	96 atm.$<P<$3800 atm. $270^{O}C<T<370^{O}C$	(68)
$1,4,C_6H_4F_2-H_2O$	80 atm.$<P<$3600 atm. $260^{O}C<T<355^{O}C$	(68)

FIGURE 2.13:   PRESSURE-COMPOSITION ISOTHERMS
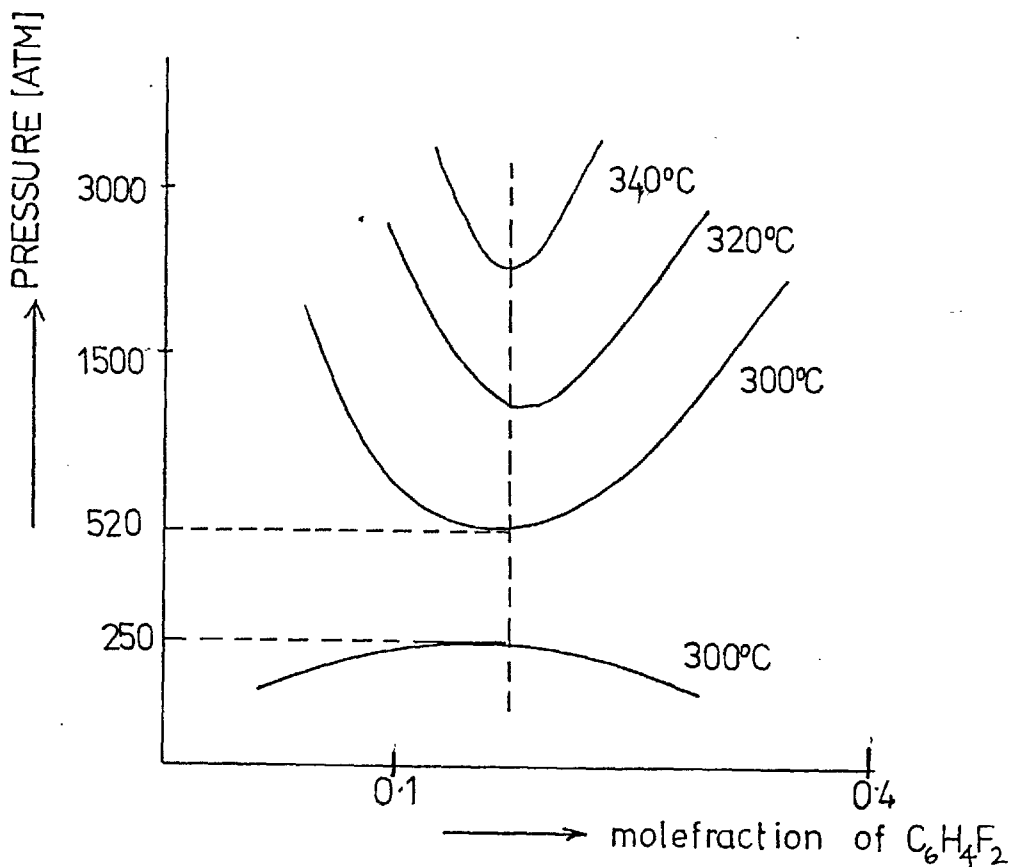FOR FLUOROBENZENE-WATER

FIGURE 2.14:   PRESSURE-COMPOSITION ISOTHERMS FOR
1, 4- DIFLUOROBENZENE-WATER

is that the system exhibits gas-gas immiscibility
under conditions which are accessible easily.

5.   Practical_Application_Of_High_Pressure_Phase_Equilibrium

The solubility of solids and liquids in supercritical
gases may provide the basis for a possible method for
separating many binary systems. Hence work in this field
is being pursued actively.

Vapor phase extraction with compressed gases is a
typical separation process operating at high pressure
which makes use of increased solubility effects at high
pressure. The principles of supercritical gas extraction
have been described by Paul and Wise [69] and the
thermodynamics of such processes have been reviewed by
Rowlinson and Richardson [70], Diepen and his colleagues [71]
and Franck [72].

According to this principle, a supercritical gas
dissolves one or more components from a mixture and the
components are separated from the supercritical gas by
reducing the pressure. In this way not only is the solute
recovered but the solvent is regenerated. In some cases it
is possible to recover the solute by heating the exit
supercritical gas. In a recent review on this subject,
Ellis [73] has outlined the advantages of compressed gases
and emphasized their solvent power but a large amount
of energy is required to compress the gas not all of which
can be recovered when the pressure is reduced.

A large number of pilot plants involving gas
extraction as a separation process have been in operation
throughout the world. Elgin and Weinstock [74] have proposed
a method for dehydrating organic compounds by using compressed
gases such as ethylene at pressures of 34-67 atm. The
ethylene under pressure is used to separate water from the
organic solution. A recent British patent [75] contains

68 examples of supercritical extraction of organic compounds. Using compressed ethylene as a solvent, a wide variety of substances (and their mixtures) were extracted.

Although a large number of patents involving gas extraction as a separation technique have been granted, very little progress appears to have been made towards developing gas extraction as a viable separation process. The major reason for this is the huge cost of running a high pressure plant and as a result the process is not an immediate substitute for the standard separation techniques such as distillation, liquid extraction, etc. However it is widely believed that the potential application of this technique lies in the extraction of solid substances which are sensitive to high temperature using gases having low critical temperatures.

Of more immediate relevance to this thesis is the granting of a U.S. Patent [76] for the demineralisation of sea water using gas-gas immiscibility.

Figure 2.15(a) illustrates schematically the arrangement of plant used for carrying out the process. Cumene is brought into contact with the brine solution (sea water) in pressure vessel (1) at an elevated temperature and pressure e.g. 260-315°C and 66-135 atm. to extract water from the brine and form a single phase mixture comprising water and cumene substantially free from organic salts. The mixture, which is in the dense gas phase at elevated pressure, is immiscible with residual brine and is separated from the latter by gravity. After separation, the mixture of water and cumene is subjected to increased pressure in vessel 2 sufficiently
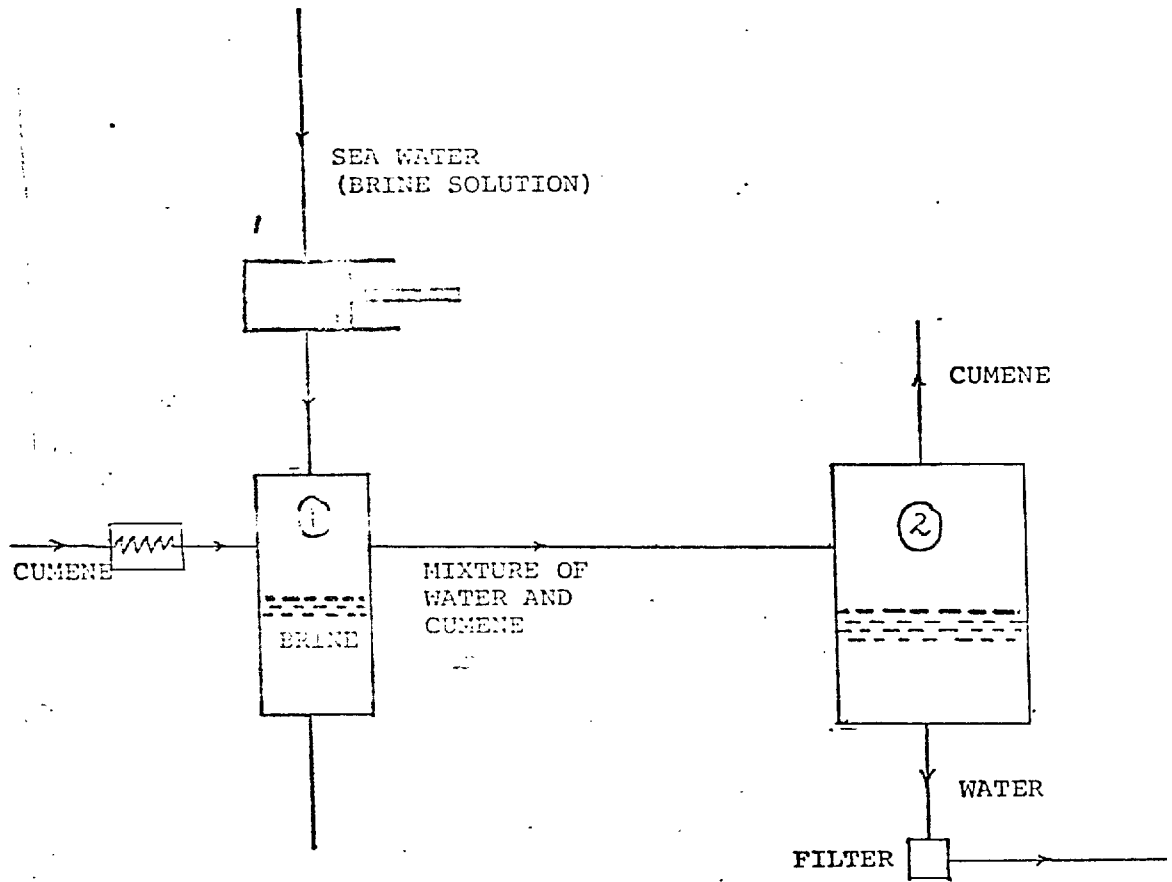
SEA WATER
(BRINE SOLUTION)

CUMENE

CUMENE

MIXTURE OF
WATER AND
CUMENE

BRINE

WATER

FILTER

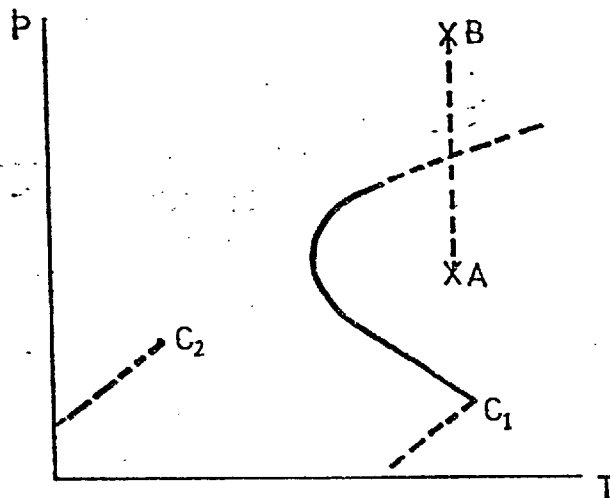**FIGURE 2.15(a): SCHEMATIC DIAGRAM OF DESALINATION PROCESS**

FIGURE 2.15(b): PRINCIPLE OF THE PROCESS

above the extraction pressure to cause cumene and water
to separate from one another as two immiscible gas phases.
The water, residual brine or salts liberated from the
brine may be recovered as products of the process while
the cumene is recycled back to the extraction column (1).
Residual cumene contained in the de-salinated water may be
eliminated by passing the water through a suitable
purifying filter.

The principle of the process can be seen from
Figure 2.15(b). The mixture of cumene and water leaving
extractor column (1) is at, say, state A. As the pressure
of the mixture is increased, the path of the process
crosses the critical locus and the mixture splits into
two gas phases which are separated at, say, state B in
column 2.

Another potential application of high pressure
phase equilibria is the development of supercritical
fluid chromatography (SFC). This is a relatively new
technique in which compressed fluids at supercritical
temperature are used as mobile phases.

Myers and Giddings [77] and Gouw and Jentoft [78],
in a recent review, have discussed the practical details
of this technique and have shown that SFC is potentially
superior to liquid chromatography in separating
efficiency and speed, since a supercritical fluid has
better transport properties than a liquid. It has been
pointed out by Bartman and Schneider [79] that several
substances whose gas or liquid chromatographic separation
is difficult or even impossible, can be separated by
this technique. Unfortunately none of the high sensitivity

detectors for gas chromatography is suitable for high
pressure use and this problem has been solved by Sie
and Rijnders by using a UV absorption detector, by Myers
and Giddings [77] by decompressing the exit gas from the
column and using flame ionization detectors for the
subsequent analysis. Recently, a microadsorption detector
has been successfully used in a SFC system.

Although SFC can be used as a rapid chromatographic
tool for the separation of heavy molecular weight compounds,
it will obviously not replace gas or liquid chromatography
except in some special application. The primary reason
for this is that the cost of running a SFC system is quite
high and the detector section is a major problem for many
applications.

It is obvious from the above discussions that although
separation processes involving high pressure phase equilibria
can be used for various commercial processes, it has not
been competitive enough with the well established means of
separation. However, this can be a basis of separation
where other standard techniques fail.

CHAPTER_3

PRINCIPLE_OF_CORRESPONDING_STATES_AND_ITS_EXTENSION_FOR
THE_PREDICTION_OF_GAS-GAS_EQUILIBRIA

It was shown in the previous chapter that gas-gas
immiscibility can be understood from the shape of critical
locus of fluid mixtures in pressure-temperature co-ordinates.
Hence the prediction of the phenomenon is basically that
of predicting which fluid mixtures will give a critical
locus of the required shape.

Methods for the prediction of critical locus fall
into four main categories:-

a)   Empirical_methods

A number of correlations for the prediction of
critical locus in mixtures have been reviewed by Grieves
and Thodos [80] and Reid, Prausnitz and Sherwood [81].
However, these correlations may be very inaccurate when
used for conditions outside the range which has been
explored experimentally and are, therefore, of limited
applicability.

b)   Use_of_equations_of_state

This method has been already discussed in the previous
chapter. It was used by both Spear, Robinson and Chao [82]
and Joffe and Zudkevitch [83] in conjunction with Redlich-
Kwong equation of state to predict the critical properties
of binary mixtures. Joffe and Zudkevitch performed
calculations using this equation of state in conjunction with
the critical state equations. A graphical procedure was
used to solve the simultaneous equations that define the
critical state. Quantitative results were reported for
ethane-CO_2 and n-butane-CO_2 systems. Spear, Robinson and

Chao [82] determined the critical properties of binary
mixtures by a procedure that follows the boundary curve
of material instability in search of an extremum pressure.
A program was developed to apply the procedure to simple
mixtures for which the extremum pressure is a maximum.
The R-k equation of state was used. Agreement of the calculated
critical pressure and temperature (P_c, T_c) with experimental
data is quite good for binary mixtures of hydrocarbon,
CO_2, H_2S, CO, N_2 and others, with the use of an empirical
binary interaction parameter in the equation of state.
However the method fails to give a reasonable agreement
between calculated and experimental critical volumes. This
deviation is expected, since the R-k equation of state
fails to reproduce critical density of pure substances.

Van der Waal's equation has been used to calculate
the critical locus and hence to predict gas-gas immiscibility
in binary mixtures. This has been discussed in detail
in the previous chapter.

c)   Mixed_methods

The mixed method makes use of both (a) and (b)
for different parts of the problem. For example, Chueh and
Prausnitz [84] correlated the critical temperature (T_c)
and volume (V_c) of binary mixtures as quadratic functions
of the mole fractions. The values of T_c and V_c were then
substituted into the Redlich-Kwong equation of state to
obtain the critical pressure, as a function of composition.

and d)   Principle_of_corresponding_states

This approach, which has the strongest theoretical
basis, has been used by various authors for the prediction
of the critical points of a wide variety of binary mixtures.

Some of the different methods proposed will be discussed briefly and because of its importance, a more comprehensive account will be given of the procedure developed by Rowlinson and Teja [85].

Zandbergen, Knaap and Beenakker [86] used the law of corresponding states to predict gas-gas immiscibility in mixtures of helium and xenon. The method is based on the derivation of the thermodynamic properties of a mixture from those of the pure components, using a corresponding states treatment and an effective interaction potential obtained by averaging the three types of pair interactions present in the mixture. The averages were performed using a single and three liquid model. (These terms will be discussed in detail later).

A homogeneous mixture must satisfy the conditions of mechanical, thermal and material stability. The last condition can be satisfied for a binary mixture if the Gibbs free energy vs. composition curve (at constant pressure and temperature) is concave upwards for all mole fractions i.e. $(\delta^2 G/\delta x^2)_{P,T} > 0$.

Zandbergen et al calculated the excess free energy of mixing as a function of the mole fraction at a fixed pressure and temperature and looked for the boundaries of the unstable region. For a fluid mixture that is unstable $(\frac{\delta^2 G}{\delta x^2})_{P,T} < 0$.

Geometrically, this corresponds to the region which lies between B and C in Figure 3.1. The portion BC is unstable and is surrounded by the portions AB and CD which are materially stable. The two phases in equilibrium have compositions A and D. This approach has been used to study the gas-gas immiscibility in the He-Xe system and the
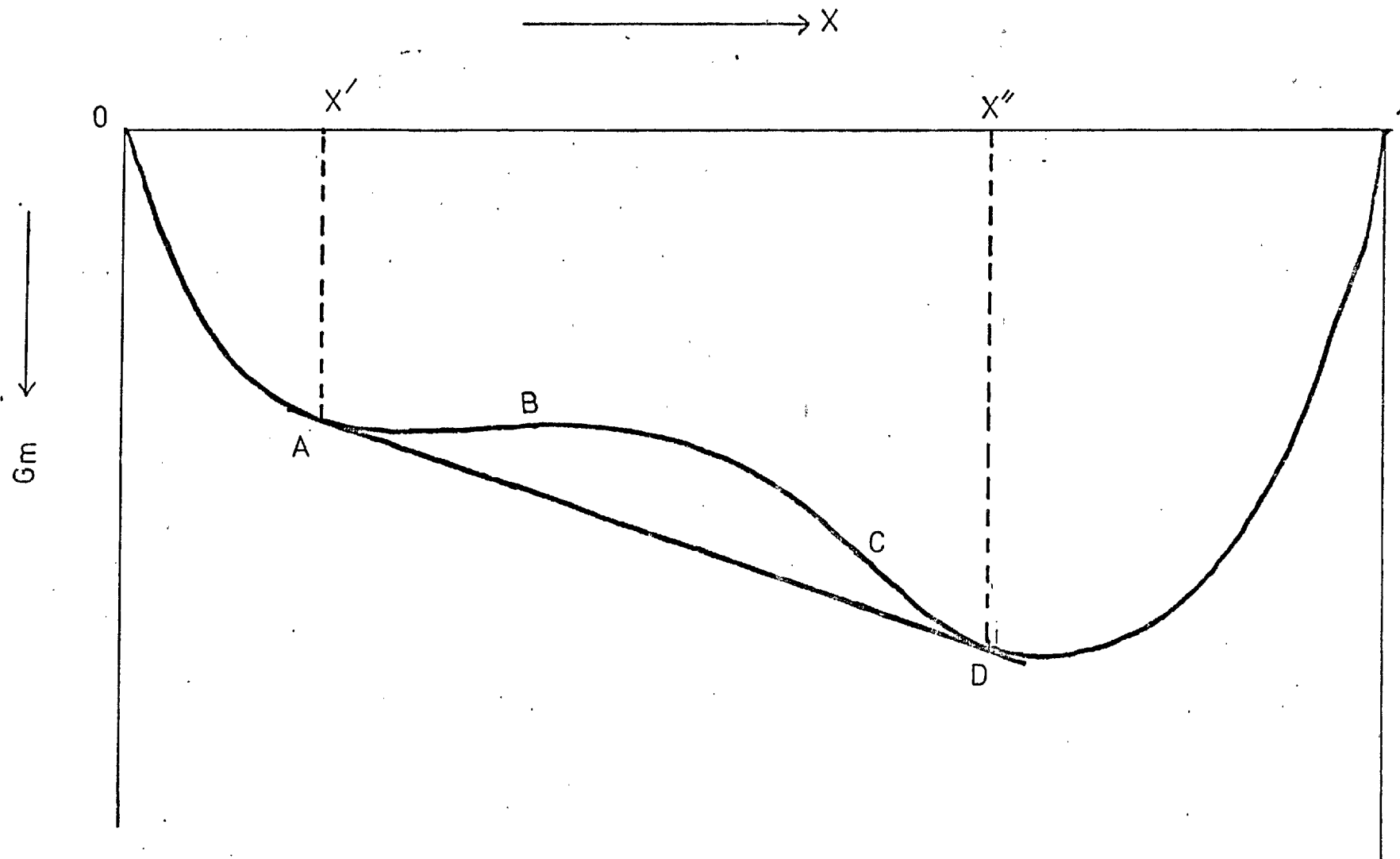
FIGURE 3.1:   MOLAR FREE ENERGY OF MIXING AS A FUNCTION OF MOLE FRACTION

agreement between predicted and experimental results was satisfactory. Using the same method it was predicted that phase separation would occur in kr-He system but not in the system Ar-He.

In order to use the principle of corresponding states to predict gas-gas immiscibility, Breveld and Prausnitz [87] have extended the existing corresponding states correlation for the estimation of the thermodynamic properties of simple fluids at reduced pressures up to 2,000 and reduced temperatures up to 50. The correlations were extended to polar molecules (e.g. ammonia and water) through introduction of effective temperature-dependent critical parameters as suggested originally by Rowlinson [88]. Van der Waal's two fluid model, in conjunction with these charts, have been used to calculate the composition of co-existing phases in the region of gas-gas immiscibility. The approach of Zandbergen et al, as discussed earlier, was used for this purpose. The systems studied were He-Xe (gas-gas immiscibility of the first type) and $C_2H_6-H_2O$ (gas-gas immiscibility of the second type).

Recently Neff and Mcquarrie [89] have utilized the perturbation theory of Weeks, Chandler and Anderson and the various n-fluid corresponding states theories of fluid mixtures to predict gas-gas equilibrium over wide ranges of pressure. It was shown that van der Waal's one fluid theory is the most reliable of the n-fluid mixture theories. Their work indicates that there are actually two factors that determine the critical locus of binary mixtures: the ratio of the well depth of the mixed interaction to the largest well depth of the pure interaction ($\varepsilon_{12}/\varepsilon_{11}$) and the ratio of the molecular diameters (σ_{22}/σ_{11}). As ($\varepsilon_{12}/\varepsilon_{11}$)

becomes larger, the region of gas-gas equilibrium decreases and as $(\sigma_{22}/\sigma_{11})$ increases, the region of gas-gas immiscibility increases. A series of figures in reduced co-ordinates allows the critical locus of any binary mixture to be predicted from the appropriate intermolecular potential parameters of the pure components.

Rowlinson and Teja [85] have utilized the principle of corresponding states and its extensions to predict critical points and critical end points in binary and ternary mixtures. The calculation procedure involves the use of shape factors to account for the deviation from the simple corresponding states principle. It was found that the predictions are in good agreement for mixtures which do not deviate too far from conformality with the reference substance. Since the principal aim of the present work is to test the model proposed by Rowlinson and Teja in case of (fluorocarbon + hydrocarbon) mixtures, the method is discussed in detail subsequently.

Thermodynamics of Critical States

A critical state for a system of m components which obeys a classical equation of state, can be defined in terms of the molar Helmholtz free energy (A) and its derivatives with respect to volume and (m − 1) mole fractions.

It can be shown that a critical point is defined by two equations. These equations can be derived by first considering a one component system. For such a system the thermodynamic conditions for equilibrium can be demonstrated by a plot of Helmholtz free energy (A) against volume at constant temperature as shown in Figure 3.2(a) together with the corresponding plot of pressure against volume at constant temperature shown in Figure 3.2(b).
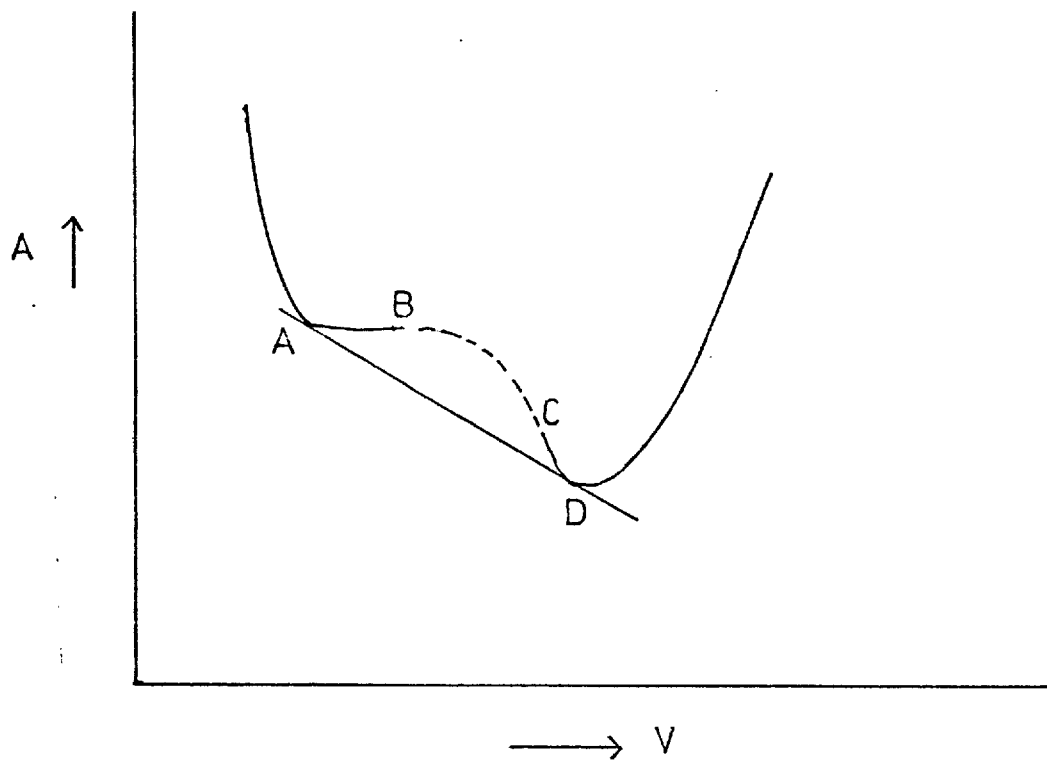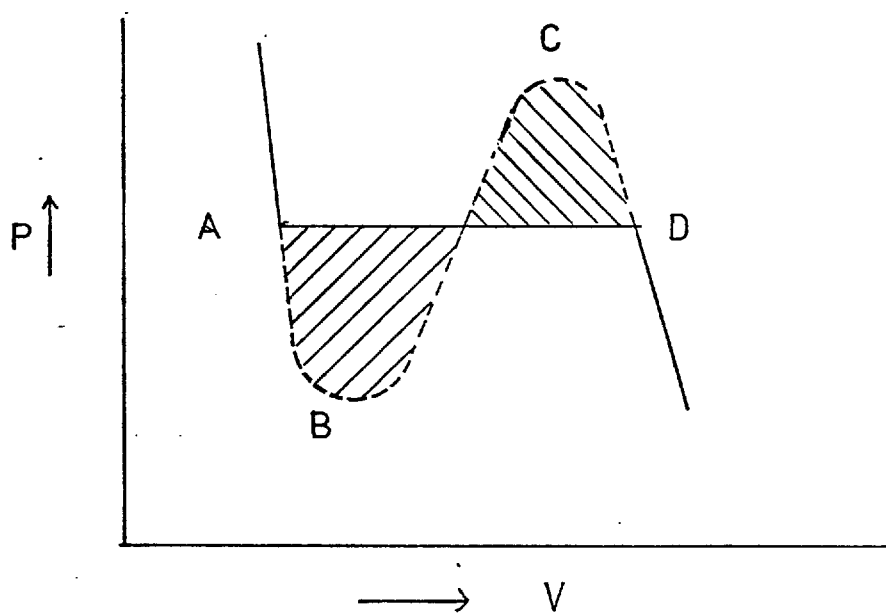
FIGURE 3.2(a): PLOT OF A AGAINST VOLUME

FIGURE 3.2(b): PLOT OF PRESSURE AGAINST VOLUME

Thermodynamic states for the co-existing vapour and liquid phases lying between A and D (Figure 3.2(a)) are unstable and since there are unstable states within the saturation boundary in the immediate vicinity of the critical point, it follows that the critical point must lie on the boundary between the stable and unstable regions. This provides one condition for the critical point. The second condition is that variations along the critical isotherm must be stable.

Münster [90] has generalized these two conditions for a system of m components and has come up with a set of homogeneous linear equations which has a solution only if the determinant of the coefficients vanishes.

Let $A(ix,jy)$, where x, y can be v or x_k, denote the derivative $(\delta^{i+j}A/_{\delta x^i \delta y^j})$. If the determinant "D" is defined by

$$D = \begin{vmatrix} A(2v) & A(v,x_1) & \text{------} & A(v,x_{m-1}) \\ A(x_1 v) & A(2x_1) & \text{-------} & A(x_1,x_{m-1}) \\ \vdots & & & \vdots \\ A(x_{m-1},v) & \text{------------} & & A(2x_{m-1}) \end{vmatrix}$$

and D' is defined as the determinant formed from D by replacing any row by

$$D(v) \quad D(x_1) \cdots \cdots \cdots D(x_{m-1})$$

(D(v) being the derivative of the determinant with respect to v and so on), then the equations for the critical point are:-

$$D = 0 \quad \text{and} \quad D' = 0 \tag{3.1}$$

For a binary system equation (3.1) can be written as

$$D = \begin{vmatrix} A_{2v} & A_{xv} \\ A_{xv} & A_{2x} \end{vmatrix} = 0 \quad \text{and} \quad D' = \begin{vmatrix} D_v & D_x \\ A_{xv} & A_{2x} \end{vmatrix} = 0 \qquad (3.2)$$

where

$$D_v = \begin{vmatrix} A_{3v} & A_{xv} \\ A_{x2v} & A_{2x} \end{vmatrix} + \begin{vmatrix} A_{2v} & A_{x2v} \\ A_{xv} & A_{2xv} \end{vmatrix}$$

and

$$D_x = \begin{vmatrix} A_{x2v} & A_{xv} \\ A_{2xv} & A_{2x} \end{vmatrix} + \begin{vmatrix} A_{2v} & A_{2xv} \\ A_{xv} & A_{3x} \end{vmatrix} .$$

Equations (3.2) can be written explicitly as

$$A_{2x} - SA_{xv} = 0 \qquad (3.3)$$

and

$$A_{3x} - 3A_{2xv}S + 3A_{x2v}S^2 - A_{3v}S^3 = 0 \qquad (3.4)$$

where $S = (A_{xv}/A_{2v})$

Equations (3.3) and (3.4) can be solved to obtain two of the critical constants v^c, T^c, x^c when one is specified. Composition was chosen as the independent variable and equations (3.3) and (3.4) were solved for v^c and T^c, P^c being calculated from an equation of state.

Prediction of Helmholtz Free Energy (A)

It was shown in the previous section that in order to solve equations (3.3) and (3.4) a knowledge of the Helmholtz free energy (A) of a mixture is required. This may be obtained from the principle of corresponding states and its extensions.

In its simplest form the principle of corresponding states postulates that the surface $\frac{P}{P_c} = f\left\{\frac{v}{v_c}, \frac{T}{T_c}\right\}$ is the same for all members of a given set of substances. It is equivalent to saying that the thermodynamic properties of a substance, α, can be calculated from those of a reference

substance "O" and the critical constants $v_\alpha{}^c$ and $T_\alpha{}^c$.

In terms of Helmholtz free energy A:

$$A_\alpha (v,T) = f \; A_O \left\{ \frac{v}{h_{\alpha\alpha}}, \; \frac{T}{f_{\alpha\alpha}} \right\} - RT \ln h_{\alpha\alpha} \qquad (3.5)$$

where

$$f_{\alpha\alpha} = \frac{T_\alpha{}^c}{T_O{}^c} \quad \text{and} \quad h_{\alpha\alpha} = \frac{v_\alpha{}^c}{v_O{}^c} \qquad (3.6)$$

This simple form of the corresponding states principle has the following limitations:-

a) The substances, in question, must be conformal. The inert gases e.g. Ar, kr, Xe have spherical molecules and these form an example of the conformal set of substances.

b) This law is applicable only to pure substances. Various methods have been proposed for overcoming these difficulties.

1. Extension_to_non-conformal_substances

The corresponding states treatment may be extended to non spherical molecules by the introduction of Pitzer's acentric factor [91] which is defined by:-

$$\omega = - \log_{10} (P^R) - 1.00 \qquad (3.7)$$

The reduced saturation pressure (P^R) being measured at a reduced temperature of 0.7. It is believed that the factor "ω" accounts for the deviation from conformality between the substances "α" and "O". The three parameter law of corresponding states which results may be defined as:-

$$\frac{P}{P_c} = f \left\{ \frac{v}{v_c}, \; \frac{T}{T_c}, \; \omega \right\} \qquad (3.8)$$

Alternatively Leland and his colleagues [92] have introduced shape factors $\theta_{\alpha\alpha}$ and $\phi_{\alpha\alpha}$ to account for the deviations from conformality, which are defined by:-

$$f_{\alpha\alpha} = (T_\alpha{}^C/T_o{}^C) \; \theta_{\alpha\alpha} \qquad\qquad (3.9)$$

$$h_{\alpha\alpha} = (v_\alpha{}^C/v_o{}^C) \; \phi_{\alpha\alpha} \qquad\qquad (3.10)$$

These shape factors are slowly varying functions of the volume and temperature which accounts for the deviations of the scaling parameters from the ratios of critical constants.

Leach [92] has derived the following empirical correlations for the shape factors of hydrocarbons relative to methane as the reference substance.

$$\theta_{\alpha\alpha} = 1 + (\omega_{\alpha\alpha}-\omega_{oo})\left\{0.0892-0.8493 \ln T_\alpha{}^R + (0.3063-0.4506/T_\alpha{}^R) \right.$$
$$\left. (v_\alpha{}^R-0.5)\right\} \qquad\qquad (3.11)$$

$$\phi_{\alpha\alpha} = \frac{(z_o{}^C)}{(z_\alpha{}^C)} \left[1 + (\omega_{\alpha\alpha}-\omega_{oo})\{0.3903(v_\alpha{}^R-1.0177)-0.9462 \right.$$
$$\left. (v_\alpha{}^R-0.7663)\ln T_\alpha{}^R\}\right] \qquad (3.12)$$

where the acentric factor of methane $\omega_{oo} = 0.005$ and $v_\alpha{}^R$ and $T_\alpha{}^R$ are the reduced volume and reduced temperature for the substance "α".

$$v_\alpha{}^R = v/v_\alpha{}^C \qquad\qquad (3.13)$$

$$T_\alpha{}^R = T/T_\alpha{}^C \qquad\qquad (3.14)$$

Equations (3.11) and (3.12) are applicable for values of $T_\alpha{}^R$ such that $0.6 \leqslant T_\alpha{}^R \leqslant 1.6$.

2. Extension to mixtures

The simplest way to extend the principle of corresponding states to mixtures is to assume that configurational free energy (A_m) of a mixture can be replaced by that of a single equivalent substance plus an ideal mixing term.

This can be represented mathematically as follows:-

$$A_m(v,T,x_\alpha) = A(v,T,x_\alpha) + RT\sum_\alpha x_\alpha \ln x_\alpha \qquad (3.15)$$

where $A(v, T, x_\alpha)$ is the Helmholtz free energy for the equivalent substance and can be related to that of the reference substance as:-

$$A(v, T, x_\alpha) = f \, A_o \left\{ \frac{v}{h}, \frac{T}{f} \right\} - RT \ln h \qquad (3.16)$$

This approximation is known as "one fluid" model. Two and multi fluid models have been proposed by Bett et al [91] and Leland, Rowlinson and Sather [93], but since there is no reason to believe that these are superior to one fluid model, the latter was used for prediction purposes.

Various approximations have been proposed for the evaluation of f and h for the equivalent substance. Rowlinson [94] prefers the one used originally by van der Waal which states that

$$h = \sum_\alpha \sum_\beta x_\alpha x_\beta h_{\alpha\beta} \qquad (3.17)$$

$$fh = \sum_\alpha \sum_\beta x_\alpha x_\beta f_{\alpha\beta} h_{\alpha\beta} \qquad (3.18)$$

The cross terms $f_{\alpha\beta}$ and $h_{\alpha\beta}$ can be obtained from a modified form of Lorentz and Berthelot rules which give:-

$$f_{\alpha\beta} = \xi_{\alpha\beta} (f_{\alpha\alpha} f_{\beta\beta})^{\frac{1}{2}} \qquad (3.19)$$

$$h_{\alpha\beta} = \eta_{\alpha\beta} \{ \frac{1}{2} (h_{\alpha\alpha}^{\frac{1}{3}} + h_{\beta\beta}^{\frac{1}{3}}) \}^3 \qquad (3.20)$$

where $\xi_{\alpha\beta}$ and $\eta_{\alpha\beta}$ are adjustable parameters which may be estimated from available experimental data.

Equations (3.15) to (3.20) provide a route for the prediction of Helmholtz free energy (A) of a mixture from that of a reference substance and the parameters $f_{\alpha\beta}$ and $h_{\alpha\beta}$ if these parameters are constants i.e. shape factors are unity. However, if the substances are not conformal, the shape factors are to be taken into account and under these circumstances the reduced volume and temperature are

given by:-

$$v_\alpha^R = (v\phi_{\alpha\alpha}/v_o^C h) \qquad\qquad (3.21)$$

$$T_\alpha^R = (T\theta_{\alpha\alpha}/T_o^C f) \qquad\qquad (3.22)$$

The equations for "f" and "h" can be written as:-

$$f_{\alpha\alpha}\{T,v,x_\alpha\} = (T_\alpha^C/T_o^C)\ \theta_{\alpha\alpha}\left\{\frac{T\theta_{\alpha\alpha}}{T_o^C f}\ ,\ \frac{v\phi_{\alpha\alpha}}{v_o^C h}\right\} \qquad (3.23)$$

$$h_{\alpha\alpha}\{T,v,x_\alpha\} = (v_\alpha^C/v_o^C)\ \phi_{\alpha\alpha}\left\{\frac{T\theta_{\alpha\alpha}}{T_o^C f}\ ,\ \frac{v\phi_{\alpha\alpha}}{v_o^C h}\right\}\ .\ (3.24)$$

and solved iteratively.

Calculation for the Reference Fluid

The corresponding states approach assumes a complete knowledge of the thermodynamic properties of a reference substance "O". Rowlinson and Watson [94] have shown that the molar Helmholtz free energy for the reference substance can be written as:-

$$A_o(v,T)\ /RT = -\ln v - 1 - \int_\infty^V (Z-1)\ \frac{dv}{v} \qquad (3.25)$$

Methane was used as a reference substance and the equation of state proposed by Vennix and Kobayashi [95] was used to solve equation (3.25).

It is clear that equation (3.25) can be used together with equations (3.15) to (3.24) to obtain the Helmholtz free energy of a mixture, which, in turn, can be used in equations (3.2), (3.3) and (3.4) to obtain the critical volume (v_c) and the critical temperature (T_c). The critical pressure (P_c) can then be calculated from an equation of state. The following method of computation is based on the work of Rowlinson and Teja [85] and may be used to predict the critical properties of a fluid mixture.

Method of Computation

The following informations are assumed available:-

a)   An equation of state such as that proposed by Vennix and Kobayashi [95] for the reference substance, Methane.

b)   The critical constants T^c, p^c, z^c and Pitzer's acentric factor "ω" for each component and for the reference substance. They are listed in Appendix 2.

On the basis of the above information the cross parameters $f_{\alpha\beta}$ and $h_{\alpha\beta}$ are calculated from equations (3.19) and (3.20). These parameters given in Table 6 have been obtained by the one fluid model.

c)   In addition, the shape factors $\theta_{\alpha\alpha}$ and $\phi_{\alpha\alpha}$ are determined from equations (3.11) and (3.12). The cross factors $\theta_{\alpha\beta}$ and $\phi_{\alpha\beta}$ appear only in the combinations $f_{\alpha\beta}$ and $h_{\alpha\beta}$ and hence are eliminated by equations (3.19) and (3.20).

Steps in Computation

1.   The composition vector for the critical point to be computed is set.

2.   A guess is made for the critical temperature and critical density. (The density is used instead of volume because Vennix equation for Methane is written in terms of the density.)

3.   First estimates of f and h are obtained by putting shape factors equal to unity (equations (3.23), (3.24), (3.19), (3.20), (3.17) and (3.18)).

4.   First estimates of v^R and T^R are obtained from equations (3.21) and (3.22) by setting shape factors (θ and ϕ) equal to unity. From these values of v^R and T^R, the shape factors are calculated using equations (3.11) and (3.12).

5.   These values of ϕ and ϕ are used to obtain new values of "f" and "h" until the values of θ, ϕ, f and h are consistent

with the initial choice of T and P.

6. All derivatives of f and h up to third order in $\underline{x}$ and P are calculated for the given value of T, P and $\underline{x}$. These derivatives are obtained by the analytical differentiation of equations (3.17) and (3.18).

7. Given T, P, $\underline{x}$, f, h and the derivatives obtained in step 6, the extended principle of corresponding states is used to obtain "A" for the mixture and all its derivatives in $\underline{x}$ and P. The steps involved are as follows:-

    a) The Holmholtz free energy (A_O) of the reference substance is obtained by solving equation (3.25). The equation of state proposed by Vennix and Kobayashi was used for this purpose.

    b) The Helmholtz free energy (A) of the mixture is calculated by using equations (3.15) and (3.16).

    c) The Helmholtz free energy (A) is differentiated analytically to give derivatives up to third order in $\underline{x}$ and P. The mathematical procedure involved in this operation is given in Appendix 4.

8. From a knowledge of the derivatives obtained in 7(c), the determinants D and D' (equation (3.2)) are evaluated at the known values of T, P and $\underline{x}$.

9. The sum of the squares ($D^2 + D'^2$) is minimized with respect to the variables T and P using Powell's method [96].

10. At the minimum D=0 and D'=0, hence the minimum gives the critical point of the mixture (T^C, P^C) at the set composition $\underline{x}^C$.

11. The critical pressure (P^C) is computed from a knowledge of T^C, P^C, x^C, f and h from an equation of state.

12. The composition vector x^C is varied to obtain critical points at other compositions.

Table 6

System	$\xi_{\alpha\beta}$	$\eta_{\alpha\beta}$	$\xi_{\alpha\beta}^*$ (obtained by Prausnitz)[84]
$CH_4-C_2H_6$	1.00	1.06	0.99
$CH_4-n-C_{10}H_{22}$	0.80	0.94	(0.84)
$C_2H_6-n-C_3H_8$	1.00	0.97	1.00
$C_2H_6-n-C_{10}H_{22}$	0.94	0.88	(0.94)
CO_2-CH_4	0.95	1.00	0.93
$CO_2-n-C_5H_{12}$	0.80	1.00	0.80
$CO_2-C_2H_4$	0.94	1.00	0.94

CHAPTER 4

A BRIEF REVIEW OF THE EXPERIMENTAL METHODS USED TO INVESTIGATE GAS-GAS IMMISCIBILITY

The methods used for investigating gas-gas immiscibility are essentially the same as those used for gas-liquid equilibrium. Hala [97] has discussed these techniques and in general, the methods can be divided into four categories:-

a)   Analytic Method

A vessel is charged with the substances under investigation and the temperature and pressure of the heterogeneous (two phase) region are adjusted and maintained at the required values. After equilibrium is reached by suitable stirring, samples of the different phases are withdrawn and analyzed at normal or moderate pressure. The samples should be small so that the resulting reduction in pressure when the samples are withdrawn does not cause a large disturbance to the equilibrium. This so called analytic method enables several isotherms to be investigated with one filling of the vessel only. However, the method should not be used near the critical or barotropic regions where the phases are of similar density. Since separation of the phases in these regions is difficult, this may lead to the introduction of analytical errors.

b)   Synthetic Method

A gas-liquid mixture of known composition is charged into a vessel and pressure and temperature in the homogeneous region are adjusted to the required values. Pressure is varied at constant temperature or vice versa until the homogeneous mixture separates into two phases. Usually the

presence of a second phase is determined by visual observation of turbidity or the formation of a meniscus through a window in the wall of the vessel. This is the so called synthetic method. This method is used only for measurements near the critical region; barotropic systems can also be studied. However, visual observation of those systems which are iso optic is impossible.

c)   Discontinuity in the First Derivative of PVT Properties

A constant mass of a mixture of known composition is confined in a vessel. Of the three variables pressure (P), temperature (T) and volume (v), one is varied and the effect on a second value is measured whilst the third is maintained constant. For convenience it is customary to measure pressure as a function of volume at constant temperature but in principle the volume or the pressure could be held constant whilst the other variables are changed. The conditions under which a phase transition occurs may be detected by a discontinuity in the slope of one variable when plotted against other.

Although this method has been used extensively for liquid-solid systems to identify the solid phase boundary, its use in liquid gas system has been very restricted [23] because it is difficult to apply at or near critical condition.

d)   Partition Chromatography

A gas elutant which may be either a single component or a binary mixture, but which is appreciably soluble in the liquid phase maintained on the column matrix material, can be used to form a multicomponent liquid phase within a chromatographic column. From elution data, the vapor-liquid equilibrium ratios or k values can be calculated by expressions relating the solute retention volume to the

solute k value in the vapor-liquid system maintained within the chromatographic column.

This technique has advantages over the other methods in that it offers a direct way for measuring infinite dilution data. It is suitable for non-volatile liquids. However, this method is not well suited for studying highly volatile solutes because of the error present in the measurement of column void volume if a thermal conductivity detector is used. k value information is required for the lightest component of the elution gas mixture.

These methods are discussed in detail subsequently.

Analytic Method

The analytic method has been used extensively by many workers particularly the Russian scientists [98] to investigate the phase equilibria. The special feature of the apparatus used by the Russians is the mercury piezometer into which a mixture of known composition is admitted. The pressure and temperature in the piezometer are adjusted so that the two phases are formed. Then upper phase is displaced at constant pressure by a mercury piston and analyzed. When all the upper phase has been removed, the heavier phase is forced out and analyzed. While sampling, the pressure is kept constant by continuously pumping mercury into the piezometer. This equipment cannot be used at temperatures above 200°C because of the increasing solubility of mercury in the compressed gas and mercury-free equipment has to be used.

A similar method has been used by Rogers and Prausnitz[99], Mcketta[100], Lindros and Dodge[7], Kennedy[101], Street[102], and others.

The problems in using the analytic method are twofold:-

a)   Firstly the problem of designing an efficient mechanism to ensure that equilibrium between phases is established, and

b)   Secondly the problem of sampling the phases without disturbing the equilibrium conditions.

Methods for Attaining Equilibrium

Basically three methods are used for stirring a two phase mixture to bring the phases into equilibrium. These involve the use of rocking mechanisms, mechanical or magnetic stirrers and circulation of vapor through the liquid.

Rocking mechanisms have been used by Krichevskii and his colleagues [98], and Mcketta [103]. The usual arrangement is to mount the equilibrium vessel in a bath which, in turn, is supported on blocks and connected to a mechanism designed to rock both the cell and the bath. This procedure is an inefficient way of stirring the contents of the pressure vessel. Furthermore, flexible pipes have to be used to connect the pressure vessel with the rest of the apparatus and there is always the possibility of a fatigue failure in the flexible pipe which may have to withstand repeated large strains.

Stirring has been frequently used to attain equilibrium. To avoid the difficult problem of sealing a rotating shaft against high pressure, magnetic agitators have been used by several authors [99, 102]. Tsiklis [98] used a stirrer actuated by a solenoid placed inside the pressure vessel. There are two drawbacks to this arrangement. Firstly, the heat generated by the solenoid disturbs the isothermal conditions in the system and secondly, the additional space taken up by the solenoid increases the dimensions of the pressure vessel.

To overcome these difficulties, Lindroos and Dodge [7]

encased the top of the stirrer shaft in a head of non-
magnetic material, so that the solenoid could be located
externally, as shown in Figure 4.1. When the solenoid
was switched on and off, the piece of soft iron attached
to the stirrer shaft moved up and down inside the pressure
vessel, so that the ensuing oscillating motion mixed the
two phases. A similar arrangement was employed by Reynolds[104],
in which a large permanent magnet was rotated around the
outside of the non-magnetic vessel head. The magnetic flux
of the rotating permanent magnet caused a smaller magnet
placed inside the head and to which was attached a stirrer
shaft to rotate.

It is very difficult to obtain permanent or electro-
magnets which are sufficiently strong to stir viscous
material and hence this method is limited to mobile fluids.

A further factor associated with stirring (mechanical
and magnetic) is the optimum diameter and wall thickness
of the pressure vessel. In the design of pressure vessel
it is customary to make the internal diameter of the vessel
small relative to the length, so as to reduce the required
wall thickness, but the small area of contact between the
two phases results in a long time being taken for equilibrium
to be attained. If on the other hand the internal diameter
of the vessel is increased so as to increase the contact
area the wall thickness of the vessel is correspondingly
increased and this makes it difficult to stir the contents
of the vessel using a magnet located on the outside surface.
A small electric motor used to drive a stirrer shaft may
be placed inside the vessel [105] but the heat dissipated
by the motor makes it difficult to maintain isothermal
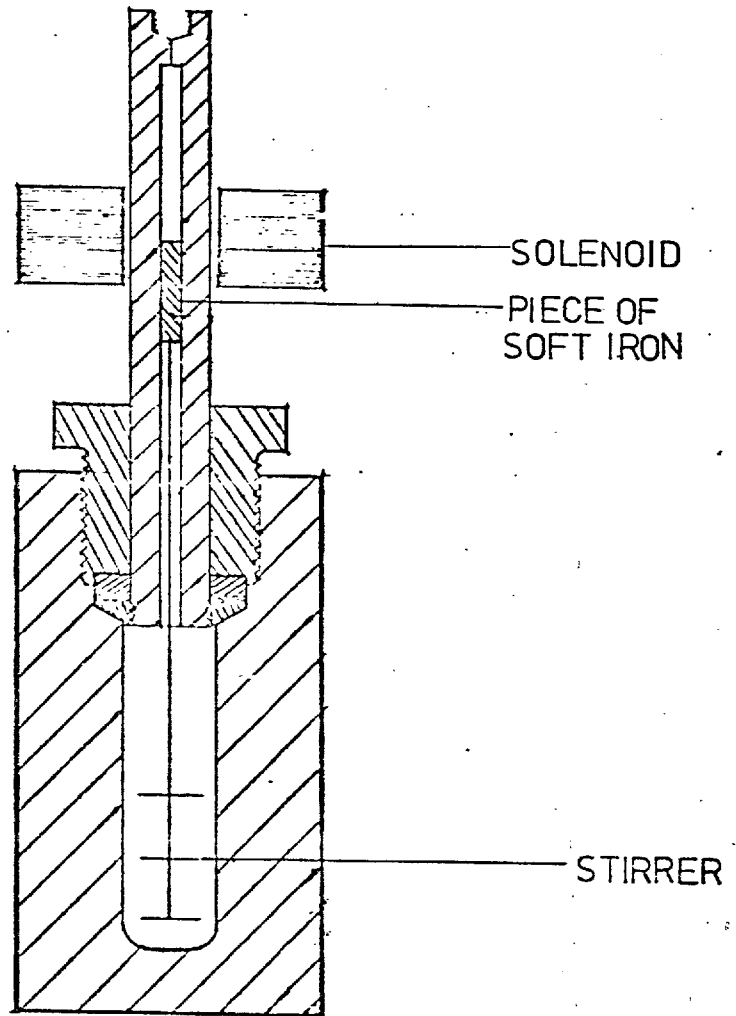conditions. Furthermore the arrangement is limited to those

FIGURE 4.1: SKETCH SHOWING MAGNETIC STIRRER (7)

fluids which do not attack the electrical insulation on the wiring in the motor.

The vapor circulation method of attaining equilibrium has been used by Michels [106], Roberts and Mcketta [107], Dodge and Dunbar [108], Streett [109] and others. In essence this method consists of continuously withdrawing the lighter phase from the top of the vessel and passing it through the heavier phase at the bottom of the vessel. Although the procedure results in an increased contact area between the two phases which allows equilibrium to be established rapidly, the saturated vapor is subjected to small pressure variations caused by the mechanical operation of the circulating pump and hence its composition may vary slightly at various part around the circulation loop. This may be of some importance if as is usually the case, the sample of the lighter phase is taken from the circulation loop whilst that of the heavier phase is taken from the vessel. Since it is very difficult to seal a rotating shaft against high pressure the circulation pump has to be sealed inside a casing fabricated from non-magnetic stainless steel and actuated by a permanent magnet placed outside the casing.

Reynold [104] used both magnetic stirring as well as circulation for the attainment of equilibrium as shown in Figure 4.2. The apparatus consisted of a pressure vessel (E) in which two fluid phases were well mixed by a magnetic stirrer (A). Whilst the contents of the pressure vessel were being stirred, the lighter phase was circulated around the system by a magnetically operated circulating pump (B). A hot wire anemometer (C) was used to ensure that the lighter phase is being continuously circulated through the
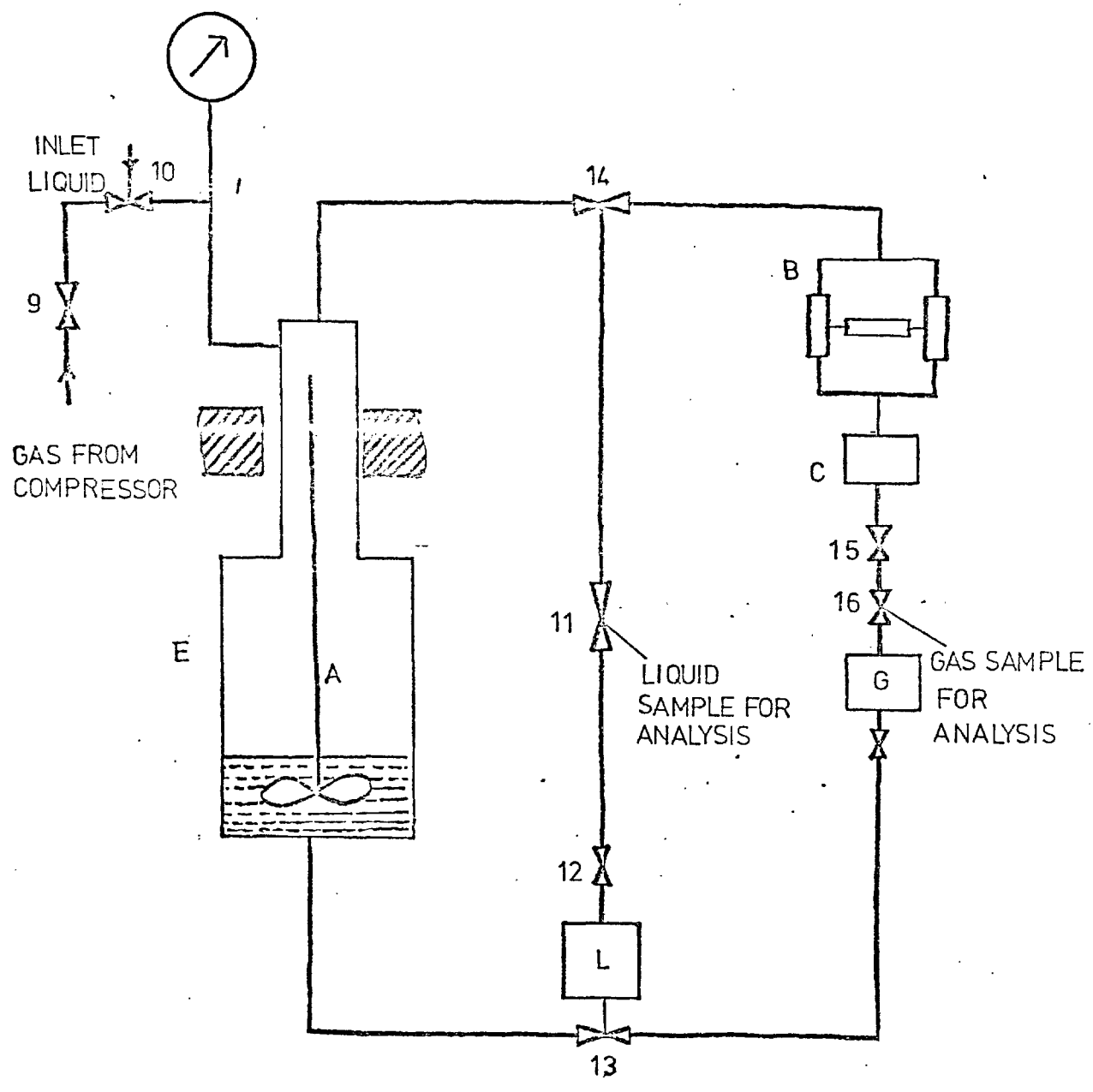
INLET
LIQUID

10

GAS FROM
COMPRESSOR

9

14

B

C

15

16

11

LIQUID
SAMPLE FOR
ANALYSIS

GAS SAMPLE
FOR
ANALYSIS

G

E

A

12

L

13

FIGURE 4.2: SCHEMATIC DIAGRAM OF EQUILIBRIUM CELL (104)

heavier phase under high pressure conditions.

Sampling of the Phases

Various methods have been proposed for the sampling of the two phases so that the equilibrium is not disturbed. Mcketta [103], in their equipment, maintained constant pressure by pumping mercury into the equilibrium cell while sampling the phases. Although this approach is convenient, the solubility of mercury in compressed gases lead to error particularly at high temperatures.

Tsiklis [98] compensated for the drop in pressure during sampling by injecting more of the liquid component. The change in total composition of the mixture (brought about by this process) influences only the relative amount of the two phases, but it does not influence the composition of the phases so long as the total composition of the mixture is within the limits of the heterogeneous equilibrium.

Rogers and Prausnitz [99] have used what they describe as a sample extruder as shown in Figure 4.3. The equipment consists of a sampling system which moves samples from the equilibrium cell to the low pressure analysis system via two sets of moving pistons A and B encased within a movable sampling framework (C). Each set of pistons, one for liquid and the other for gas, contains two pistons between which there is a variable volume. While framework (C) moves horizontally, this variable volume comes into contact with the analysis system and the sample (both liquid and gas) expands through the capillary tubing into the low pressure zone.

Streett and others [109] solved the problem of pressure drop by isolating both phases (gas and liquid phase) in the external portion of the loop so that equilibrium cell

TO LOW PRESSURE ANALYSIS SYSTEM

VAPOUR SAMPLE PISTONS [A]

MAGNETIC STIRRER

MOVING SAMPLING FRAMEWORK [C]

LIQUID SAMPLE PISTONS [B]

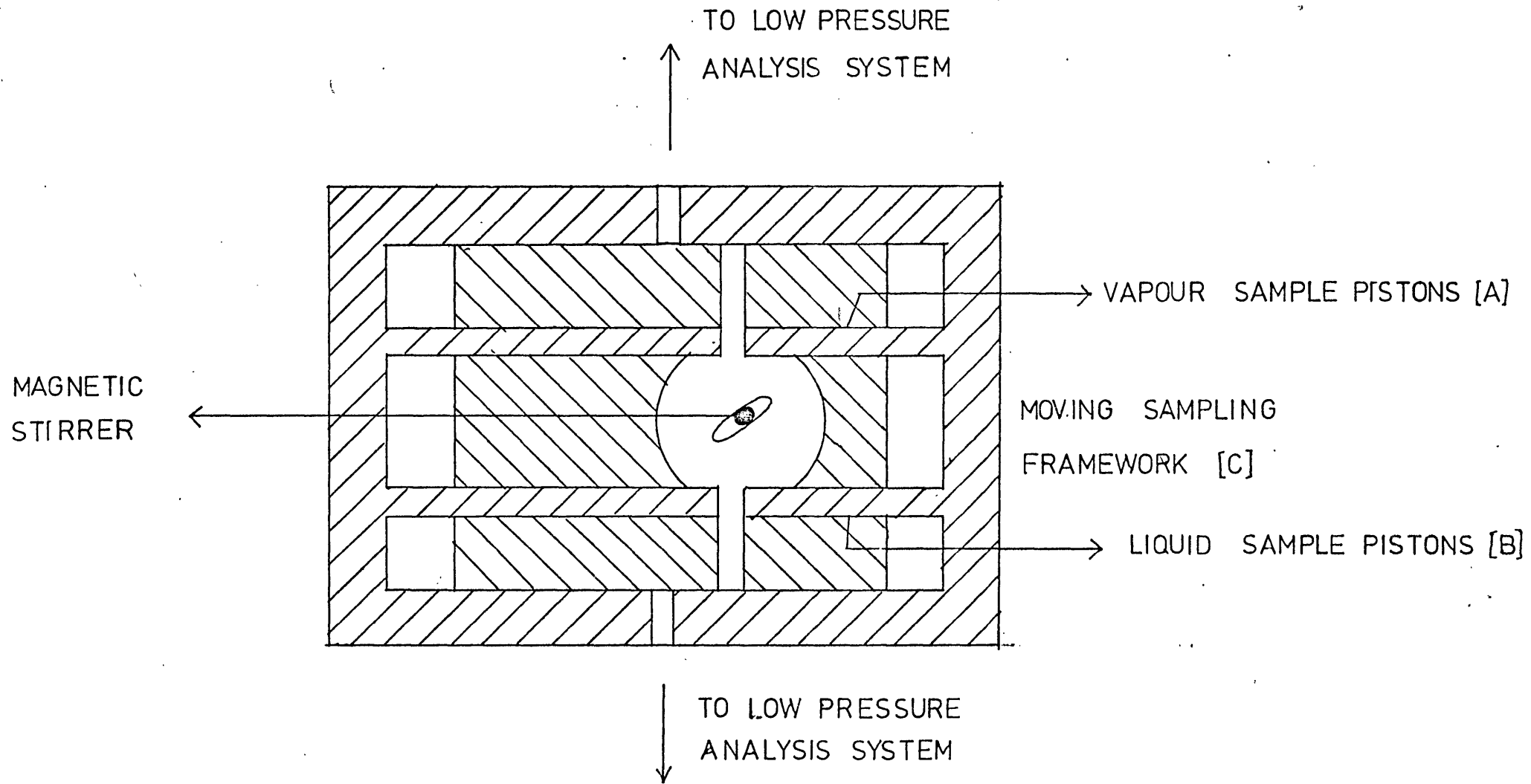TO LOW PRESSURE ANALYSIS SYSTEM

FIGURE 4.3: EQUILIBRIUM CELL AND SAMPLING SYSTEM (99)

was not disturbed during sampling.

This procedure may be illustrated by reference to Figure 4.2. After attainment of equilibrium in vessel E, the lighter phase is isolated in vessel G, by closing valves 15 and 17 and then removed for analysis through valve 16. Simultaneously the heavier phase is allowed to flow under gravity into sampling vessel, L, by opening valve 13, valves 12 and 14 being open. Thus when the valves 12, 13 and 14 are closed the heavier phase is isolated in L. The tubing between 14 and 12 is evacuated and the heavier phase is taken in the tubing between 14 and 12 by opening valve 12. The sample is then removed for analysis through valve 11.

Synthetic Method

This method has been extensively used by De Swaan Arons and Diepen [10], Schneider and his colleagues [110], Lentz [111] and others. The principle of all these methods is the same as that discussed earlier and may be illustrated by the apparatus used by De Swaan Arons and Diepen to study gas-gas immiscibility in helium-xenon system up to a pressure of 2000 atm. and a temperature of $65^{\circ}C$.

The apparatus used by De Swaan Arons and Diepen [10] is shown in Figure 4.4.

The fluid mixture of known composition is enclosed in a glass piezometer (3) mounted in a pressure vessel (1). It is separated from the pressure transmitting medium water (7) by mercury (5). The appearance or disappearance of the meniscus in the upper capillary tube of the piezometer caused by a change in the pressure and/or temperature may be observed through two windows (2). The mixture is stirred by a small permanent magnet (11) which is pushed up and down
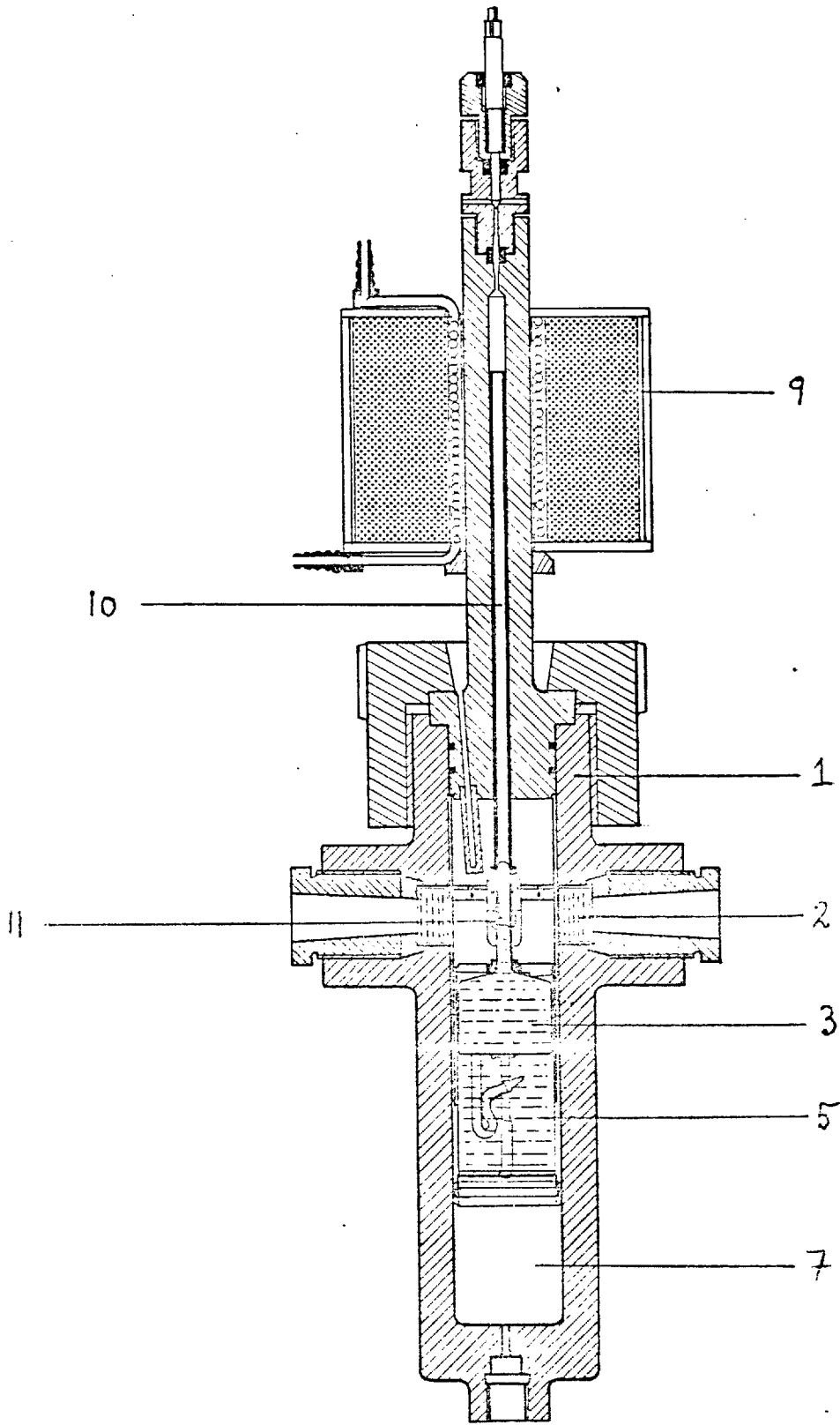
FIGURE 4.4:   APPARATUS USED BY DIEPEN

from outside the piezometer by a second permanent magnet
fastened at the lower end of an iron tube (10) actuated by
a magnetic solenoid (9).

Gas-Liquid Partition Chromatography (G.L.P.C.) Method

In gas-liquid partition chromatography a non-volatile
liquid phase is fixed on the surface and in the pore space
of an inert, porous solid support. This solid support
containing liquid is packed into a column through which a
gas phase is caused to flow. A solute which distributes
itself between both phases is injected into the column
and eluted by the gas phase. In this way a vapor-liquid system
is established within the packed column composed of the
mobile elution gas, the immobile liquid on the column
packing material and the solute being eluted through the
column. From the elution data, vapor-liquid equilibrium
ratios or k values may be calculated from the solute
retention volume and the solute k values for the vapor-
liquid system maintained within the chromatographic
column.

A schematic diagram of the experimental apparatus
used [112] for determining vapor-liquid equilibrium by
G.L.P.C. is shown in Figure 4.5. The apparatus is similar
to a conventional G.L.P.C. unit used in analytical work
except that tubing, fittings, etc. are designed for use
at high pressure. Pressure regulation in the G.L.P.C. column
was achieved with a sensitive diaphragm pressure regulator (A)
whilst small gaseous samples were injected into the
elution gas stream at high pressure through sample valve B.
The flow rate through the column and the reference side of
the system was adjusted by small needle valves (C and D)
which served not only to control the flow rate but also

THERMAL
CONDUCTIVITY
CELL

DIFFERENTIAL
PRESSURE GUAGE

GAS CYLINDER

CONSTANT
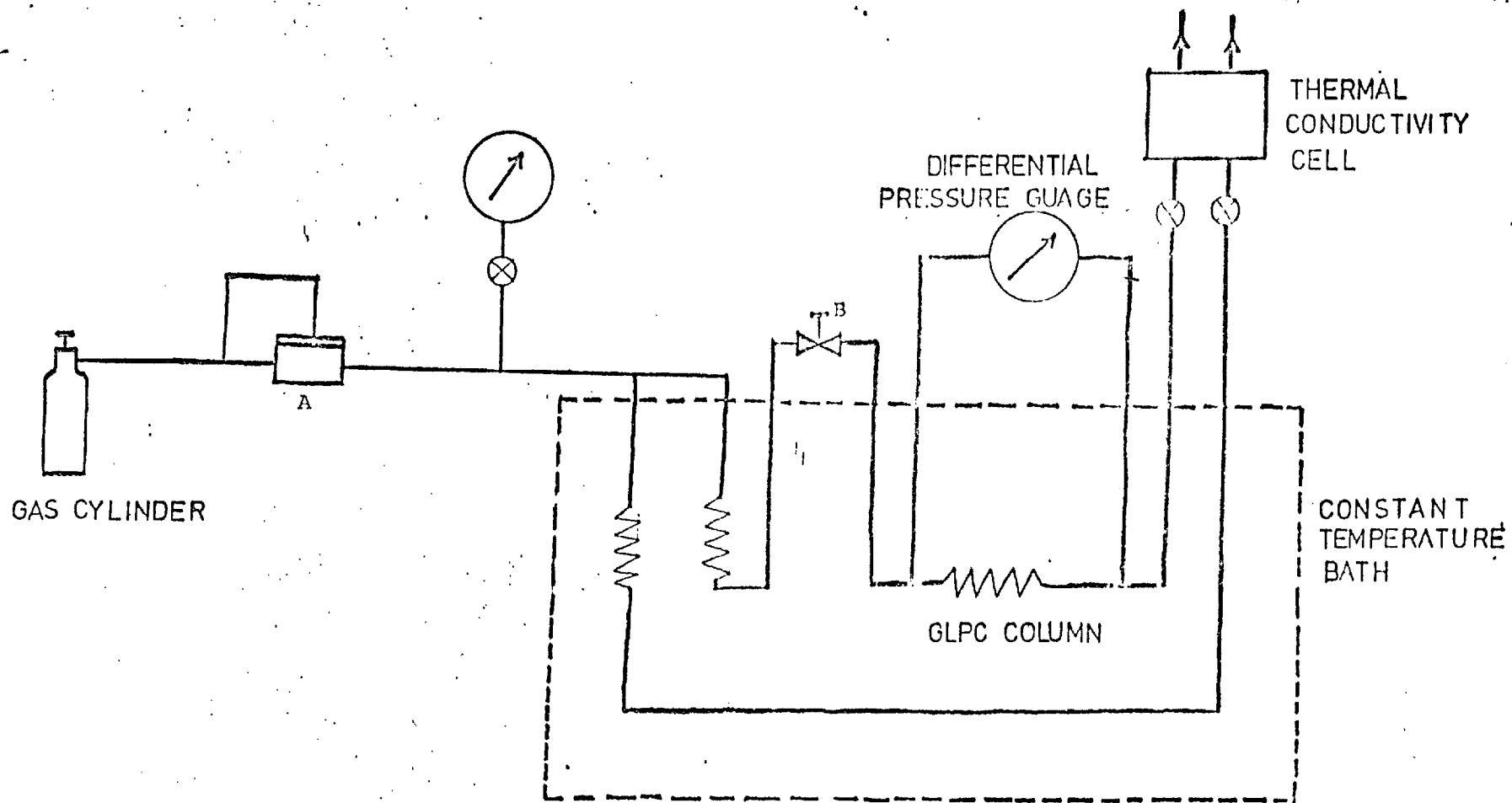TEMPERATURE
BATH

GLPC COLUMN

FIGURE 4.5:   SCHEMATIC DIAGRAM OF GLPC APPARATUS

to reduce the elution gas pressure to atmospheric so that
a conventional hot wire thermal conductivity detector
could be employed.

CHAPTER 5

DESCRIPTION OF APPARATUS

An apparatus was designed to measure gas-liquid equilibrium over a pressure range of 30 to 700 atm. at temperatures between 0 and 100°C. In essence the apparatus consists of an equilibrium cell in which two fluid phases are mixed by a magnetically operated stirrer. The cell is provided with two diametrically opposite sapphire windows in order to observe the position of the gas-liquid interface. A sampling probe (through which both liquid and gas phases are withdrawn separately for analysis) is located in the field of view and both the gas and liquid phases are sampled in turn by raising or lowering the position of the interface relative to the sampling probe by means of two pistons moved by oil pressure.

The apparatus consists of four main parts:-

a) A compressor, used to deliver gas at pressures up to 700 atm.

b) A pump and intensifier, used to deliver pressure transmitting fluid at pressures up to 700 atm.

c) The equilibrium cell which enables equilibrium to be attained between the two fluid phases.

d) Equipment for the analysis of samples withdrawn from the equilibrium cell.

Each of these major components will be described in detail.

The Gas Compressor

The compressor used in this work is of the mercury piston type and was supplied by W.C.T. Hart and Z.N. Holland. The operation of this type of compressor may be followed

by reference to Figure 5.1. Oil (mixture of liquid paraffin and paraffin oil to prevent the oil from freezing at a temperature of 0°C and a pressure of 700 atm.) from reservoir, A, is pumped by hand pump, B, to the compression cylinder, E, via mercury trap, D, the three way valve, 1, being used to release pressure. Valve, 3, acts as the inlet valve to the compression cylinder, F, and valve, 4, is the outlet valve for the compressed gas. Bourdon tube gauge, C, indicates the oil pressure which is the same as that of compressed gas.

The gas to be compressed is introduced, usually at storage cylinder pressure, into compression cylinder, F, through valve, 3, until the mercury piston has displaced oil from cylinder, E, through valves 2 and 1 into reservoir A. Oil is then pumped into cylinder, E, through valves 1 and 2 to force mercury into compression cylinder, F, thereby compressing the gas confined above the mercury. The high pressure gas is introduced into the equilibrium cell by opening valve 4. If after opening valve 4 the pressure reached in the equilibrium cell is not sufficiently high, the compression cylinder, F, is recharged and after compression, the gas is admitted to the equilibrium cell. This process is continued until the required pressure is built up.

To avoid displacement of mercury through the inlet and outlet valves (valves 2 and 4 respectively) the compressor must be provided with some means to indicate the position of the mercury piston. Usually an electrical device is employed for this purpose but in this instance the simple expedient of calibrating the position of the mercury column in compression cylinder, F, against the
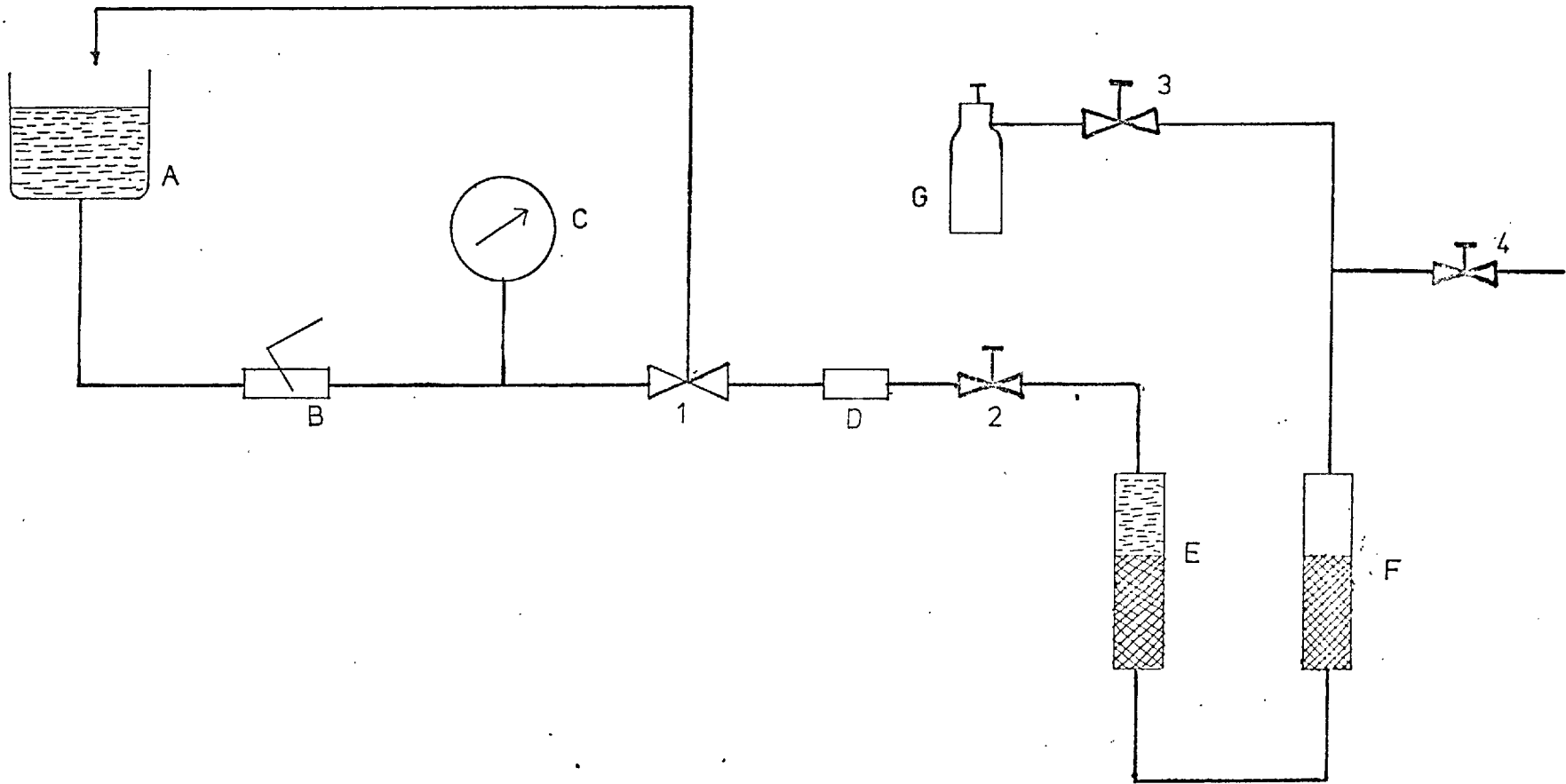
FIGURE 5.1: SCHEMATIC DIAGRAM OF GAS COMPRESSOR

OIL

MERCURY

GAS

position of the oil level in reservoir, A, was used.
The compression stroke was discontinued when the oil level
in the reservoir fell to the position corresponding to
maximum permitted mercury level in cylinder, F. Similarly
when the compressor was being charged with gas, the oil
level was only permitted to rise to a position corresponding
to the maximum permitted mercury level in cylinder, E.

A general arrangement drawing of the gas compressor
used is shown in Figure 5.2. This differs from that
illustrated in schematic diagram (see Figure 5.1) in that
the two cylinders A and B are arranged one above the other
and connected together with a valve block C. Gas at cylinder
pressure is introduced into the compression cylinder, A,
through inlet valve, I. Oil from the reservoir is pumped
into the compression cylinder, B, through valve, F, and
displaces mercury from cylinder, B, through the tube, R, into
cylinder, A, in which the gas is compressed. When the
required pressure is reached, the gas is introduced into
the apparatus through the outlet valve, H.

Mercury piston compressors are widely used in the
laboratory for compressing small quantities of gas, since
the only moving parts likely to fail are confined to
the hand pump. However, there are a few practical
difficulties with this equipment. Bridgeman [113] found
that steel in contact with high pressure mercury may be
embrittled and thereby fail if the pressure is sufficiently
high. The cause of failure was attributed to diffusion of
mercury into steel through very small cracks and the
subsequent formation of an amalgam thereby causing
embrittlement. However torsional fatigue tests carried
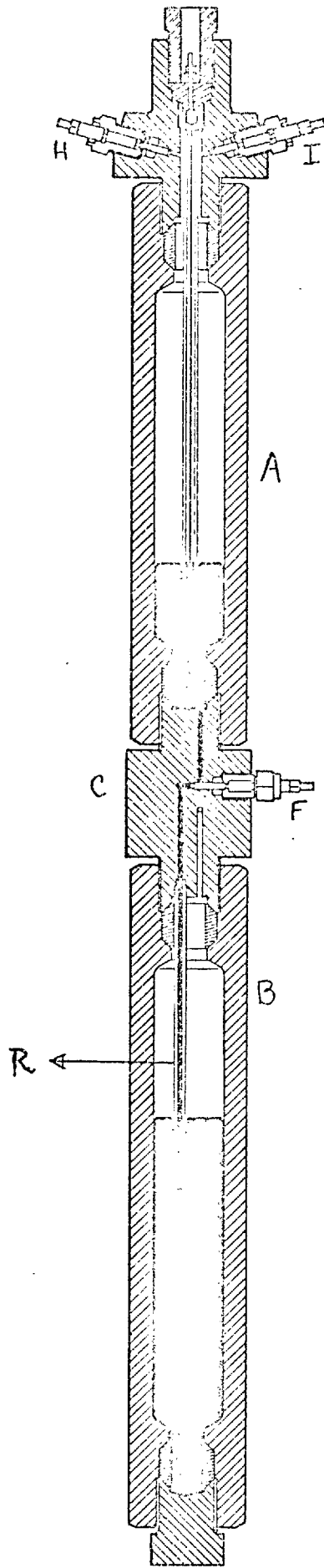out on steel in contact with mercury at high pressure

FIGURE 5.2:   ARRANGEMENT OF GAS COMPRESSOR

showed that mercury attack is unlikely to be a problem at pressures up to 3000 atm.

Another difficulty of this type of compressor is that oil tends to seep past the mercury piston and contaminate the compressed gas. This is caused by the fact that mercury does not wet the walls of the vessel whereas oil does. Bett and Reynold [114a] have pointed out that rate of oil seepage is a function of the bore surface finish of the steel cylinder in contact with mercury and care must be taken to avoid scratches on the surface if seepage is to be avoided. In practice care was taken to remove the small quantities of oil which seeped past the mercury piston from time to time.

Pressure Intensifier

A schematic diagram of the oil pump and pressure intensifier which provides high pressure oil to move the pistons in the equilibrium cell is shown in Figure 5.3. Oil from reservoir, A, is pumped using hand pump, B, via valve, 1, to the low pressure side of intensifier, I, whilst valves 2, 3 and 4 are closed. Pressure P_1 acting on the low pressure side of the piston of area A_1 gives rise to a force P_1A_1 which is balanced by the higher pressure, P_2, acting on the piston, M, of smaller area A_2. Thus, to a first approximation, the pressure intensification ratio P_2/P_1 is equal to A_1/A_2, the ratio of the area of the low pressure piston to that of the high pressure piston. The intensifier used in this work had a pressure intensification factor of 15 and this enabled very fine control to be exercised over the oil pressure admitted to the equilibrium cell.

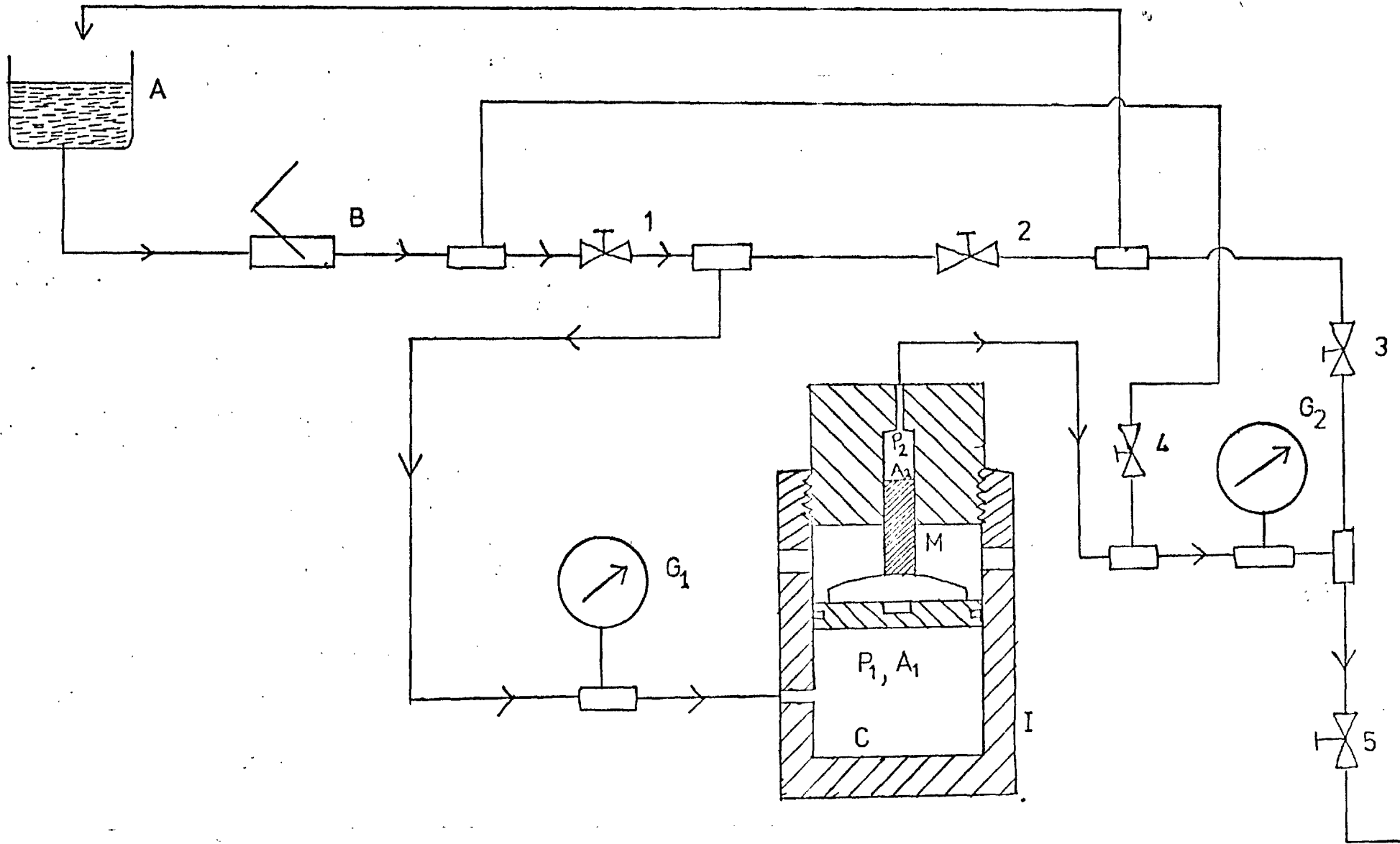When the piston is at the end of its stroke, it is

FIGURE 5.3: SCHEMATIC DIAGRAM OF PRESSURE INTENSIFIER

88

returned to its initial position by closing valve, 1,

(see Figure 5.3) and opening valves 2 and 4 so that when

oil is pumped to the high pressure side of the intensifier,

it forces the piston down and displaces oil from the

low pressure side into reservoir, A. When the piston comes

down to the lowest level valves 2 and 4 are closed and

1 opened.

Equilibrium Cell

The equilibrium cell is that part of the apparatus

where the binary fluid-fluid mixture is brought to

equilibrium. A schematic diagram of the equilibrium cell

and its associate pipework is shown in Figure 5.4.

Sectional side and plan views of the equilibrium

cell are shown in Figures 5.5 and 5.6 respectively. The

pressure vessel which forms the body of the cell is

fabricated from stainless steel, is 16.5 cm long,

has a bore diameter of 3.25 cm, a wall thickness of 1.7 cm

and an internal volume with both pistons as far apart

as possible of approximately 94 cm^3. The joints between

the pressure vessel and the two screwed end-caps are

pressure sealed by means of an o-ring and an anti-extrusion

ring. The pressure vessel is provided with two movable

pistons. The upper piston (see Figure 5.5) is made of

stainless steel sleeved with screwed aluminium bronze

rings. The area between the two aluminium bronze rings is

pressure sealed against the bore of the vessel, which was

honed to give a surface finish of 8 micro inches, by an

o-ring located between two PTFE rings. This piston is

drilled through the centre and connected to a 0.635 cm O.D.

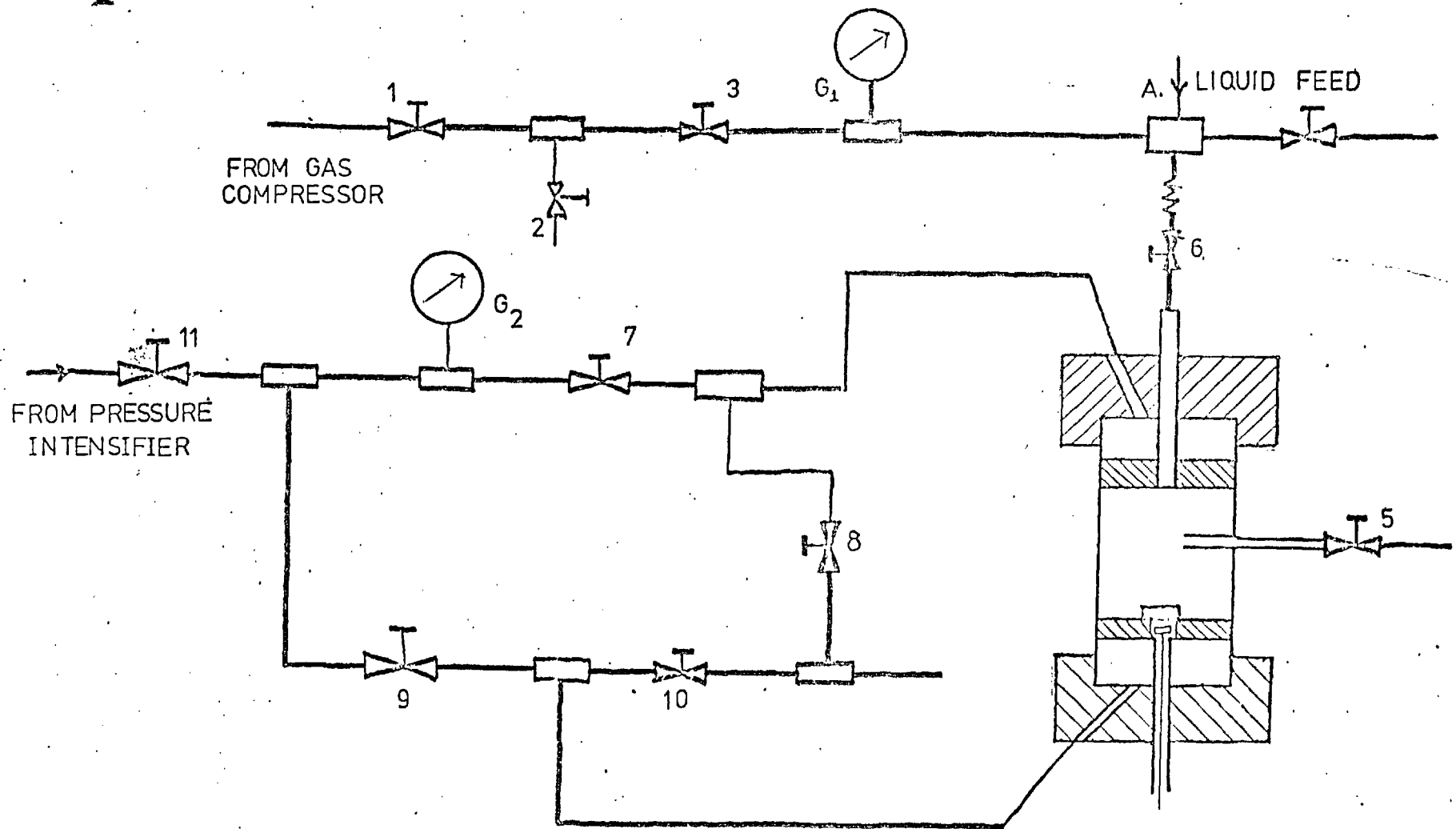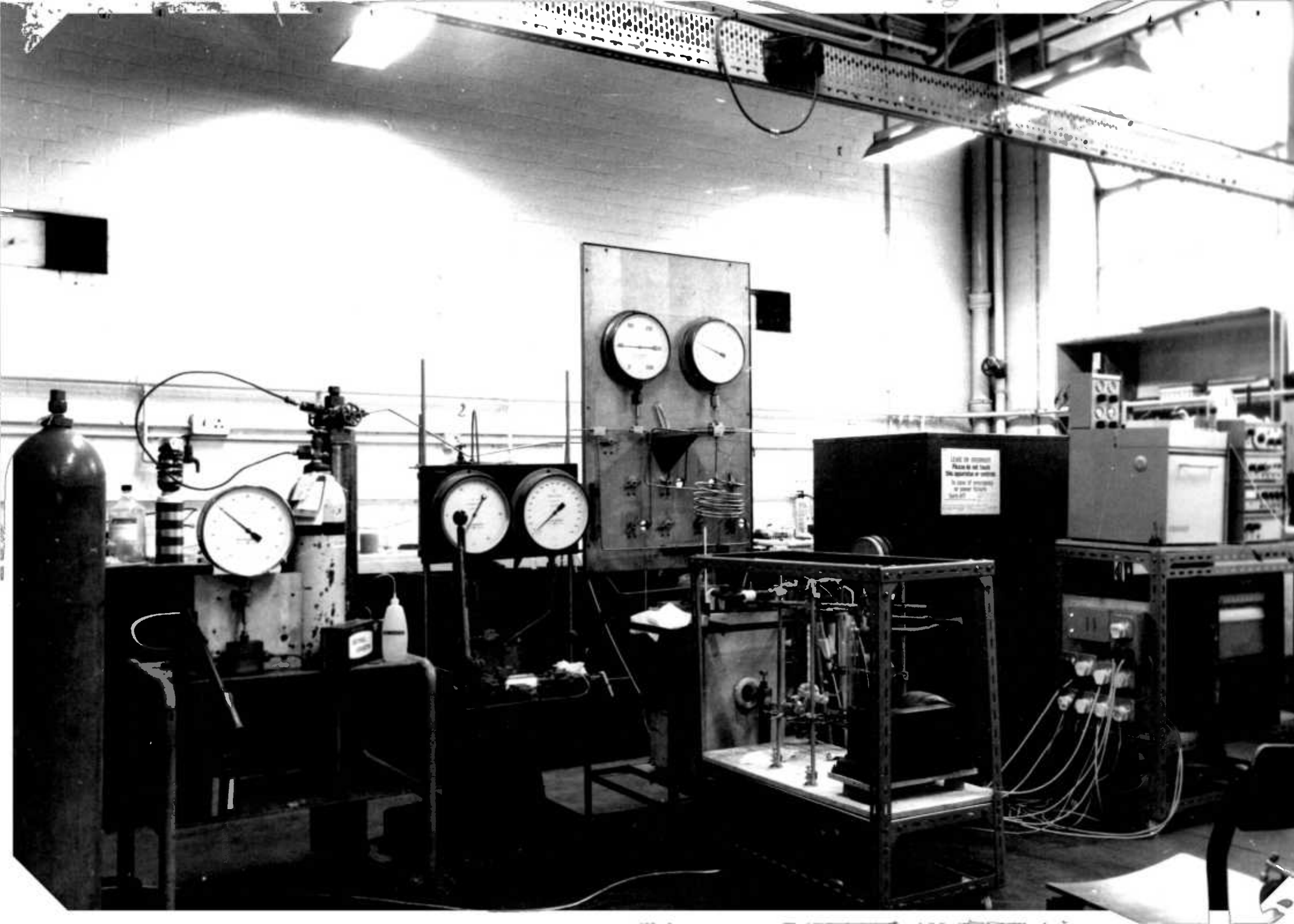stainless steel tube with a screwed joint sealed by hard

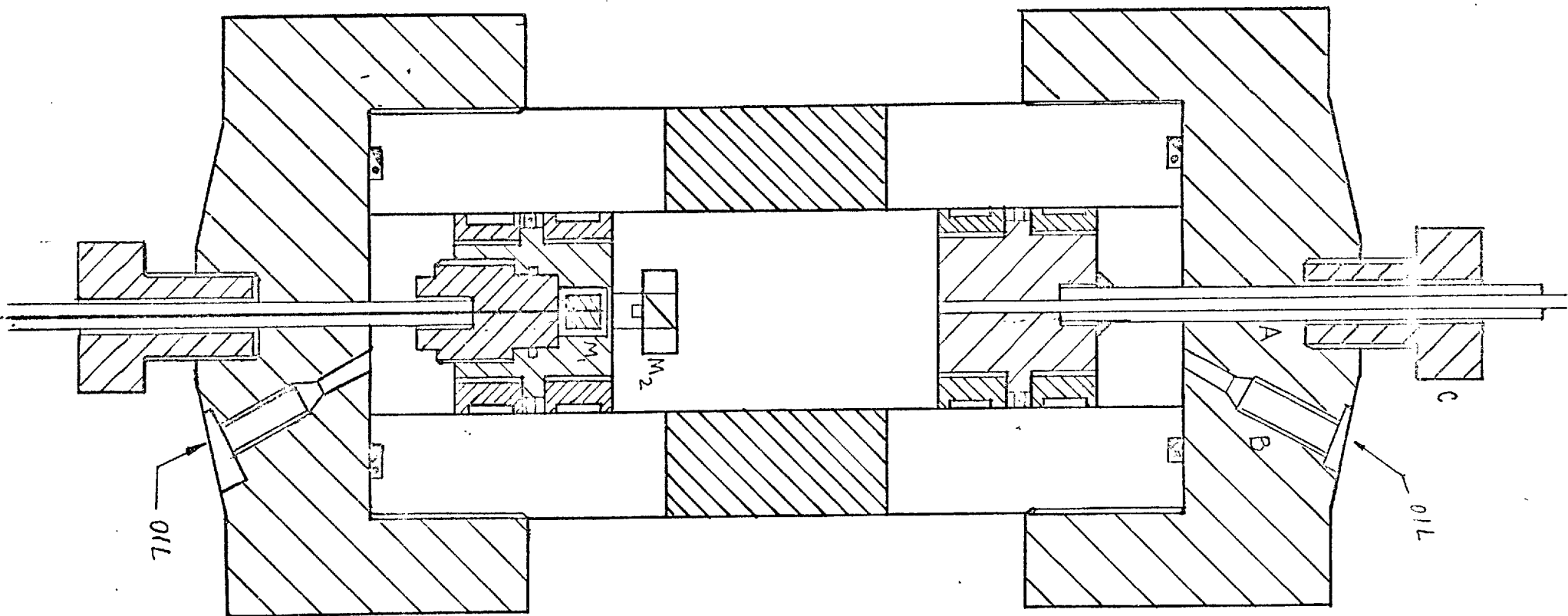FIGURE 5.4:   SCHEMATIC DIAGRAM OF EQUILIBRIUM CELL

FIGURE 5.5: Sectional front view of the pressure vessel

solder. The tube passes through the central hole, A,
in the upper screwed end-cap and is sealed with two
o-rings and a PTFE ring held in place with a gland nut C.
The end of the stainless steel tube is connected to the
gas supply line also of stainless steel but coiled so that
the piston can be moved freely when oil is admitted through
inlet B.

The lower piston (see Figure 5.5) is of similar
construction to the upper one except that it is provided
with a recess to accommodate a permanent magnet, M_1,
connected to a shaft which is rotated by an electric
motor geared to run at 300 r.p.m. As magnet, M_1,
rotates, so a second permanent magnet (M_2) resting on the
piston surface and to which is attached a four bladed brass
propeller also rotates so providing stirring inside the
vessel. The thickness of the diaphragm separating M_2 and
M_1 had to be kept small to achieve high magnetic flux
yet sufficient to prevent permanent distortion as a result
of the stress induced by the internal pressure.

In order to observe the gas-liquid interface the
equilibrium cell is provided with two diametrically opposite
sapphire windows (each 1.9 cm diameter x 1.27 cm thick)
arranged as shown in Figure 5.6. The sapphire windows,
held in place by the gland nuts, C, are pressure sealed by
means of o-rings and two anti-extrusion rings, shown in
detail in Figures 5.7(a) and 5.7(b). The anti-extrusion
ring on the outer side of the o-ring is made of copper
whereas the inner one is made of brass. The inner anti-
extrusion ring prevents the o-ring from distortion when
pressure is released from the apparatus. A lamp is placed
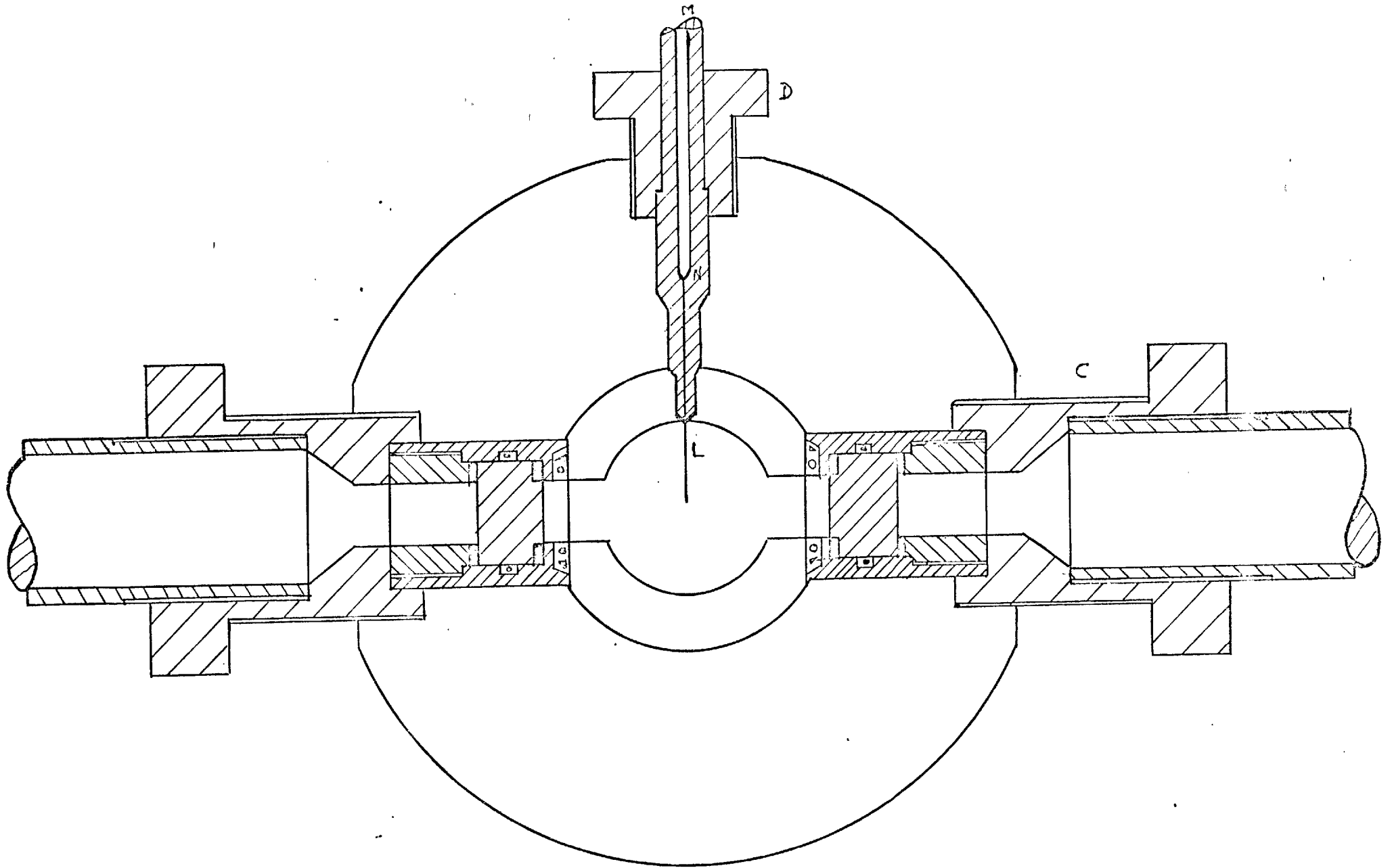adjacent to one of the sapphire window and the gas-liquid

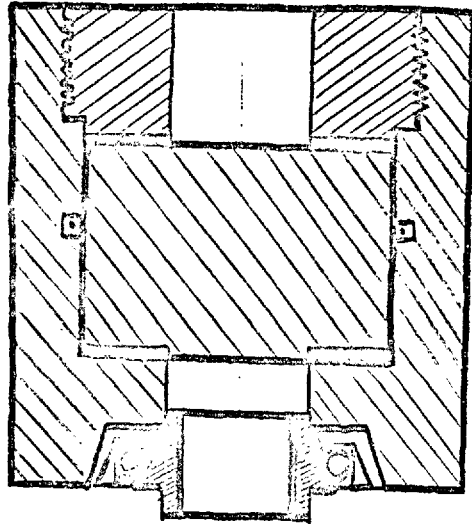FIGURE 5.6 Sectional Top view of the pressure vessel assembly
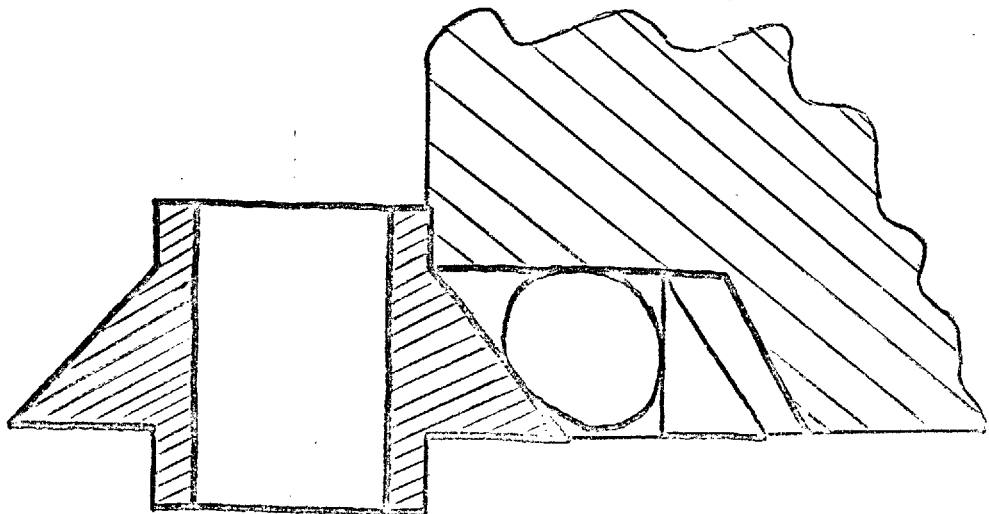
FIGURE 5.7(a): SEALS IN THE WINDOW

FIGURE 5.7(b): ENLARGED DRAWINGS OF WINDOW SEALS

interface was observed through the other window from a remote distance using a periscope.

In order to take samples from the pressure vessel for analysis, the vessel is provided with a sampling probe as shown in Figure 5.6. The sampling probe is held in place by the threaded gland nut D and is sealed against the vessel. In order to minimize the pressure drop in the equilibrium cell during sampling, every effort was made to reduce the internal volume of the sampling tube first by using a stainless steel thin walled capillary tube, L, inside the vessel and secondly by inserting a steel rod of 0.159 cm diameter inside tube MN. By this process the volume of the sampling tube (from the centre of the pressure vessel to the sampling valve) was reduced to 0.09 cm^3. The sampling tube is placed in the field of view through the windows so that the phase being sampled can be identified.

The associated pipework can be divided into two sections, the gas line through which gas-liquid mixture is introduced inside the vessel and the oil line, through which oil is pumped to adjust the position of the pistons (See Figure 5.4). The gas-liquid mixture is confined within the pressure vessel by closing valve 6. Both the oil lines (oil lines for top and bottom piston) are provided with valves 8 and 10 through which oil can be pumped back to the reservoir so that the pistons can be moved to the extreme end positions. Care was taken to ensure that the pistons were not moved far enough to hit the sampling tube which is situated at the centre of the equilibrium cell. Gauge G_1, indicates the gas pressure whereas, G_2, indicates the oil pressure.

The equilibrium cell is mounted in a steel tank of

rectangular shape having dimensions (30.48 cm x 30.48 cm x 60.96 cm) which acts as a thermostatic bath. The tank is provided with coil made of 0.63 cm O.D. copper tubes. Ethylene glycol is circulated from a refrigerator through this coil when the experiment is to be conducted at low temperature of $0^{\circ}C$ or $-2^{\circ}C$. Support for the pressure vessel is provided by two viewing tubes which extend out of the tank through openings in the 'sides of the tank. To facilitate the dismantling of the pressure vessel, the tank is provided with a removable front-panel through the centre of which the sampling tube passes. For higher temperatures ($26-50^{\circ}C$) Shell Tellus 23, which has a low viscosity at $25^{\circ}C$ and fumes to a limited degree at $100^{\circ}C$, is used as the thermostatic liquid inside the tank. When the experiment is conducted at $0^{\circ}C$ or $-2^{\circ}C$, a mixture of water and antifreeze (a specially inhibited blend of methanol and ethylene glycol) is used in the thermostatic bath.

The thermostatic liquid is circulated by a 12.7 cm dia. propeller located near the bottom of the tank and driven by a 118 r.p.m. motor. To avoid vibration, the end of the propeller shaft fits into a bearing located at the bottom of the tank.

Electric motors for both the thermostatic liquid stirrer and the magnetic stirrer are mounted on a plate fixed to the top of the tank. At higher temperatures ($26-50^{\circ}C$) heat is supplied to the oil by an immersion heater having a maximum rating of 1 kw. To prevent carbonization of the oil, the power dissipated by the heater is reduced using a variable transformer. The heater is controlled using an electronic relay, actuated by a

mercury-toluene thermoregulator such that the temperature can be controlled to $\pm$ 0.1^{O}C. The actual temperature of oil is measured by a mercury-in-glass thermometer, calibrated to $\pm$0.1^{O}C. When the apparatus is to be operated at 0°C or -2^{O}C, the refrigerator is switched on and the ethylene glycol is constantly circulated through the copper coil placed in the thermostatic bath. The refrigerator is set at a temperature slightly below that of the bath and the temperature of the bath is controlled to $\pm$0.05^{O}C using an electronic relay actuated by a mercury-toluene regulator. In order to minimize heat loss the tank is provided with a 1.905 cm thick fibre board insulation on all sides.

Before using the equilibrium cell for experimental purposes, it was tested at pressures up to 1000 atm. The testing was divided into two phases:-

a)   Overall pressure testing using liquid paraffin as the pressure transmitting fluid.

b)   Testing of the piston seals using nitrogen as the pressure transmitting fluid.

The piping arrangement used for the overall pressure testing of the equilibrium vessel is shown in Figure 5.8. During assembly of the pressure vessel the two pistons are placed at the extreme end positions. The lower piston containing the stirrer is moved from this position by pumping oil through valves 1 and 5. Similarly the top piston is moved from the extreme position by pumping oil through valves 1 and 4. With valves 4 and 5 closed, oil is pumped into the centre of vessel through valve 2. Oil forces the two pistons outwards but since valves 4 and 5 are closed, pressure builds up in the system. When the pressure registered by gauge, G, reaches 1000 atm., valve, 2,
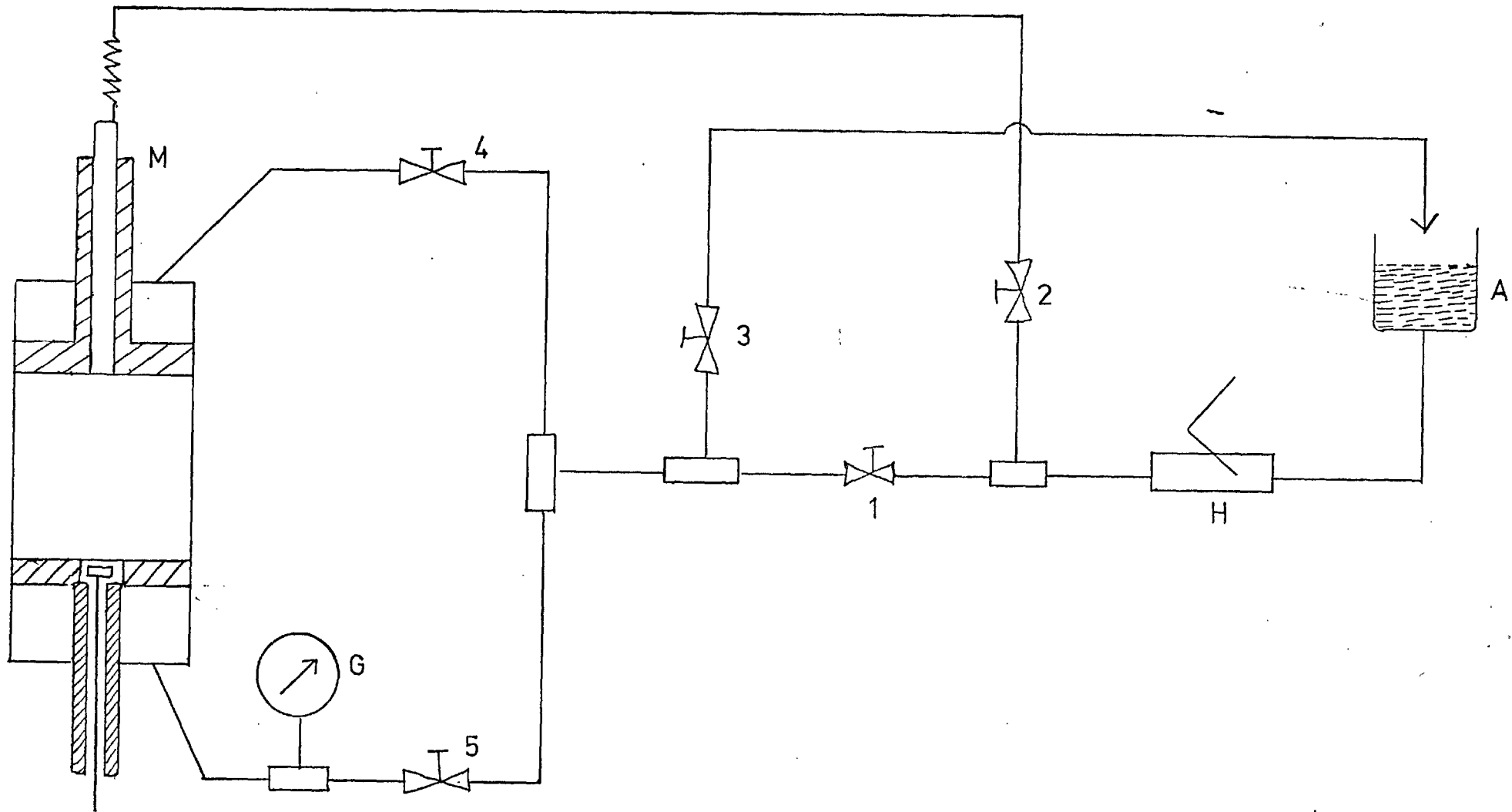
FIGURE 5.8: TEST RIG FOR EQUILIBRIUM CELL

M   4   3   2   A   1   H   G   5

is closed and the system is allowed to stand for about
24 hours to ensure that there is no reduction in pressure
due to leakage.

Since the gas-liquid mixtures studied were confined
between the two hydraulically actuated pistons special
tests were undertaken to ensure that no leakage would occur
across the sealing rings which might result in contamination
of the mixture by hydraulic fluid. The arrangement made
for the test on the piston sealing rings is shown in
Figure 5.9.

In these tests the pistons are kept at the extreme
ends of the vessel. In the case of the test on the upper
piston seal, (see Figure 5.9) the lower end is sealed
by a dummy piston, A, the oil inlet, B, to this end of
the vessel is closed and that to the upper piston, C, is
kept open. Nitrogen at cylinder pressure of 130 atm. is
introduced into the vessel through valve 1. Leakage past
the piston seal was detected by an escape of gas through
oil inlet C. A similar technique was used to test for gas
leakage past the lower piston. It was found from experience
that if the piston seals would withstand a differential
gas pressure of 130 atm. when tested statically, leakage
past the seals when they were made to move under a very
small differential pressure was negligible.

Experimental Set-Up for the Analysis of Gas and Liquid Phases

Both the gas and liquid phases from the equilibrium
cell are analyzed by a Pye series 104 gas chromatograph
fitted with a katharometer detector cell, the output from
which is connected to a Honeywell recorder (Model No.
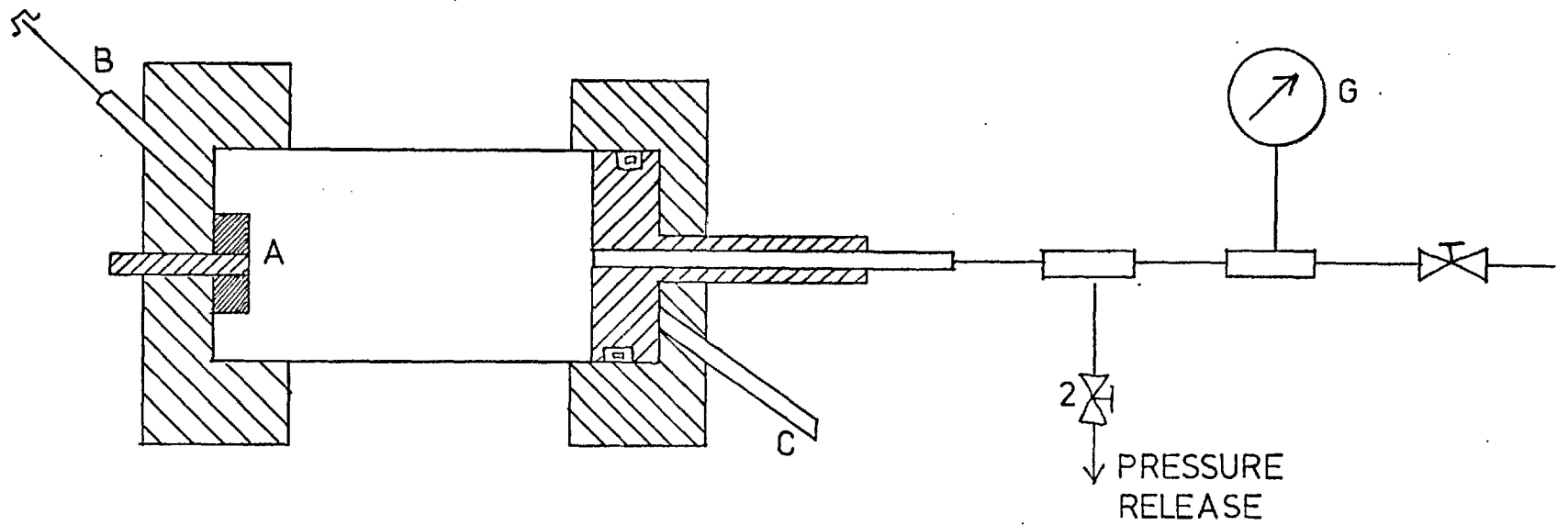y153x18-VH-II-III-118-P14P15). Two columns are used,

FIGURE 5.9:   ARRANGEMENT FOR TESTING UPPER PISTON SEAL

one providing the sample input and the other the
reference input to the katharometer. This arrangement
enables the flow rates through the system to be balanced
and so minimizes the effects of small changes of
temperature. The active column consists of 150 cm length
of 4 mm bore glass tube formed into a coil 17.8 cm in
diameter and packed with Porapak-Q. The column terminates
in two straight sections to facilitate connection to the
detector and injection head which consists of a septum
through which the sample in the vapor phase was injected
by a 0.1-1.0 cm^3 syringe. Before using the column it
was conditioned using the process recommended by Goodfellow
and Weber [114b]. The column is operated at a temperature
of 212°C using Helium as the carrier gas at a flow rate
of 64 cm^3/min.

A schematic diagram of the sampling assembly, in which
samples taken from the equilibrium cell at high pressure
are isolated at low pressure for analysis is shown in
Figure 5.10. In addition to sampling valve, 5, which is
connected to the sample probe within the equilibrium
vessel, the assembly consists of greaseless ball and
cup joint, B, septum, S, (through which the samples are
taken out for analysis) greaseless stopcocks and a
rotary vacuum pump protected by trap, T. The pressure
gauge, P, can be used to read a vacuum.
The line was made as short as possible and in order to
avoid condensation of the liquid phase, it is warmed
by an electrical resistance heating tape, the input to
which is controlled by a variable transformer.

The chromatograph was calibrated using mixtures of
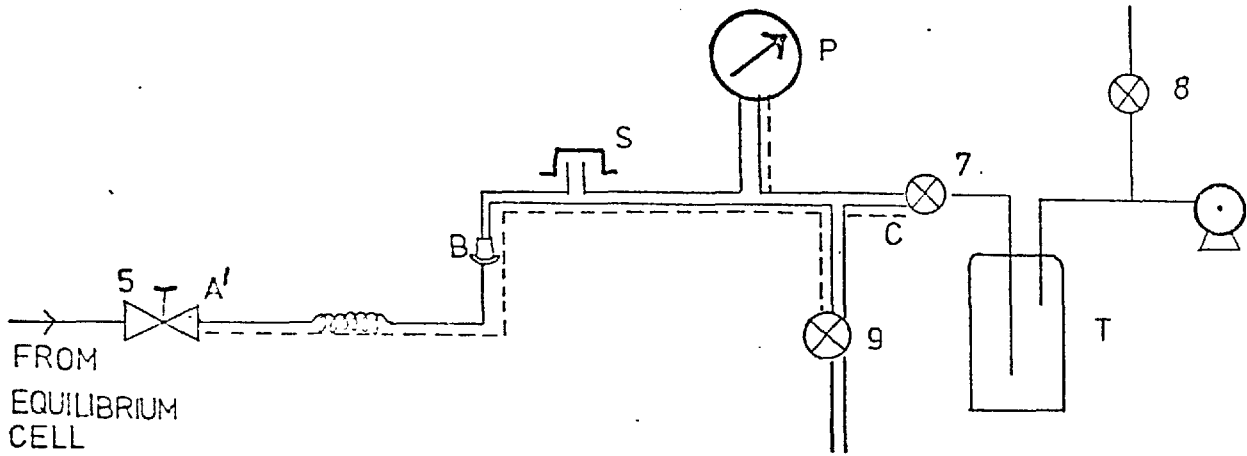known composition with the equipment shown in Figure 5.11.

FIGURE 5.10: SCHEMATIC DIAGRAM OF SAMPLING ASSEMBLY
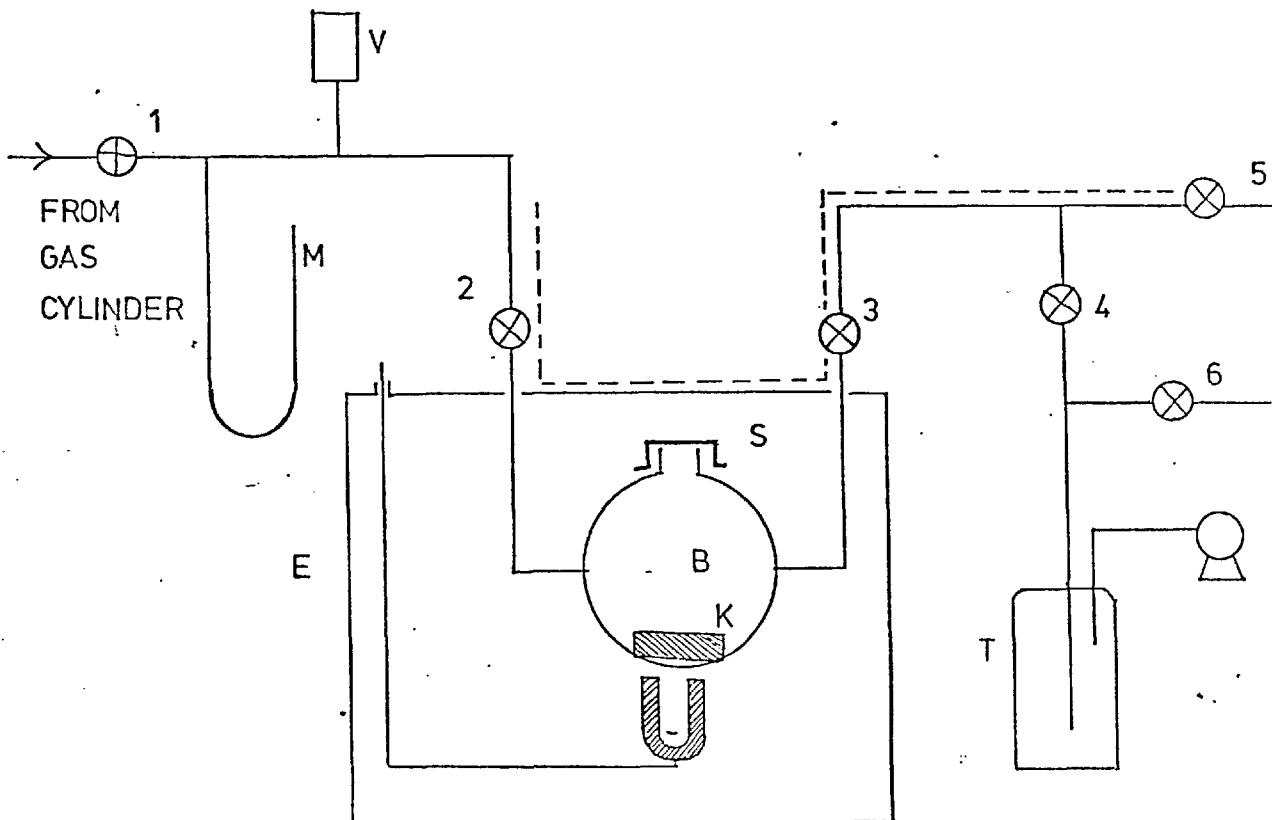(------- signifies heating tape)

FIGURE 5.11: SCHEMATIC DIAGRAM OF THE SET-UP USED TO CALIBRATE
GAS CHROMATOGRAPH

These mixtures were prepared by varying the partial
pressure of the gas and the volume of liquid added to a
250 cc glass bulb , B, so that total pressure of the
vapor phase mixture was 1 atm.

After closing stopcocks 1, 5 and 6 and opening
stopcocks 2, 3 and 4 the apparatus (see Figure 5.11)
was evacuated to 0.1 mm mercury, the pressure being read
on vacustat V. The oven, E, was switched on and sufficient
time was allowed for the temperature set to a value
above the boiling point of liquid in the mixture to attain
a steady value. Stopcocks 3 and 4 were then closed and the
gas from the storage cylinder was introduced into the glass
bulb, B, by opening stopcock 1 until the required pressure
as indicated by the manometer, M, was achieved. Since the
oven is above ambient temperature the pressure increases as
the temperature of the gas increases and sufficient time
was allowed for equilibrium to be established. Stopcock, 2,
was then closed so that the bulb, B, was isolated from the
rest of the apparatus. The required volume of liquid was
introduced into bulb, B, through septum, S, and the
magnetic stirrer, K, was switched on. Sufficient time was
allowed for the liquid to vaporize completely and form a
homogeneous mixture. Samples (0.3 cm^3) of the mixture
of known composition were removed through the septum from
bulb, B, by a syringe maintained at a temperature above
the the boiling point of the heavier liquid and injected
into the chromatograph. This had to be carried out quickly
so that the mixture did not condense in the syringe. Mixtures
ranging from 1 to 92 mole per cent with an estimated accuracy
of $\pm$ 1 mole percent were used to calibrate the chromatograph.
The ratios of the peak areas at various attenuator levels

were plotted against the ratios of the number of moles of the two components in the binary mixture and these plots provided the necessary calibration curves. For a mixture of unknown composition, the ratio of the peak areas was calculated and the corresponding ratio of the number of moles of each component and hence the composition was obtained from the calibration curves.

Accessories

Apart from equilibrium cell, compressor and pressure intensifier, the apparatus contains standard high pressure equipment such as valves, elbow joints, tees, cross, tubings and pressure gauges.

The high pressure tubing used throughout the equipment is made of 316S grade stainless steel and has a dimension of (0.635 cm O.D. x 0.23 cm nominal bore). Standard AMINCO fittings have been used to connect the various parts of the apparatus.

All the elbow joints, tees and crosses are capable to withstand a maximum working pressure of 6500 atm. The high pressure valves are suitable for a maximum working pressure of 3000 atm. An important feature of their design is that the spindle is easily removable so that they may be cleaned whenever necessary.

A total of five bourdon tube gauges have been used in the apparatus, one in the gas compressor, two in the pressure intensifier and two in the equilibrium cell. For reasons of safety each pressure gauge is fitted with a special safety glass.

CHAPTER 6

EXPERIMENTAL PROCEDURE

Operation of the Gas Compressor

Initially the mercury level in compression
cylinder, F, (see Figure 5.1) is set at its highest position
so that the oil level in reservoir, A, is at its lowest
position. Gas is introduced into the compression cylinder, F,
at cylinder pressure by opening valve, 3, and so displaces
oil into reservoir, A. When the oil level in A is at its
highest position valve, 1, is closed and when the pressure
indicated by bourdon tube gauge, C, attains cylinder gas
pressure, valve, 3, is closed and oil from reservoir, A,
is pumped into compression cylinder, E, through valve, 2.
The oil displaces the mercury which, in turn, compresses
the gas, the pressure of which is monitored by bourdon
tube gauge, C. When the desired pressure is reached, gas
is allowed to pass directly into the equilibrium cell by
opening valve, 4.

If the pressure of the compressed gas in the equilibrium
cell is not sufficiently high, the compression cylinder is
recharged and after compression the gas is admitted to the
equilibrium cell. This process is continued until the
required pressure is built up.

Operation of the Equilibrium Cell

After thoroughly cleaning and assembling the
equilibrium cell (see Figure 5.4) the thermostatic bath
is brought to the desired temperature which is measured
on the mercury-in-glass thermometer. When the bath
temperature is constant, the apparatus is purged with gas

several times to ensure that the system is free from air.
With all the valves (except valve 3) closed, the pure
solvent is introduced into the equilibrium cell through
inlet, A. Since the liquid will not flow by gravity into
the vessel, sampling valve, 5, which is connected to a
vacuum pump, is cracked open and sufficient liquid is
sucked into the cell so that the level of the liquid
coincides with that of the sampling tube. Inlet, A, is
closed and several hours are allowed for the solvent
temperature to reach that of the thermostatic bath.
Hydraulic fluid from the pressure intensifier (see Figure
5.3) is pumped to the back of the top piston by opening
valves, 11 and 7, so causing the top piston to move
from its upper position. Valve, 7, is now closed and the
lower piston is moved upwards by pumping hydraulic fluid
through valves, 11 and 9. After closing 11 and 9 and opening
valve, 7, gas is allowed to enter the apparatus slowly
through valve, 1, until the desired pressure is reached.
The force on the piston arising from the pressure of the
hydraulic fluid will balance that induced by the pressure
of the gas within the equilibrium cell and as a result,
the oil pressure, as indicated by the bourdon tube gauge,
G_2, will increase.

The magnetic stirrer is switched on and as the gas
dissolves in the liquid, the pressure in the apparatus
falls and the liquid level, as observed through the windows,
rises. When the system reaches equilibrium after
approximately half an hour of mixing, the pressure attains
a constant value. The magnetic stirrer is then turned off
and additional time is allowed for the liquid and gas
to separate completely before sampling the two phases.

During the experiment, the gas-liquid interface is kept within the field of view. Both the gas and liquid phases are sampled through the same sampling probe through valve, 5.

The liquid phase is sampled by raising the gas-liquid interface so that the sampling probe is immersed in the liquid. This is done by pumping hydraulic fluid to the back of the stirrer position through valves, 11 and 9 (see Figure 5.4), while the valve, 8, on the top piston side is opened very slowly. The pressure is thus maintained constant while the gas-liquid interface is being raised. The sampling probe is purged with the liquid phase before a sample of the liquid phase is taken for analysis.

Virtually the same procedure is adopted for sampling the gas phase except that hydraulic fluid is pumped to the back of top piston through valves, 11 and 7, whilst valve, 10, on the stirrer piston side is opened very slowly in order to maintain the pressure constant. This enables the interface between the two phases to be lowered, so that the sample probe is immersed in the gas phase.

If the system exhibits barotropic inversion, the same procedure is adopted for sampling the phases except that gas and liquid phases interchange positions. Since the volume of the sampling tube has been reduced to approximately 0.09 cc by filling the 0.635 cm O.D. tube connecting the sampling probe to valve, 5, with a rod of 0.159 cm diameter, the fall in pressure in the equilibrium cell during sampling is very small and may be neglected.

Analysis_of_Gas_and_Liquid_Phases

Before sampling both phases the heating tape is switched on to a temperature above the boiling point and the

sampling line (see Figure 5.10) is evacuated by opening

stopcock, 7, whilst valve, 5 and stopcocks, 8 and 9 are

closed. Before sampling the liquid phase for analysis

the sampling probe is purged with the liquid to be

sampled. This is generally done by first opening the

sampling valve, 5, very slowly until the pressure in the

sampling line is slightly above atmospheric pressure and

then opening stopcock, 9, so that the excess vapor pressure

generated by the liquid is purged to atmosphere. After

purging the sampling line with the liquid phase, valve, 5

and stopcock, 9, are closed and the apparatus is again

evacuated through stopcock, 7. After evacuation,   stopcock,

7, is closed and the liquid phase is sampled by opening

valve, 5, very slowly until the pressure in the sampling

line is atmospheric. The sample of vaporised liquid is

taken by a syringe (the temperature of which is above

the boiling point of liquid) through septum, S, and is

injected immediately into the chromatograph.

The same experimental procedure was applied when

sampling gas phase except that the sampling line was

purged with gas in order to remove any trace of vapor

from the liquid sample remaining in the sampling line.

To re-establish equilibrium at another pressure,

either fresh gas is introduced into the apparatus

(see Figure 5.4) through valve, 1, or valve, 4, is opened

to remove some of the vapor phase depending on whether

measurements are required at higher or lower pressure.

After allowing the system to attain equilibrium at the new

pressure The procedure for analyzing the samples is repeated.

In this way it is possible to obtain the composition of

the two co-existing phases at various pressures under

isothermal conditions and thereby construct pressure-
composition isotherms. This process is continued until
the critical condition is reached. The first sign of
critical opalescence is that the field of view is obscured
in the vicinity of the meniscus and this enlarges and
expands until the entire field of view is opaque to
transmitted light. The gas-liquid interface disappears when
the opalescence clears. If the system shows gas-gas
immiscibility, the pressure is raised further (above the
critical pressure) until the critical mixture separates
into two phases.

CHAPTER 7

RESULTS AND DISCUSSION

Accuracy and Reproducibility of Results

In order to check the accuracy and reproducibility of the apparatus and the proposed experimental technique, the compositions of the co-existing phases in the CH_4-n-C_7H_{16} system at $30^\circ C$ at pressures up to the critical point were measured. This system has been investigated by Juren [115] and Sage and Lacey [116] and the results are shown in Figure 7.1 along with the results from this experiment.

The curve in Figure 7.1 has been drawn to pass through the mean of the results obtained by Juren [115] and Sage and Lacey [116]. Juren's results have a mean deviation of 0·01 mole fraction about the curve whereas those of Sage and Lacey deviate by 0·01 mole fraction. The comparable deviation of the results reported here is only 0·015 mole fraction. Moreover according to Juren's results the system shows critical phenomenon at 240 atm. and 0.85 mole fraction of CH_4 whereas according to this experiment the system shows critical opalescence at 241 atm. and 0.842 mole fraction of CH_4. These observations support the belief that the apparatus can be used for precise measurement of phase equilibria in binary mixtures of (CF_4 + n-C_6H_{14}) and (CF_4 + n-C_5H_{12}).

Accuracy

During each experiment the equilibrium pressure, equilibrium temperature, the composition of gas in the light and heavy phase samples were measured.

FIGURE 7·1

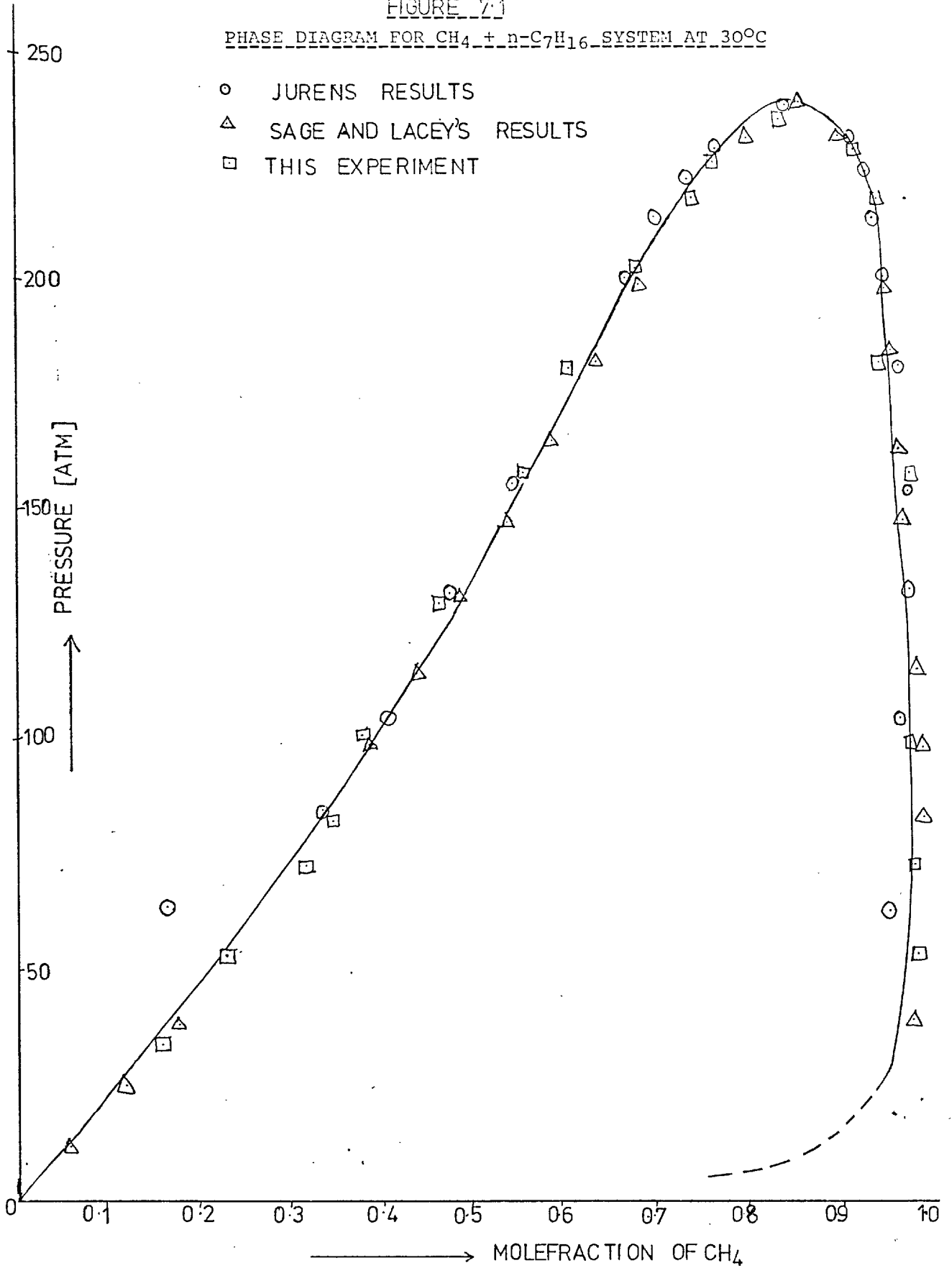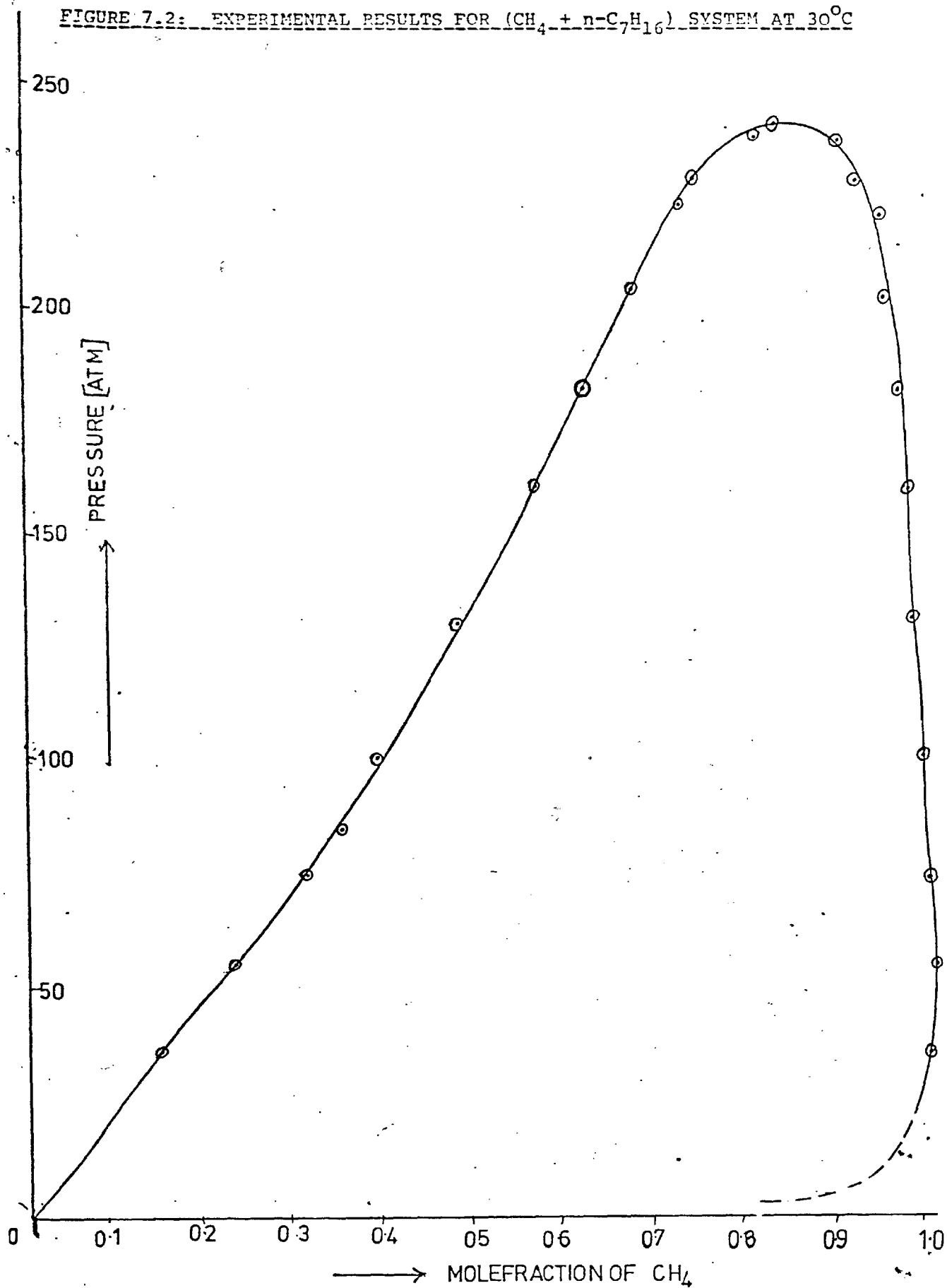PHASE DIAGRAM FOR CH_4 + n-C_7H_{16} SYSTEM AT 30°C

    ○   JURENS RESULTS
    △   SAGE AND LACEY'S RESULTS
    □   THIS EXPERIMENT

PRESSURE [ATM]

MOLEFRACTION OF CH_4

FIGURE 7.2: EXPERIMENTAL RESULTS FOR (CH₄ + n-C₇H₁₆) SYSTEM AT 30°C

The pressure gauge used for reading the equilibrium pressure was calibrated against a dead weight tester, was not subject to any systematic error and was found to be reproducible to $\pm$ 5 atm. from 50 to 1000 atm.

The equilibrium temperatures were recorded by mercury-in-glass thermometers graduated in $0.1^{\circ}C$ which were read to $0.05^{\circ}C$. The temperature of the thermostatic bath was controlled to $\pm$ $0.1^{\circ}C$ with a toluene regulator and the temperature variation inside the equilibrium cell is unlikely to exceed $\pm$ $0.05^{\circ}C$. When the experiment is conducted at a temperature lower than ambient (e.g. $0^{\circ}C$ or $-2^{\circ}C$), the temperature of the thermostatic bath can be controlled to $\pm$ $0.05^{\circ}C$ and hence the temperature variation in the equilibrium cell is unlikely to exceed $\pm$ $0.02^{\circ}C$. This was achieved with the help of two controllers, one in the refrigeration unit and the other (toluene-regulator) in the thermostatic bath.

There are two sources of error in the measurement of the composition of the co-existent phases, that arising from systematic error and that due to random experimental error. Since the mixtures with an estimated accuracy of $\pm$1 mole % were used to calibrate the chromatograph, the systematic error in the composition has been reduced to less than $\pm$ 0.01. The experimental error has been reduced to a minimum by keeping the sampling arrangement the same as that used in the calibration of the chromatograph. The random experimental error was estimated by checking the reproducibility of the results from time to time and was found to be $\pm$ 0.01. Therefore, the overall error in the measurement of composition is $\pm$ 0.02.

In order to check the accuracy of the experimental

data, the pressure-composition data were smoothed by

least square technique. The results were fitted to a

seven order polynominal of the form:

$$y = a + bx + cx^2 + dx^3 + \ldots\ldots\ldots\ldots$$

The standard deviation in the critical region was found

to be $\pm$ 8 atm.

Presentation of Results

Having checked the reproducibility of the apparatus

with (CH_4 + $n-C_7H_{16}$) system, the liquid-gas phase

equilibria for the system (CF_4 + $n-C_6H_{14}$) were determined

at temperatures from 26-50°C over a range of pressure

from 30-700 atm. The experimentally recorded data are

tabulated in Appendix 5 and the isothermal results are

presented in the form of pressure - mole fraction curves

in Figure 7.3. The corresponding critical pressure (P_c) -

critical temperature (T_c) plot is shown in Figure 7.4.

In order to plot the points of double contact against

the number of carbon atoms in the n-alkane, the phase

equilibria data for the system (CF_4 + $n-C_5H_{12}$) were

determined at temperatures of 0° and -2°C over the pressure

range of 30-700 atm. As stated earlier, the isothermal

results have been tabulated in Appendix 5 and are presented

in the form of pressure vs. mole fraction curves in

Figure 7.5.

Discussion of Results

The experimentally determined p-x diagram for

(CF_4 + $n-C_6H_{14}$) system, see Figure 7.3, shows that the

binary mixture exhibits gas-gas immiscibility of the

second type. The liquid and gas curves remain open at

28°C and show solubility maxima and minima respectively
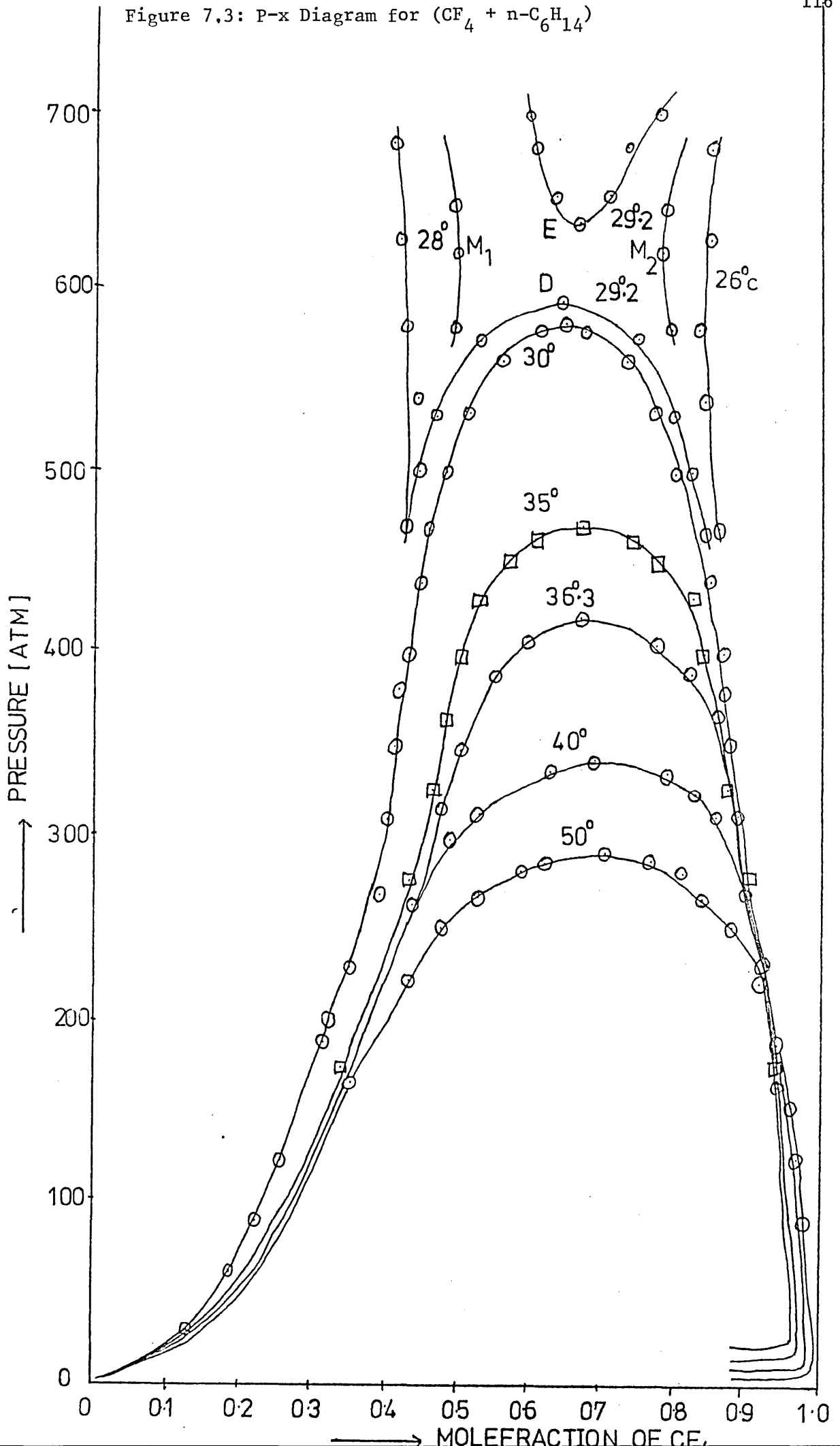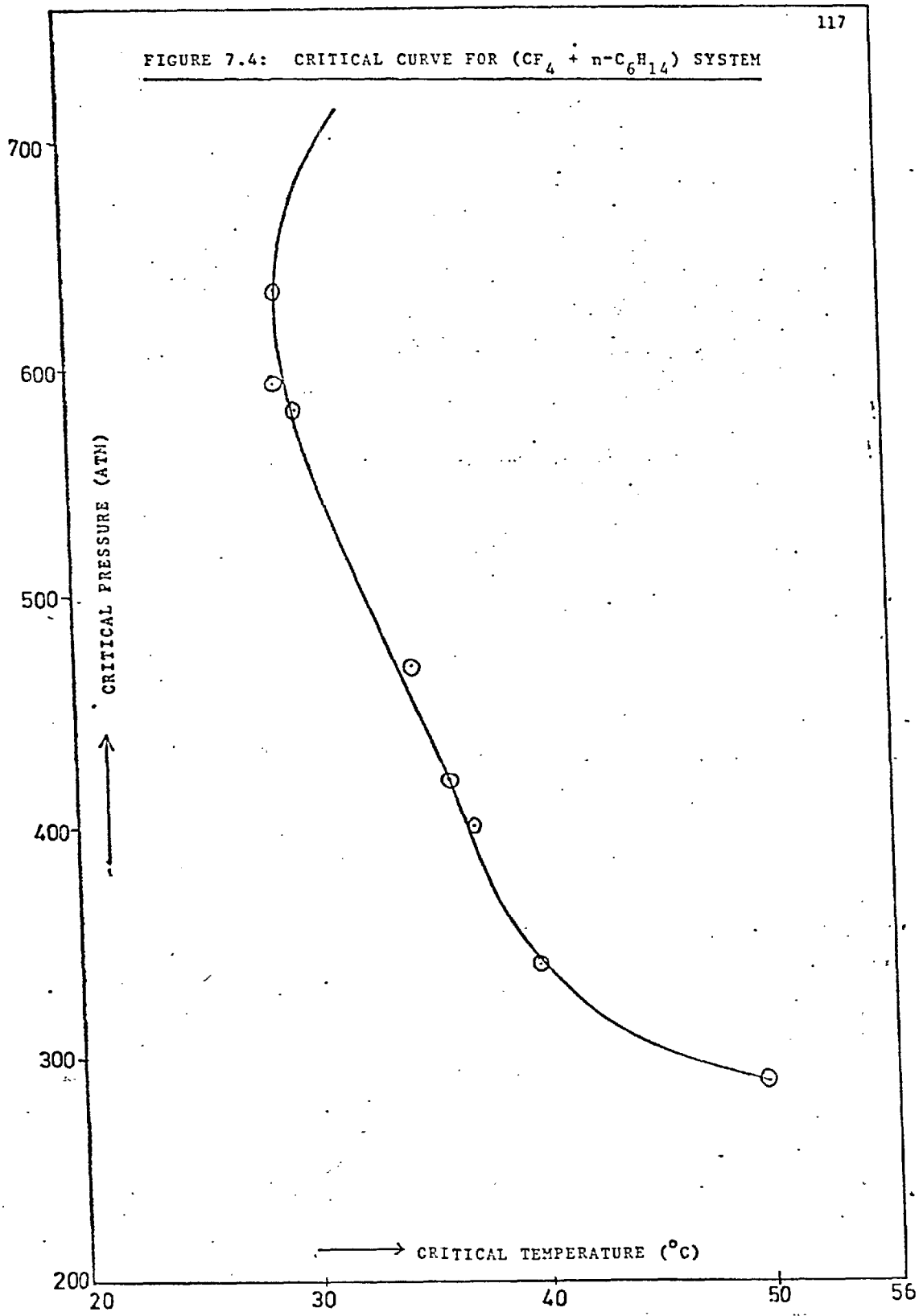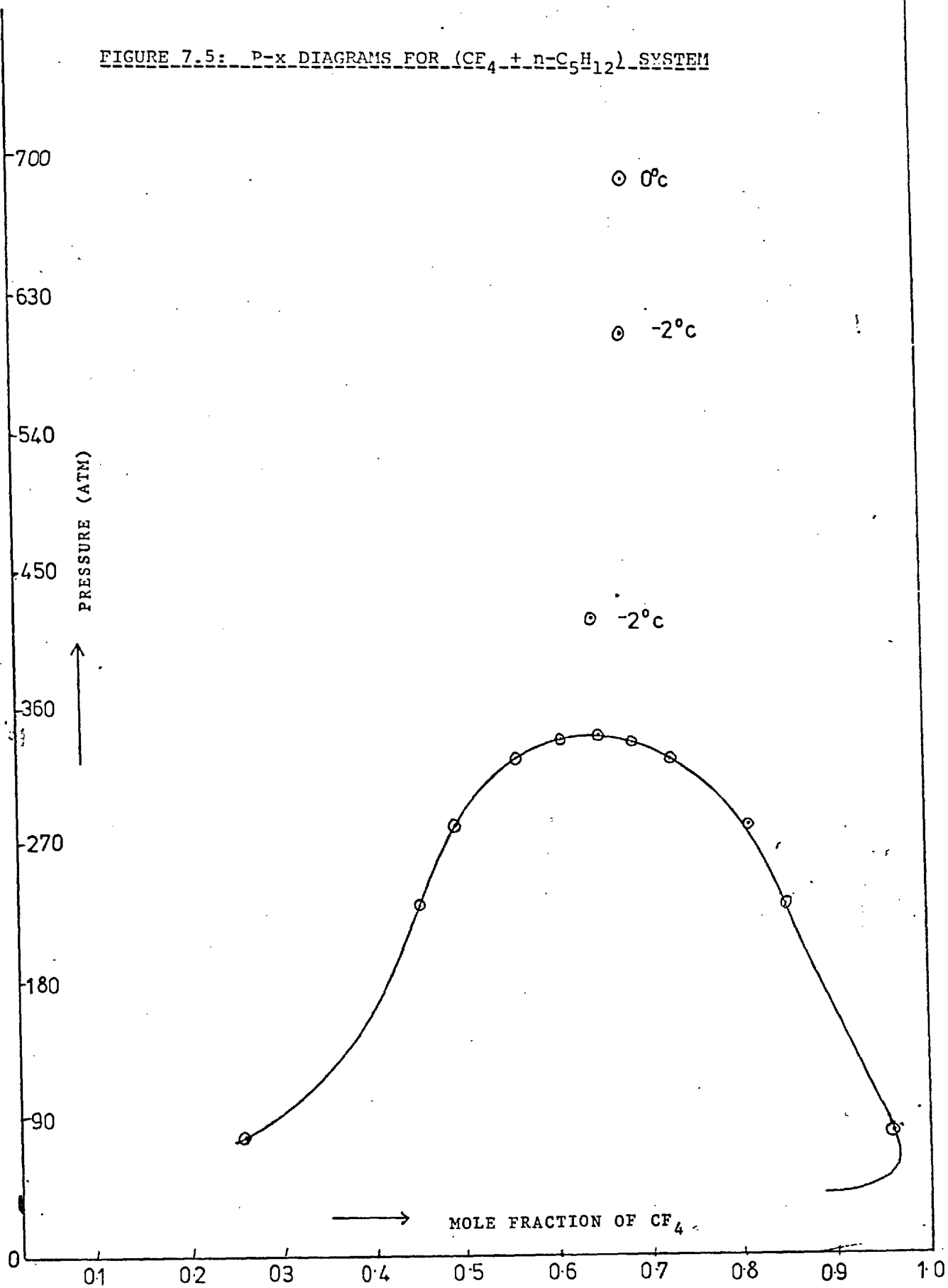
Figure 7.3: P-x Diagram for (CF_4 + n-C_6H_{14})

FIGURE 7.4: CRITICAL CURVE FOR $(CF_4 + n\text{-}C_6H_{14})$ SYSTEM

FIGURE 7.5: P-x DIAGRAMS FOR (CF$_4$ + n-C$_5$H$_{12}$) SYSTEM

(points M_1 and M_2). When the temperature is raised to 29.2°C, the liquid-gas region splits into two parts; a gas-liquid region below the lower critical point, D, and a gas-gas immiscibility region above the upper critical point E. The point, D, is marked by critical opalescence. It was observed that when the pressure was increased slightly above D, the gas-liquid interface expanded until the entire field of view became opaque to transmitted light. After thorough stirring over a considerable period, the opalescence cleared and it was found that the gas-liquid interface had disappeared.

If the pressure of the fluid mixture is increased in steps above D under isothermal conditions then when the p-x co-ordinates of the system lie above the upper critical point, E, the critical mixture separates into two phases and as a result a meniscus is formed such as that shown in Figure 7.6. This is the so called gas-gas immiscibility region. Point D corresponds to a pressure of 595 atm. whereas point E corresponds to 635 atm. The point of double contact where the p-x curve just splits into two regions may be estimated from the critical pressure (P_c) - critical temperature (T_c) plot shown in Figure 7.4. At a temperature of 29°C and a pressure of 615 atm. the critical curve changes direction and these conditions correspond to the point of double contact.

Gas-gas immiscibility of the second type has also been observed for the $(CF_4 + n-C_5H_{12})$ system as shown in Figure 7.5. At 0°C the pressure of the lower critical point, D, is 340 atm. and that of the upper critical point, E, when the critical mixture separates into two gas phases is approximately 700 atm. In order to verify
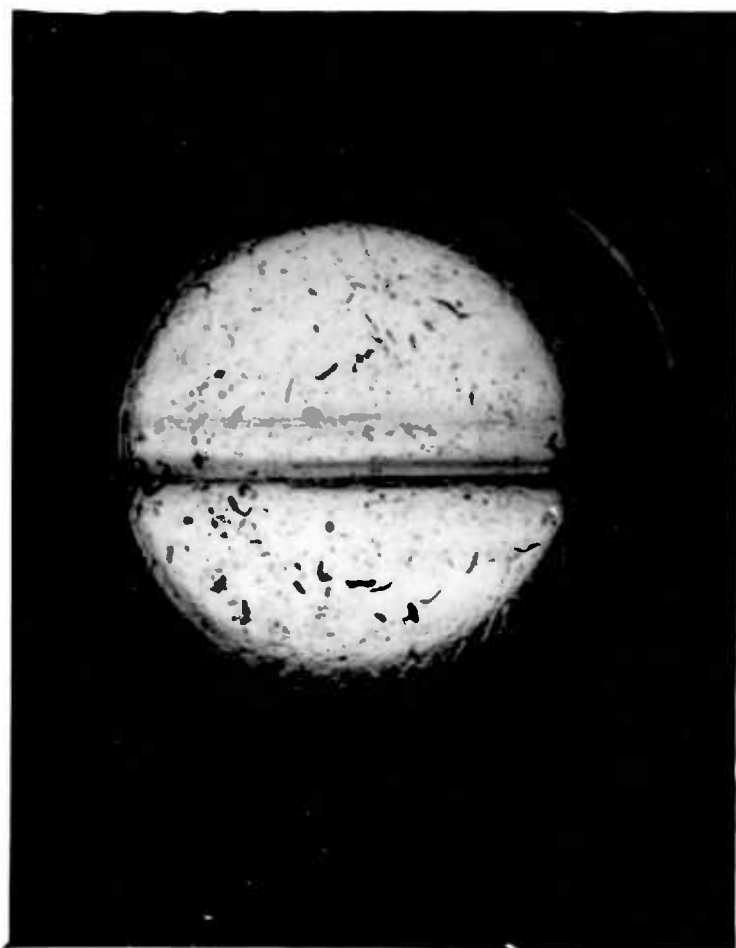
FIGURE 7.6: The Meniscus in the Gas-gas Immiscibility Region

these observations, an experiment was carried out at a temperature of $-2^{\circ}C$ when it was observed that the lower critical point, D, was raised to 415 atm. whereas point, E, was lowered to 600 atm. It was intended to carry out further experiments at temperatures lower than $-2^{\circ}C$ to study the phase equilibria of this system in greater detail but insufficient time was available to complete this work.

From a knowledge of other systems which exhibit gas-gas immiscibility it is expected that the point of double contact for the $(CF_4 + n-C_5H_{12})$ system will lie approximately half-way between D and E (see Figure 7.5) i.e. at a pressure of 510 atm. and a temperature estimated to be $-3^{\circ}C$. The pressure and temperature co-ordinates of the estimated points of double contact decreases as the number of carbon atoms in the n-alkane decrease as shown in Figure 7.7.

Prior to the work of Sideras [1] the occurrence of gas-gas immiscibility in both the $(CF_4 + n-C_6H_{14})$ and $(CF_4 + n-C_5H_{12})$ systems would have been unexpected since neither of the systems conforms to the criteria proposed by Kreglewski, Kaplan and Temkin which were discussed earlier.

The difference in solubility parameter $(\Delta\delta^2)$ between CF_4 and $n-C_6H_{14}$ is 29 atm. whereas that between CF_4 and $n-C_5H_{12}$ is only 14 atm. These values are much less than those of other systems known to exhibit gas-gas immiscibility.

According to Kaplan's criterion, neither system should exhibit gas-gas immiscibility since it is not observed in the $(CH_4 + n-C_6H_{14})$ $\{\Delta\delta^2 = 67$ atm.$\}$ and $(CH_4 + n-C_5H_{12})$ $\{\Delta\delta^2 = 52$ atm.$\}$ systems. Furthermore the values of van der

FIGURE 7.7: POINTS OF DOUBLE CONTACT AGAINST NUMBER OF CARBON ATOMS IN n-ALKANE
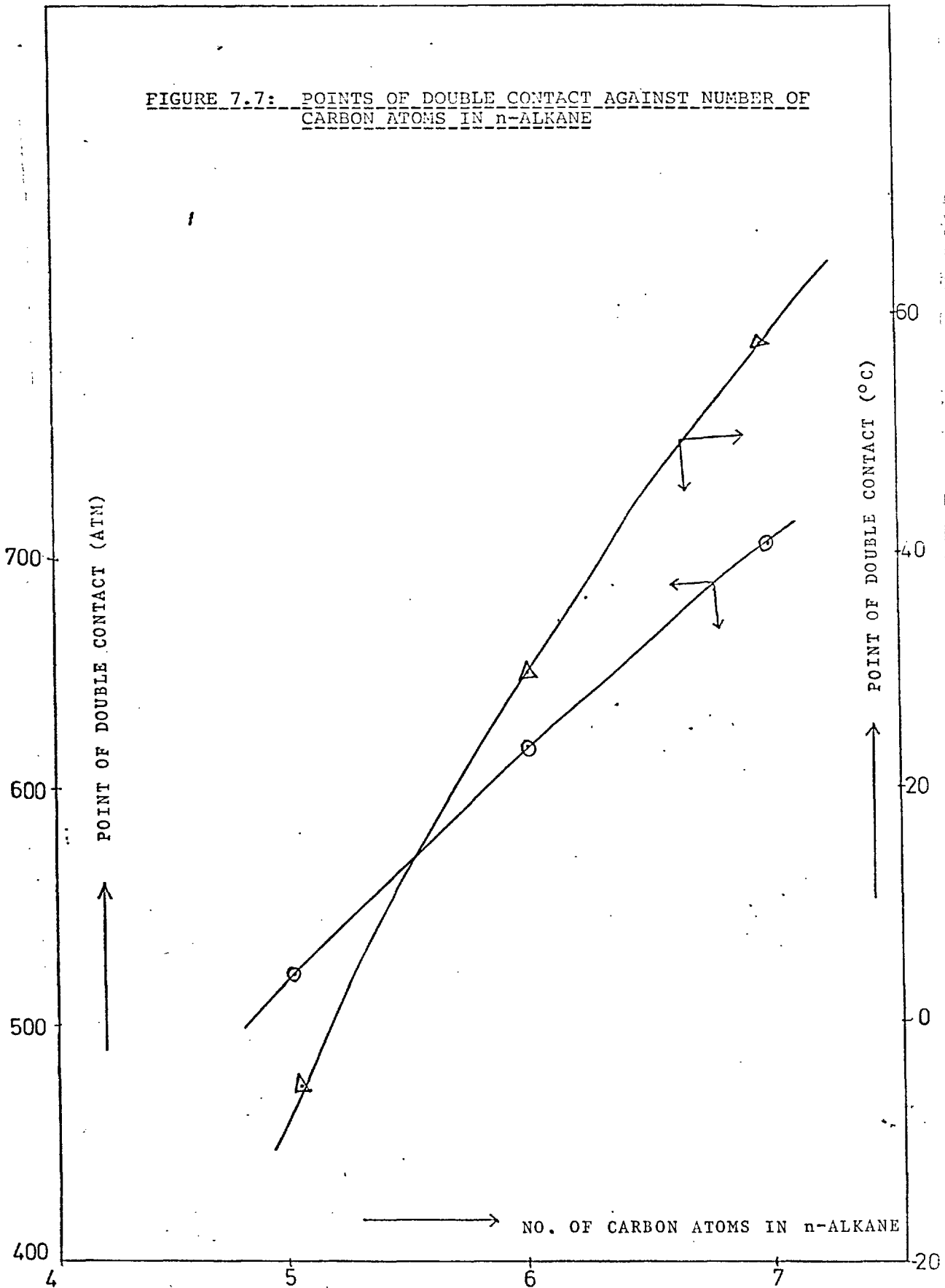
Waal's constants for the pure components (a_{11} and a_{22}) should satisfy the Temkin criterion discussed in Chapter 2. The van der Waal's constants for CF_4, $n-C_6H_{14}$ and $n-C_5H_{12}$ are 3.984, 24.39 and 19.01 atm. litre^2/mole^2 respectively, thus

$$a_{CF_4} > 0.053\ a_{C_6H_{14}} \quad \text{and} \quad a_{CF_4} > 0.053\ a_{C_5H_{12}}$$

which shows that Temkin's criterion is not applicable to the systems studied.

In view of the failure of all known criteria to predict gas-gas immiscibility in (CF_4 + n-alkane) systems it is neccessary to examine the effect of the molecular interactions of the two components on this phenomenon. It has been established that gas-gas immiscibility results from a change in the sign of the slope of the critical locus of fluid mixtures in pressure-temperature co-ordinates. Rowlinson and Teja [85] have developed a procedure to predict the critical locus of a wide variety of binary mixtures utilizing the principle of corresponding states.

The critical curves for the (CF_4 + $n-C_7H_{16}$) system predicted by Teja [85] are given in Figure 7.8, the assumed values for the interaction parameter ξ_{12} and η_{12} are given in parenthesis adjacent to each curve. It can be seen from this figure that the shape and position of the critical loci change significantly with the assumed value of interaction parameter, ξ_{12}, given by the Lorentz and Berthelot rule, see equation (3.19):-

$$f_{12} = \xi_{12}\ (f_{11}f_{22})^{\frac{1}{2}}$$
$$h_{12} = \eta_{12}\ \{\tfrac{1}{2}(h_{11}^{\frac{1}{3}} + h_{22}^{\frac{1}{3}})\}^3$$

where $f_{11} = (\frac{T_1^C}{T_0^C})\ \theta_{11}\ (T_1^R, V_1^R)$ and $f_{22} = (\frac{T_2^C}{T_0^C})\theta_{22}\ (V_2^R, T_2^R)$
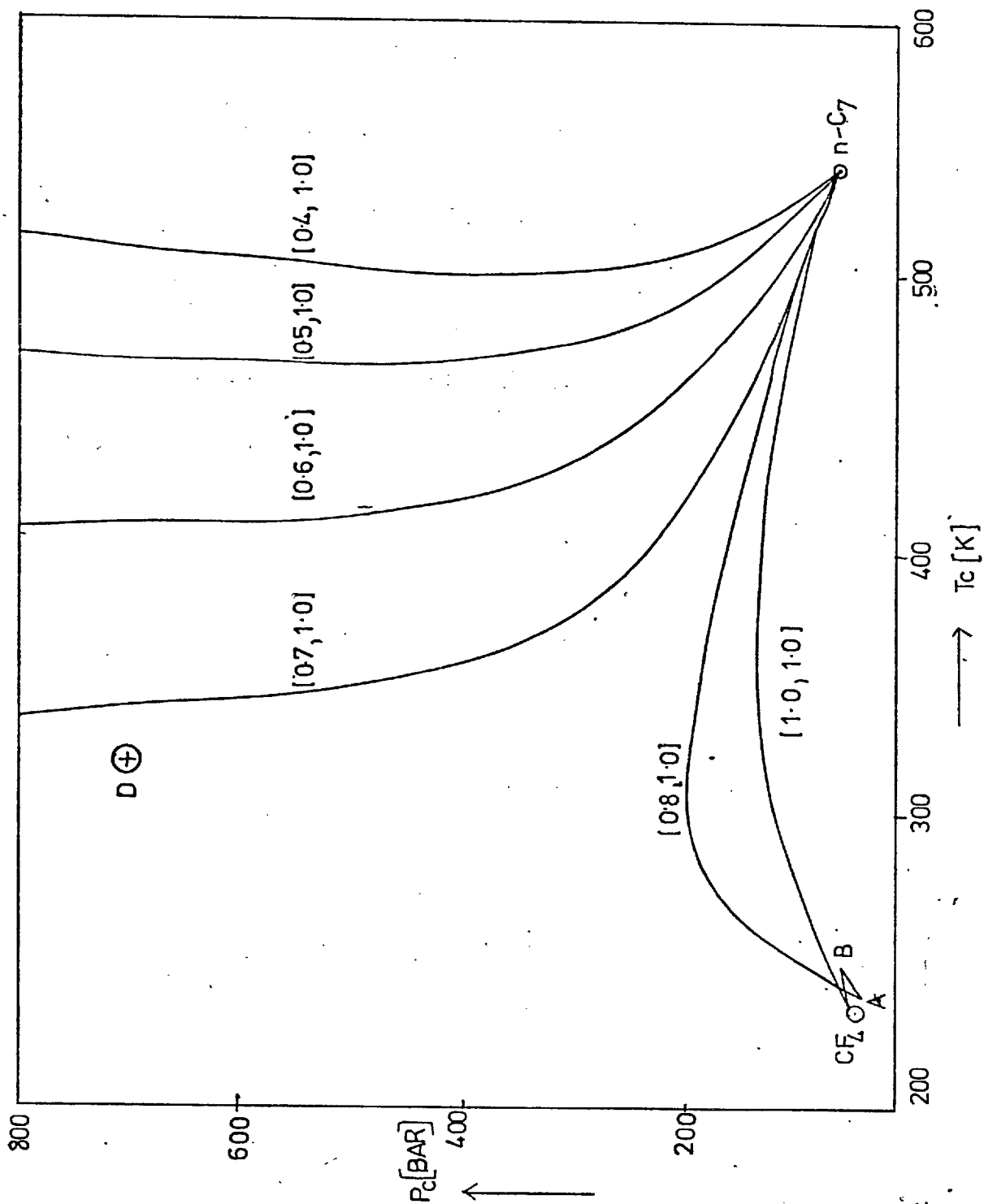
FIGURE 7.8: CRITICAL CURVE FOR (CF$_4$ + n-C$_7$H$_{16}$) SYSTEMS

$T_1{}^c$, $T_2{}^c$ and $T_0{}^c$ are the critical temperatures of the components 1, 2 and reference substance respectively and θ_{11} and θ_{22} are the shape factors discussed in Chapter 3.

According to the experimental results of Mendonca [20], the $(CF_4 + n\text{-}C_7H_{16})$ system shows gas-gas immiscibility above a temperature of $57^{\circ}C$ and a pressure of 700 atm. (point D in Figure 7.8). Although the co-ordinates of the point of double contact would lie on the critical curve predicted assuming a value of ξ_{12} slightly greater than 0.7 the slope of the curve in the vicinity of the point would not change sign but would remain negative as may be seen from Figure 7.8. It is possible that the accuracy of the predicted curve might be improved by varying the value of η_{12} which was assumed to be unity in calculating the curves in this figure. Similar results would be obtained if calculations were to be made for the $(CF_4 + n\text{-}C_6H_{14})$ and $(CF_4 + n\text{-}C_5H_{12})$ systems.

It follows that if Rowlinson and Teja's procedure is to be used to predict phase equilibria in the critical region, a method for estimating ξ_{12} is required. It has been pointed out by Scott [55] that the weak interaction between fluorocarbon and hydrocarbons may be attributed to the failure of the Lorentz-Berthelot rule.

Hudson and McCoubrey [57] have modified the mixing rule by taking into account the ionization potentials and collision diameters of the two pure substances. According to them, the interaction parameter ξ_{12} is given by:

$$\xi_{12} = \left\{ \frac{2(I_1 I_2)^{\frac{1}{2}}}{I_1 + I_2} \right\} \left\{ 2^6 \frac{\sigma_1{}^3 \sigma_2{}^3}{(\sigma_1 + \sigma_2)^6} \right\} \qquad (7.1)$$

where I_1 and I_2 are the ionization potentials and σ_1 and σ_2 are the collision diameters of molecules 1 and 2 respectively.

For CF_4, $I = 17.8$ eV, $\sigma = 4.66$ $\overset{o}{A}$ [56, 81] where as for $n-C_6H_{14}$ $I = 10.43$ eV, $\sigma = 5.95$ $\overset{o}{A}$ [56, 81] and for $n-C_5H_{12}$ $I = 10.55$ eV, $\sigma = 5.78$ $\overset{o}{A}$ [56, 81].

Substituting these values in equation (7.1) the following values of ξ_{12} are obtained:-

$\xi_{12} = 0.921$ for the system ($CF_4 + n-C_6H_{14}$)

$\xi_{12} = 0.963$ for the system ($CF_4 + n-C_5H_{12}$)

Similar values of ξ_{12} have been obtained by Young and his colleagues [119, 120] from U.C.S.T. and gas-liquid critical point measurements on a wide variety of (perfluoroalkane + n-alkane) mixtures as shown in the adjacent table.

System	ξ_{12}
Perfluoromethyl cyclohexane + n-pentane	0.88
Perfluoromethyl cyclohexane + n-decane	0.85
Perfluoromethyl cyclohexane + n-hexadecane	0.79
Perfluoroheptane + n-pentane	0.934
Perfluoroheptane + n-octane	0.969

The values of ξ_{12} for all these systems are less than unity and in case of (perfluoromethyl cyclohexane + n-alkane) mixtures the value of ξ_{12} decreases systematically as the chain length of n-alkane increases in accordance with the calculation made using equation (7.1).

It has been recently shown by Schneider and his colleagues [65, 66, 117] that the systems ($CF_4 + CH_4$) and ($CF_4 + C_2H_6$) show liquid-liquid immiscibility in the temperature range -153 to -53°C and at pressures up to 1900 atm. It would be of great interest to calculate the value of ξ_{12} required by Rowlinson and Teja's theory to

predict liquid-liquid immiscibility in these systems.
It is worth noting that the theory predicts a liquid-
liquid immiscibility region AB for the $(CF_4 + n-C_7H_{16})$
system when $\xi_{12} = 0.8$, as shown in Figure 7.8.

In view of the results obtained for $(CF_4 + CH_4)$ and
$(CF_4 + C_2H_6)$ systems and the experimental results contained
within this thesis, it is possible to predict the phase
behaviour of $(CF_4 + C_3H_8)$ and $(CF_4 + n-C_4H_{10})$ systems.
Figure 7.9 shows the predicted critical curves of a series
of $(CF_4 + n-alkane)$ systems starting from CH_4 to $n-C_6H_{14}$.
It is observed that the system $(CF_4 + CH_4)$ shows liquid-
liquid immiscibility, the immiscibility region being
situated well below the critical temperature of CF_4. For
$(CF_4 + C_2H_6)$ system the liquid-liquid immiscibility region
is situated at a higher temperature than that in
$(CF_4 + CH_4)$ system. Since liquid-liquid immiscibility
region for this system is below the critical point of
CF_4, the liquid-gas critical locus for this system will be
a continuous curve between the critical points of the two
pure components, as in the case with $(CF_4 + CH_4)$ system.
In view of the fact that the systems $(CF_4 + n-C_5H_{12})$ and
$(CF_4 + n-C_6H_{14})$ show gas-gas immiscibility of the second
type and the liquid-liquid immiscibility region for
$(CF_4 + n-alkane)$ systems extends to higher temperatures
as the number of carbon atoms in the n-alkane is
increased, it is anticipated that the critical locus for
the systems $(CF_4 + n-C_3H_8)$ and $(CF_4 + n-C_4H_{10})$ will be
represented by curves 3 and 4 respectively. This form
of transition (curve 1 to curve 6) is expected in view
of the fact that disparity between CF_4 and n-alkane increases
in the order $(CF_4 + CH_4)$ to $(CF_4 + n-C_6H_{14})$. This is
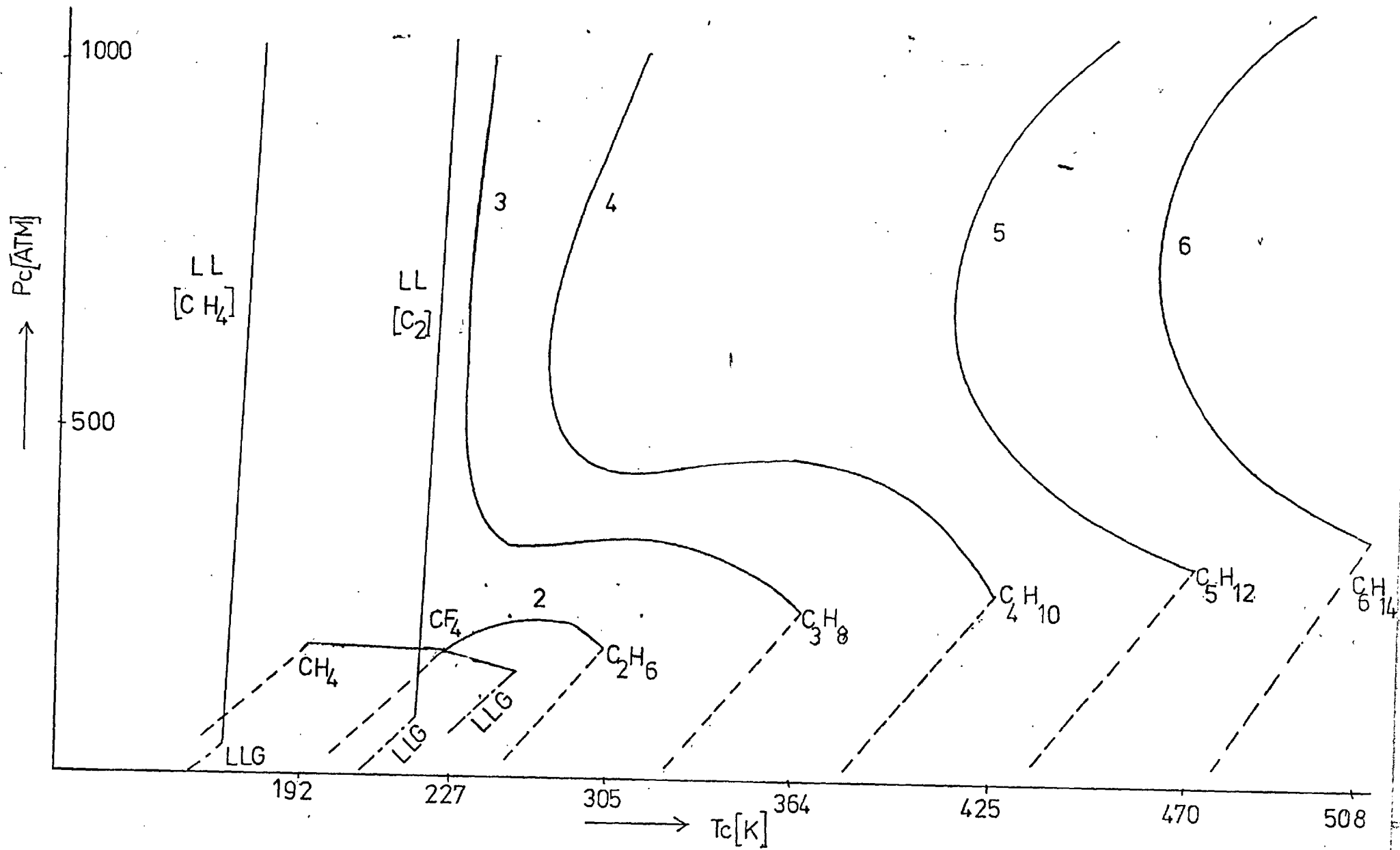
FIGURE 7.9: PREDICTED CRITICAL CURVE FOR A SERIES OF $(CF_4 + n\text{-ALKANE})$ SYSTEMS
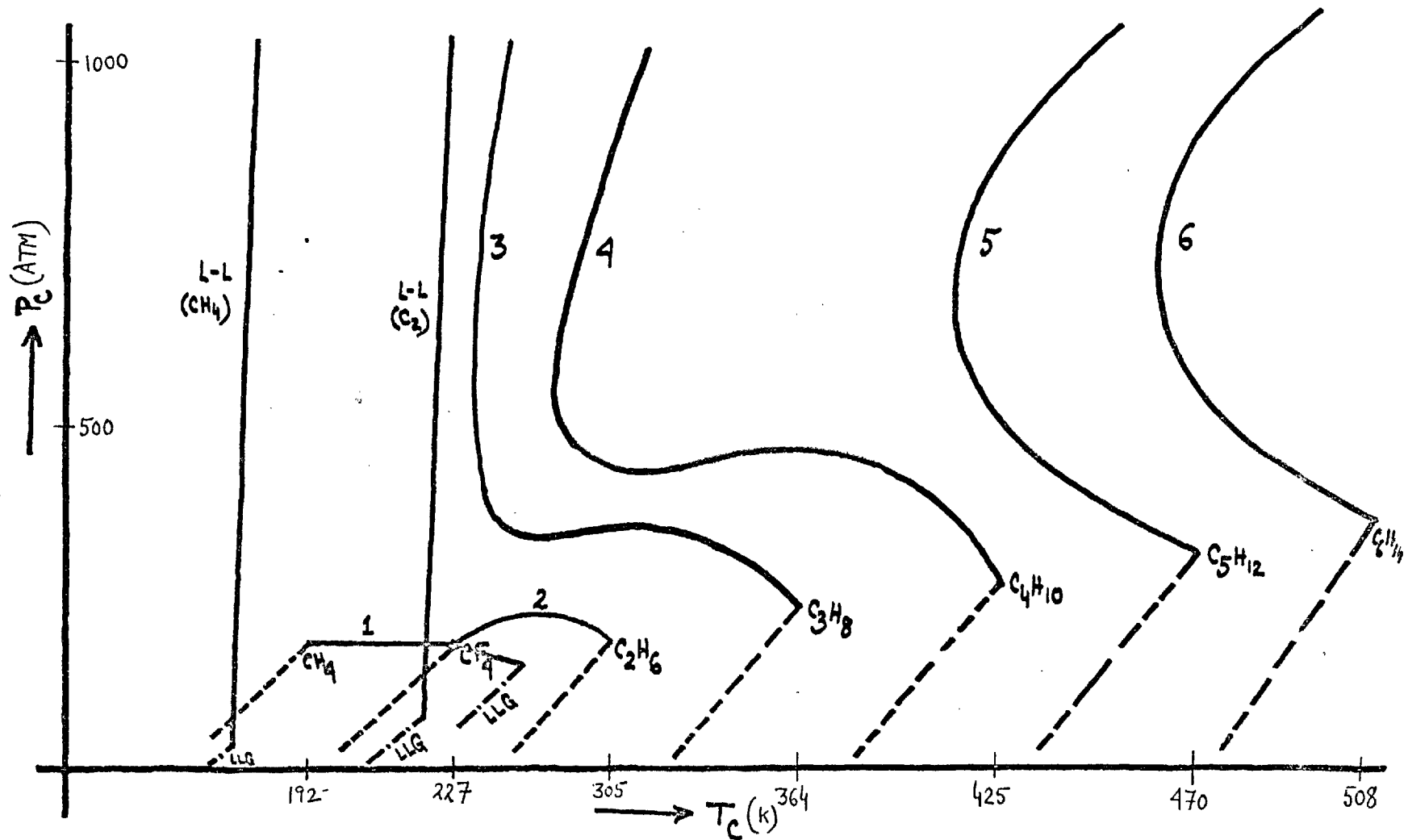
FIGURE 7.9: PREDICTED CRITICAL CURVE FOR A SERIES OF $(CF_4 + n\text{-ALKANE})$ SYSTEMS

verified theoretically from the value of interaction parameter, ξ_{12}, which decreases from 0.943 for $(CF_4 + CH_4)$ system [28] to 0.7 for $(CF_4 + n\text{-}C_7H_{16})$ system [85] so that the prediction conforms with the experimental results.

It is evident that insofar as the $(CF_4 + n\text{-}C_7H_{16})$ system is concerned, the calculated values of ξ_{12} are significantly higher than the values of ξ_{12} needed to bring the predicted curves based on Rowlinson and Teja's [85] theory into agreement with experiment. Consideration will now be given to the phase behaviour of other binary systems such as (Ar + n-alkanes), $(CH_4 + n\text{-}alkanes)$, $(CO_2 + n\text{-}alkanes)$ and $(H_2O + n\text{-}alkanes)$ to see if they behave in the same way.

Ar and n-alkanes form simple mixtures and as a result the critical loci for these systems take the form of continuous curves between the critical properties of the pure components. The predicted curves conform well with the experimental observations without modifications to the Lorentz and Berthelot combining rules (i.e. $\xi_{12} = \eta_{12} = 1$). In the absence of experimental data on (Ar + higher n-alkane) mixtures, it is not possible to verify whether the agreement extends to n-alkanes $> C_7$.

With $\xi_{12} = 1$ and $\eta_{12} = 1$, Rowlinson and Teja's treatment [85] reproduces well the observed maximum in the critical pressure for $(CH_4 + C_2H_6)$, $(CH_4 + C_3H_8)$ and $(CH_4 + n\text{-}C_4H_{10})$ mixtures. The predicted maximum in the critical pressure for $(CH_4 + n\text{-}C_5H_{12})$ and higher n-alkanes differs considerably from the experimental observations. However this discrepancy can be reduced considerably by assuming ξ_{12} less than 1. It has been shown that with ξ_{12} significantly less than 1 $(\xi_{12} = 0.9)$ the predicted

maximum in the critical curve for (CH_4 + $n-C_5H_{12}$) to (CH_4 + $n-C_8H_{18}$) systems does not differ from the experimental observations. Liquid-liquid immiscibility is predicted for (CH_4 + $n-C_6H_{14}$) systems if $\xi_{12} = 0.85$. However the treatment fails to give accurate results for (CH_4 + $n-C_{10}H_{22}$) and higher n-alkanes even when ξ_{12} is well below unity. This discrepancy is probably due to the fact that the higher n-alkanes are highly non-conformal with the reference substance CH_4 and as a result the values of ξ_{12} are significantly lower than expected.

The experimentally measured critical curves for (CO_2 + n-alkane) systems have been shown in Figure 2.8. The predicted critical curves for (CO_2 + CH_4) to (CO_2 + $n-C_5H_{12}$) are in good agreement with experimental results and reproduce the minimum temperature exhibited by the (CO_2 + C_2H_6) system provided the value of interaction parameter ξ_{12} is decreased from 0.95 for (CO_2 + CH_4) system to 0.80 for (CO_2 + $n-C_5H_{12}$) system. Thus mixtures of (CO_2 + higher n-alkanes) deviate considerably from the Lorentz and Berthelot combining rules as verified by the fact that the critical curve for the system (CO_2 + $n-C_8H_{18}$) does not conform well with the experimental results even when $\xi_{12} = 0.70$. Calculations made by Rowlinson and Teja predict liquid-liquid immiscibility in the (CO_2 + $n-C_8H_{18}$) system extending to high pressure such that the liquid-liquid and gas-liquid critical curves are continuous, this however is not the case [14]. In view of these calculations it is likely that the predicted results for the (CO_2 + higher n-alkanes ($>C_8$)) systems will deviate more and more from the experimental results as the value of ξ_{12} is decreased.

During recent years (H_2O + n-alkane) systems have been

studied at temperatures > 300°C and pressures > 1000 atm. where parts of the critical curve could be determined. It has been experimentally observed that all the (H_2O + n-alkane) systems (up to n-octane) show gas-gas immiscibility of the second type. This behaviour could not be predicted by Rowlinson and Teja because H_2O is a strongly polar substance and does not conform to the principle of corresponding states.

Figure 7.10, which is not drawn to scale, shows the critical locus of a variety of binary mixtures containing n-hexane as one of the components. Ar and $n-C_6H_{14}$ form simple mixtures and as a result the critical locus for (Ar + $n-C_6H_{14}$) system should be a continuous curve between the critical points of the two pure components. This was reproduced for (Ar + CH_4) system by Rowlinson and Teja with ξ_{12} = 1.0. For (CO_2 + $n-C_6H_{14}$) system the critical locus is a continuous curve between the critical points of the two pure components, liquid – liquid immiscibility zone is not observed as the phases solidify before the immiscibility zone is reached [15]. The value of interaction parameter, ξ_{12}, for this system has to be < 0.80 to make the predicted curve conform well with the experimental observations. Liquid-liquid immiscibility is observed for (CH_4 + $n-C_6H_{14}$) system and this is reproduced for ξ_{12} = 0.85. Gas-gas immiscibility of the second type is observed for (CF_4 + $n-C_6H_{14}$) system and this is reproduced when ξ_{12}<0.7.

In view of these observations it can be concluded that Rowlinson and Teja's theory has been very successful in predicting the critical locus of simple mixtures (where the critical locus is a continuous curve between the critical
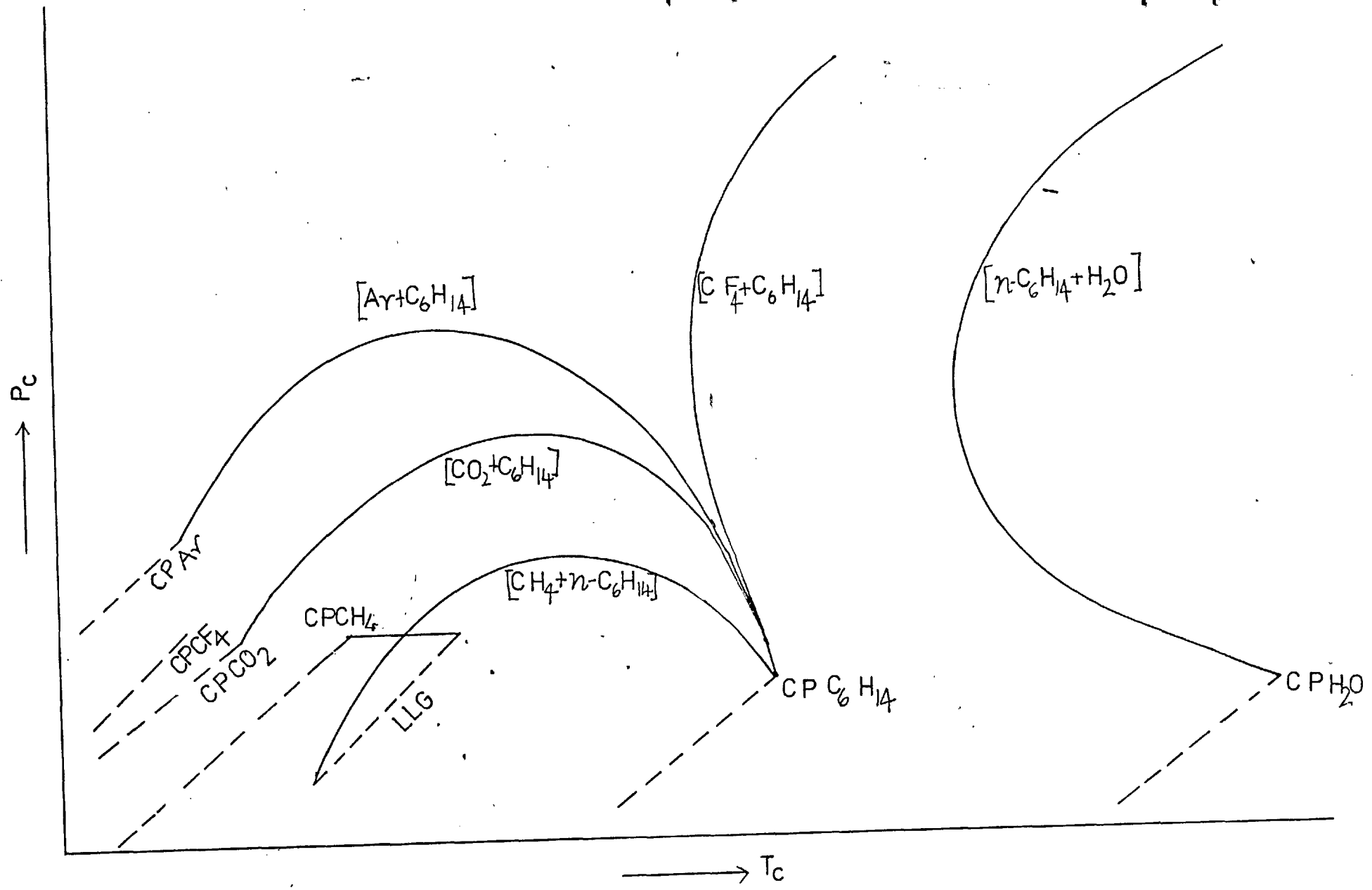
FIGURE 7.10: CRITICAL LOCUS OF BINARY MIXTURES CONTAINING n-HEXANE

properties of pure components) with $0.9 < \xi_{12} < 1.0$.
As the dissimilarity between the two components increases,
the predicted critical locus becomes more and more qualitative
and the assumed value of ξ_{12} has to be much smaller than that
predicted from Hudson and McCoubrey's rule or values
estimated from gas-liquid critical point, U.C.S.T. etc.
Moreover the value of ξ_{12} becomes smaller as the disparity
between the molecules increases. When the Redlich-Kwong
equation of state was used by Deiters and Schneider [28]
to predict the critical locus of a wide variety of binary
mixtures ranging from simple systems to systems with liquid-
liquid immiscibility and then to systems exhibiting gas-gas
immiscibility of the second and first type, the different
types of behaviour could be obtained only by a continuous
decrease of the value of ξ_{12}.

It is clear from the above discussion that there is no
reliable method for estimating the correct value of inter-
action parameter for any binary system to be used for
critical locus predictions. This is evident from
the predictions made by Rowlinson and Teja utilizing the principle
of corresponding states and by Deiters and Schneider using the
Redlich-Kwong equation of state. Rowlinson and Teja's
method is not suitable for strongly polar systems
(e.g. H_2O + n-alkanes) whereas Deiters and Schneider's
method has been able to explain the phase behaviour of
polar systems with suprising accuracy.

Barotropic Phenomenon

Barotropic inversion was observed in both the
(CF_4 + n-C_6H_{14}) and (CF_4 + n-C_5H_{12}) systems, this resulted

in the gas rich phase, which at lower pressure is the upper phase, becoming more dense and sinking to the bottom of the container as the pressure is raised. This phenomenon depends on the relative compressibility of the two phases.

In the $(CF_4 + n-C_6H_{14})$ system the pressure at which barotropic inversion occurred increases with increasing temperature. However the phenomenon is confined to pressures from 140 to 170 atm. in the temperature range 29-50°C. Inversion has also been observed with the $(CF_4 + n-C_7H_{16})$ and $(CF_4 + n-C_5H_{12})$ systems and it is found that inversion pressure and temperature decreases as the number of carbon atoms in the n-alkane decreases. (Inversion takes place at 50°C and 170 atm. for $(CF_4 + n-C_7H_{16})$, at 30°C and 140 atm. for $(CF_4 + n-C_6H_{14})$ and at 0°C and 100 atm. for $(CF_4 + n-C_5H_{12})$)

Barotropic inversion has been experimentally observed with N_2-NH_3 [6], Ar-NH_3 [106], Ar-H_2O [64], CO_2-H_2O [101], C_3F_8-n-$C_{10}H_{22}$ [118] and C_3F_8-$C_{11}H_{24}$ [118]. In all these systems molecular weight of liquid is less than that of gas, a fact that led Tsiklis [8] to suggest that barotropic phenomenon may occur when the molecular weight of liquid is less than that of gas. This criterion is satisfied in both the systems $(CF_4 + n-C_6H_{14})$ and $(CF_4 + n-C_5H_{12})$. However, this criterion is not satisfied for all systems e.g. $(CF_4 + n-C_7H_{16})$ or $(n-C_4H_{10} + H_2O)$ where barotropic inversion also takes place.

CONCLUSION

From the experimental work reported in this thesis
it is clear that the binary systems (CF_4 + n-C_5H_{12}) and
(CF_4 + n-C_6H_{14}) exhibit gas-gas immiscibility of the second
type. The pressure and temperature co-ordinates of the points
of double contact are estimated to be 615 atm. and 29°C
for (CF_4 + n-C_6H_{14}) system and 510 atm. and -3°C for the
(CF_4 + n-C_5H_{12}) system. From a knowledge of the phase
equilibria in the (CF_4 + CH_4) and (CF_4 + C_2H_6) systems
at low temperature obtained elsewhere and that for
(CF_4 + n-C_7H_{16}) obtained by another research student,
Mr. J. Mendonca, working in this Department it is
predicted that the (CF_4 + n-alkane) systems will show a
transition from liquid-liquid, through liquid-gas to gas-gas
equilibria as the chain length of n-alkane in the binary
mixture increases.

With the present state of knowledge it is impossible
to predict the detailed phase behaviour of these systems
accurately. because a procedure has yet to be developed for
estimating the weak interaction between CF_4 and the hydro-
carbon molecules based on measurements remote from critical
conditions or on the properties of the molecules.

In view of the different types of immiscibility which
are likely to be exhibited by (CF_4 + n-alkane) mixtures it
is concluded that further experimental work to study the
phase equilibria of CF_4 with C_3H_8 and n-C_4H_{10} over wide
temperature and pressure range would be rewarding. This
information together with that obtained as a result of the
work contained in this thesis will provide a critical test
of current theories of phase equilibria such as that

developed by Rowlinson and Teja. This, in turn, will lead to a better understanding of the intermolecular forces between these molecules, and so further the development of a reliable procedure for predicting phase equilibria in binary mixtures.

APPENDIX 1

PURITY OF MATERIALS

n-heptane

This was supplied by B.D.H. Chemicals Ltd. to the following specification:-

    Assay (G.L.C.): Not less than 99.5%

    Wt. per ml. at 20°C: 0.682 to 0.684 gm.

    Refractive index: 1.3880 to 1.3885

    Boiling range: Not more than 1°C between 97°C and 99°C

n-hexane

This was supplied by B.D.H. Chemicals Ltd. to the following specification:-

    G.L.C. analysis: Minimum purity of 99%

    Wt. per ml. at 20°C: 0.658 gm.

    Refractive index: 1.3750

    Boiling range: From 67.7°C to 69.2°C

n-pentane

This was supplied by Hopkin and Williams Ltd. to the following specification:-

    Maximum limit of impurity (non volatile matter): 0.01%

    Wt. per ml. at 20°C: 0.625 gm.

    Boiling range: From 34°C to 37°C

Carbon tetrafluoride

This was supplied by the British Oxygen Co. Ltd. to the following specification:-

    G.L.C. analysis: Minimum purity of 99.7%

    Specific volume at 20°C: 0.14 m^3/kg

    Boiling point: -128°C

Methane

This was supplied by the British Oxygen Co. Ltd. to
the following specification:-

Purity: 99.99%

Impurities (typical analysis):

Nitrogen - 30 vpm (parts by volume per million)

Oxygen - 1 vpm   ,,

Carbon dioxide - 1 vpm   ,,

Hydrogen - 1 vpm   ,,

Hydrocarbons 30 vpm   ,,

APPENDIX 2

Table 7 PHYSICAL PROPERTIES OF PURE SUBSTANCES

Property	Carbontetra-fluoride	n-Hexane	n-Pentane	n-Heptane	Methane
Chemical formula	CF_4	$CH_3(CH_2)_4CH_3$	$CH_3(CH_2)_3CH_3$	$CH_3(CH_2)_5CH_3$	CH_4
Molecular wt.	88.1	86	72	100.20	16
Boiling pt. (^{O}C)	-128	68.4	36.1	98.4	-161.6
Melting pt. (^{O}C)	-184	-94	-129.7	-90.5	-182.6
Density (gm/cm^3)	0.003946 at NTP	0.658 at 20^OC	0.625 at 20^OC	0.684 at 20^OC	0.424 at NBP
Refractive index	1.151 at -73^OC	1.375 at 20^OC	1.358 at 15.7^OC	1.387 at 20^OC	
Critical Temp. (^{O}K)	227.67	508	470	540.4	191.72
Critical pressure (atm.)	37.4	30.3	33	27.4	47.8
Critical volume (cm^3/mole)	140.7	368	313	426.2	94.4
Critical compressibility factor (Z_c)	0.2	0.264	0.268	0.260	0.283
Pitzer's acentric factor ω	0.174	0.298	0.252	0.349	0.013

The properties of carbontetra fluoride were taken from ASRAE Thermodynamic properties of refrigerants, New York, 1969 whereas the properties of CH_4, $n-C_5H_{12}$, $n-C_6H_{14}$ and $n-C_7H_{16}$ were taken from International Critical Tables and Handbook of Physics and Chemistry.

APPENDIX 3

REFERENCE EQUATION OF STATE

The Vennix equation of state for the reference substance, methane, is given by:

$$Z = 1 + B + \left[A + C \exp\{E(T - T_O)\} + D \exp\{(K_O - F/T)\}\right]/T$$

where $K_O = 6$

$T_O = 145.0$

$$A = \sum_{i=1}^{5} A_i \rho^i$$

$$B = \sum_{i=1}^{5} B_i \rho^i$$

$$C = \sum_{i=1}^{9} C_i \rho^i; \quad D = \sum_{i=1}^{4} D_i \rho^i$$

$$E = E_1 + E_2 \rho; \quad F = F_1 + F_2 \rho$$

In units of bars, K and moles/litre, the constants of the equations are given by:

$A_1 = -31.7635$	$C_3 = -0.9533$	$D_2 = -0.1882 \times 10^{-1}$
$A_2 = -0.4547$	$C_4 = +0.1511$	$D_3 = +0.3785 \times 10^{-2}$
$A_3 = +0.1608$	$C_5 = -0.7733 \times 10^{-2}$	$D_4 = -0.1506 \times 10^{-3}$
$A_4 = -0.01095$	$C_6 = 0.00$	$E_1 = -1.50 \times 10^{-2}$
$A_5 = +0.2098 \times 10^{-3}$	$C_7 = +0.7341 \times 10^{-5}$	$E_2 = -0.401 \times 10^{-2}$
$C_1 = -6.8888$	$C_8 = 0.00$	$F_1 = 1.60 \times 10^{3}$
$C_2 = +2.3035$	$C_9 = -0.3878 \times 10^{-8}$	$F_2 = -25.667$
	$D_1 = -0.1031$	

APPENDIX 4

THE HELMHOLTZ FREE ENERGY AND ITS DERIVATIVES FOR A MIXTURE

From the corresponding states principle (Chapter 3)

$$\frac{A_m(\tilde{P}, T, x_\alpha)}{RT} = \sum_\alpha x_\alpha \ln x_\alpha + A(\tilde{P}, T)/RT$$

and $A(\tilde{P}, T)/RT = f\, A_0\,(\tilde{P}h, T/f)/RT - \ln h$

where the quantities in brackets refer to the variables.

From thermodynamics:

$$A_0\,(\tilde{P}, T)/RT = \ln \tilde{P} - 1 + I\,(\tilde{P}, T)$$

where $I(\tilde{P}, T) = \int_0^{\tilde{P}} \{\frac{Z-1}{\tilde{P}}\}\, d\tilde{P}$

so that $A_0\,(\tilde{P}h, T/f)/RT = \left[\ln \tilde{P} + \ln h - 1 + I\,(\tilde{P}h, T/f)\right]/f$

and $A_m\,(P, T, x_\alpha)/RT = \sum_\alpha x_\alpha \ln x_\alpha + \ln \tilde{P} - 1 + I\,(\tilde{P}h, T/f)$

The differentiation of this expression is straightforward if the derivatives of the last term are known.

Now: $I(\tilde{P}, T) = \int_0^{\tilde{P}} \{\frac{Z-1}{\tilde{P}}\}\, d\tilde{P}$

From the vennix equation (Appendix 3)

$$\{\frac{Z-1}{\tilde{P}}\} = B' + (A' + C'\,\exp\left[E\{T - T_0\}\right] + D'\,\exp\left[K_0 - F/T\right])/T$$

where $B' = \frac{B}{\tilde{P}}$, $C' = \frac{C}{\tilde{P}}$, $A' = \frac{A}{\tilde{P}}$ etc.

and A, B, C, D, E, F, T_0 and K_0 are constants in the Vennix equation. Thus $I\,(\tilde{P}h, T/f)$ may be obtained by integrating the above expression between 0 and $\tilde{P}$ and replacing $\tilde{P}$ by $\tilde{P}h$ and T by T/f. The resulting expression is:-

$$I\,(\tilde{P}h, T/f) = \sum_{i=1}^{5} B_i\,\{\tilde{P}h\}^i/i + \{\frac{f}{T}\} \times \left\{ \sum_{i=1}^{5} A_i\,\{\tilde{P}h\}^i/i \right.$$

$$- \exp\left[E\{\frac{T}{f} - T_0\}\right] \sum_{i=1}^{9} P_c\{i\}\, \Omega_c\{i\} + \exp\left[E_1\{\frac{T}{f} - T_0\}\right]\sum_{i=1}^{9} \{i - 1\}!\,C_i P_c\{i\}$$

$$- \exp\left[K_O - Ff/T\right] \sum_{i=1}^{4} P_d\{i\} \, Q_d\{i\} + \exp\left[K_O - F_1 f/T\right]$$

$$\left. \sum_{i=1}^{4} \{i-1\}! D_i P_d\{i\} \right\}$$

where

$$P_c\{n\} \;=\; 1/\left[-E_2\{\tfrac{T}{f} - T_O\}\right]^n$$

$$P_d\{n\} \;=\; 1/\left[F_2 \; f/T\right]^n$$

$$Q_c\{n\} \;=\; \sum_{i=1}^{9} \frac{\{i-1\}!}{\{i-n\}!} \, C_i \, \{\rho h\}^{i-n}$$

$$Q_d\{n\} \;=\; \sum_{i=1}^{4} \frac{\{i-1\}!}{\{i-n\}!} \, D_i \, \{\rho h\}^{i-n}$$

A_i, B_i, C_i, D_i, E_i and F_i are constants in the Vennix equation.

APPENDIX 5

TABULATED EXPERIMENTAL RESULTS

Table 8

System: (Methane + n-Heptane)

$T = (30° \pm 0.1°)C$

P (atm.)	x (mole fr. of CH_4 in liquid phase)	y (mole fr. of CH_4 in gas phase)
36	0.16	0.99
55	0.24	0.99
75	0.32	0.985
85	0.37	-
101	0.39	0.981
132	0.46	0.98
160	0.55	0.98
182	0.61	0.95
203	0.68	0.95
220	0.75	0.95
228	0.77	0.92
237	-	0.90
238	0.84	-
241 (critical pt.)	0.842	0.842

The results were not subjected to regression analysis as
(CH_4 + n-C_7H_{16}) system was studied to check the reproducibility
of the apparatus and the phase equilibria data for
(CH_4 + n-C_7H_{16}) system were available at 30°C from the
experimental results of Juren [115] and Sage and Lacey [116].

System: (Freon-14 + n-Hexane)

Table 9

Temperature 26°C

Pressure (atm.)	Mole fr. of CF_4 in lighter phase	Mole fr. of CF_4 in heavier phase
470	0.43	0.86
540	0.45	0.85
579	0.43	0.84
628	0.42	0.85
680	0.42	0.86

Table 10

Temperature 28°C

Pressure (atm.)	Mole fr. of CF_4 in lighter phase	Mole fr. of CF_4 in heavier phase
580	0.50	0.79
620	0.51	0.76
.646	0.49	0.79

Table 11

Temperature 29.2°C

Pressure (atm.)	Mole fr. of CF_4 in lighter phase	Mole fr. of CF_4 in heavier phase
470	0.43	0.84
500	0.45	0.82
530	0.47	0.80
572	0.54	0.75
595	0.65	0.65

Gas-gas immiscibility region

635	0.67	0.67
652	0.64	0.71
680	0.61	0.74
700	0.595	0.78

The results were subjected to regression analysis and the standard deviation was found to be 8.69 atm.

Table 12

Temperature 30°C

Pressure (atm.)	Mole fr. of CF_4 in heavier phase	Mole fr. of CF_4 in lighter phase
30	0.13	0.99
60	0.19	0.985
90	0.23	0.98
125	0.26	0.97
152	0.96	–
188	0.94	0.32
200	0.93	0.33
228	0.92	0.36
268	0.90	0.40
309	0.89	0.40
349	0.88	0.41
380	0.87	0.425
400	0.87	0.44
440	0.85	0.455
470	0.83	0.46
500	0.81	0.49
532	0.77	0.52
560	0.74	0.57
578	0.68	0.62
581	0.65	0.65

The results were subjected to regression analysis and the
standard deviation was 9 atm.

Table 13

Temperature 35°C

Pressure (atm.)	Mole fr. of CF_4 in heavier phase	Mole fr. of CF_4 in lighter phase
40	0.169	0.971
78	0.238	0.962
114	0.290	0.952
174	0.938	0.342
225	0.929	0.391
276	0.904	0.435
325	0.872	0.47
364	0.859	0.49
399	0.84	0.505
430	0.825	0.535
452	0.78	0.58
462	0.745	0.615
470	0.675	0·675

The results were subjected to regression analysis and the standard deviation was found to be 9.24 atm.

Table 14

Temperature 36.3°C

Pressure (atm.)	Mole fr. of CF_4 in heavier phase	Mole fr. of CF_4 in lighter phase
314	0.881	0.48
348	0.865	0.505
388	0.821	0.552
406	0.721	0.602
417	0.675	0.675

The results were subjected to regression analysis and the standard deviation was found to be 3.92 atm.

Table 15

Temperature (40 $\pm$ 0.1)°C

Pressure (atm.)	Mole fr. of Freon-14 in heavier phase	Mole fr. of Freon-14 in lighter phase
35	0.18	0.96
68	0.255	0.952
110	0.289	0.947
139	0.312	0.946
180	0.94	0.355
227	0.915	0.401
262	0.902	0.435
297	0.89	0.49
312	0.862	0.53
326	0.83	0.585
335	0.795	0.631
340	0.698	0.698

The results were subjected to regression analysis and the standard deviation was found to be 0.90 atm.

Table 16

Temperature $(49.9 \pm 0.1)°C$

Pressure (atm.)	Mole fr. of CF$_4$ in heavier phase	Mole fr. of CF$_4$ in lighter phase
34	0.155	0.98
68	0.23	0.97
100	0.269	0.959
135	0.316	0.947
164	0.355	0.94
198	0.93	0.398
220	0.917	0.435
250	0.877	0.475
266	0.84	0.53
280	0.807	0.59
286	0.767	0.624
290	0.705	0.705

The results were subjected to regression analysis and the standard deviation was found to be 1.81 atm.

Table 17

System: (Freon-14 + n-Pentane)

Temperature $(0^\circ \pm 0.05^\circ)C$

Pressure (atm.)	Mole fr. of CF_4 in lighter phase	Mole fr. of CF_4 in heavier phase
80	0.96	0.255
228	0.455	0.86
279	0.495	0.815
324	0.56	0.73
338	0.61	0.69
340	0.65	0.65

Gas-gas immiscibility was observed at 700 atm.

The results were subjected to regression analysis and the standard deviation was found to be 1.56 atm.

BIBLIOGRAPHY

1. G.M. Sideras
    M.Sc. thesis, University of London (1970)

2. J.S. Rowlinson
    Paper read at the Symposium "The Physics and Chemistry
    of High Pressure" held in London, 1962

3. J.S. Rowlinson
    Liquid and Liquid Mixtures, second edition, Butterworth
    (1969)

4. J.H. van der Waals
    Zittinsvesl. Kon. Acad. V. Wetensch, Amsterdam (1894)

5. Kammerlingh Onnes and Keeson
    Comm. Phys. Lab. Leiden Suppl. No. 15 (1907)

6. I.R. Krichevskii and P.E. Bolshakow
    Acta Physicochim. U.S.S.R. $\underline{14}$, 353 (1941)

7. A.E. Lindros and B.F. Dodge
    Chem. Engg. Progr. Symp. Series $\underline{48}$ (3), 10 (1952)

8. D.S. Tsiklis and L.A. Rott
    Russ. Chemical Review $\underline{36}$, 351 (1967)

9. D.S. Tsiklis
    Dokl. Akad. Nauk S.S.S.R., $\underline{86}$, 993 (1952)

10. De Swaan Arons and G.A.M. Diepen
    J. Chem. Physics $\underline{44}$, 2322 (1966)

11. J. Zernike
    Chemical Phase Theory P.143-144, Antwerp (1956)

12. W.B. Streett
    Can. J. Chemical Engg. $\underline{52}$, 92 (1974)

13. G.M. Schneider
    Ber. Bunsenges. Phys. Chem. $\underline{70}$, 497 (1966)

14. G.M. Schneider
    Chem. Engg. Progr. Symp. Ser. $\underline{64}$ (88), 9 (1968)

15. G.M. Schneider
    Adv. in Chemical Physics $\underline{17}$, 1 (1970)

16. J. Gordon
    J. of Chemical Education $\underline{49}$ (4), 249 (1972)

17. a) A. Kreglewski
       Bull. Acad. Polon. Sci., Classe III $\underline{5}$, 662 (1957)

    b) J. Van Dranen
       J. Chemical Physics $\underline{20}$, 1175 (1952)

18. R. Kaplan
    A.I.Ch.E. Jnl., $\underline{13}$, 186 (1967)

19. R. Kaplan
    A.I.Ch.E. Jnl., 14, 821 (1968)

20. J. Mendonca
    Personal communication

21. L.A. Rott
    Russ. Jnl. of Phys. Chem. 36, 1205 (1962)

22. E.U. Franck et al
    Chem. Ingr. Tech. 39, 816 (1967)

23. Z. Alwani and G.M. Schneider
    Ber. Bunsenges. Phys. Chem. 73, 294 (1969)

24. H. Lentz and E.U. Franck
    Ber. Bunsenges. Phys. Chem. 73, 28 (1969)

25. M.I. Temkin
    Russ. Jnl. of Phys. Chem. 33, 275 (1959)

26. a) P. Van Konynenburg
       Ph. D. thesis, University of California, Los Angeles
       (1968)

    b) R.L. Scott
       Paper presented at 3rd International Conference on
       Chemical Thermodynamics (1973)

27. S. Peter and H. Wenzel
    Ber. Bunsenges. Phys. Chem. 76, 331 (1972)

28. U. Deiters and G.M. Schneider
    Ber. Bunsenges. Phys. Chem. 80 (12), 1316 (1976)

29. K. Schäfer
    Statistiche Theorie der Materie Vol. 1, Gottingen,
    Germany (1960)

30. K.G. Tan, Luks and Kozak
    J. Chemical Physics 55, 1012 (1971)

31. W.B. Kay et al
    J. Chemical Thermodynamics 4, 301 (1972)

32. E.A. Guggenheim
    Mixtures, Oxford (1952)

33. N.J. Trappeniers, Schouten
    Physica 73, 556 (1974)

34. D.S. Tsiklis
    Dokl. Akad. Nauk S.S.S.R. 86, 1159 (1952)

35. D.S. Tsiklis
    Dokl. Akad. Nauk S.S.S.R. 91, 1361 (1953)

36. D.S. Tsiklis et al
    Russ. Jnl. of Phys. Chem. 41, 1804 (1967)

37. W.B. Streett
    Chem. Engg. Progr. Symp. Ser. 63 (81), 37 (1967)

38. W.B. Streett
     Trans. Far. Soc. 65, 696 (1969)

39. W.B. Streett
     J. Chem. Phys. 46, 3282 (1967)

40. G.M. Schneider et al
     Chem. Ingr. Tech. 39, 649 (1967)

41. D.S. Tsiklis et al
     Dokl. Akad. Nauk. S.S.S.R. 161, 645 (1965)

42. E.U. Franck et al
     Z. Phys. Chem. 37, 387 (1963)

43. J.F. Connolly
     J.C.E.D. 11, 13 (1966)

44. C.J. Rebert et al
     A.I.Ch.E. Jnl. 13, 118 (1967)

45. C.J. Rebert and W.B. Kay
     A.I.Ch.E. Jnl. 5, 285 (1959)

46. G.M. Schneider
     Ber. Bunsenges. Phys. Chem. 76, 325 (1972)

47. G.M. Schneider
     Pure and Applied Chem. 47, 277 (1976)

48. N.J. Trappeniers et al
     Physica 73, 539, 546 (1974)

49. American Petroleum Institute
     Technical Data Book for Refining, Chapter 9 (1970)

50. A.J. Davenport and J.S. Rowlinson
     Trans. Far. Soc. 59, 78 (1963)

51. P.I. Freeman and J.S. Rowlinson
     Pure and Applied Chem. 2, 329 (1961)

52. A.J. Davenport, G. Saville and J.S. Rowlinson
     Trans. Far. Soc. 62, 322 (1966)

53. Z. Alwani and G.M. Schneider
     Ber. Bunsenges. Phys. Chem. 80 (12), 1312 (1976)

54. J.H. Hildebrand, Prausnitz and R.L. Scott
     Regular and Related Solutions, N.Y. (1970)

55. R.L. Scott
     J. Phys. Chem. 62, 136 (1958)

56. T.M. Reed
     J. Phys. Chem. 59, 425 (1955)

57. Hudson and McCoubrey
     Trans. Far. Soc. 56, 761 (1960)

58. F.L. Swinton
Paper presented at the Symposium "Physical
Properties of Liquids and Gases for Plant and Process
Design" (Glasgow, 1968)

59. F.L. Swinton, C.L. Young et al
J. Chemical Thermodynamics 2, 105 (1970)

60. D.S. Tsiklis and V.M. Prokhorov
Dokl. Akad. Nauk. S.S.S.R. 174, 1377 (1967)

61. D.S. Tsiklis et al
Dokl. Akad. Nauk. S.S.S.R. 178, 886 (1968)

62. D.S. Tsiklis et al
Russ. Jnl. of Physical Chem. 45 (4), 448 (1971)

63. S.M. Khodeeva
Russ. Jnl. of Physical Chem. 40, 1973 (1966)

64. D.S. Tsiklis
Phasentrennung in Gasgemischen, Leipzig (1972)

65. G.M. Schneider et al
J. Chem. Thermodynamics 8, 731 (1976)

66. G.M. Schneider et al
J. Chem. Thermodynamics 8, 741 (1976)

67. R. Paas
Ph.D. Thesis, University of Bochum, F.R.G. (1977)

68. R. Jockers
Ph.D. Thesis, University of Bochum, F.R.G. (1976)

69. P.F.M. Paul and W.S. Wise
The Principles of Gas Extraction, Mills and Boon
.monograph (1971)

70. J.S. Rowlinson and M.J. Richardson
Adv. in Chemical Physics 2, 85 (1959)

71. G.A.M. Diepen et al
J. Am. Chem. Soc. 70, 4085 (1948)

72. E.U. Franck
Chapter 4 in "Physical Chemistry - an Advanced Treatise"
(Vol. 1) edited by Eyring, Henderson and Jost (1971)

73. S.R.M. Ellis
British Chemical Engg. 16, 358 (1971)

74. Elgin and Weinstock
J. Ch. Engg. Data 4, 1, 3 (1959)

75. British Patent 1,057,911 (1967)

76. U.S. Patent No. 3,318,805 (May 1967)

77. M.N. Myers and J.C. Giddings
Progr. in Separation and Purification 3, 133 (1970)

78. T.H. Gouw and R.E. Jentoft
Jnl. of Chromatography 68, 303 (1972)

79. D. Bartman and G.M. Schneider
Jnl. of Chromatography 83, 135 (1973)

80. Grieves and Thodos
A.I.Ch.E. Jnl. 6, 561 (1960)

81. Reid, Prausnitz and Sherwood
Physical Properties of Gases and Liquids, 3rd Edition
(1977)

82. R.R. Spear, R.L. Robinson and K.C. Chao
I. and E.C. Fundamentals 8, 2 (1969)

83. J. Joffe and D. Zudkevitch
C.E.P. Symp. Ser. No. (81) 63, 43 (1967)

84. P.L. Chueh and J.M. Prausnitz
Computer Calculations for High Pressure Vapor Liquid
Equilibrium, Prentice Hall (1968)

85. A.S. Teja
Ph.D. Thesis, University of London (1971)

86. P. Zandbergen, H.F.P. Knaap and J.M. Benakker
Physica 33, 379 (1967)

87. J.F. Breedveld and J.M. Prausnitz
A.I.Ch.E. Jnl. 19, 783 (1973)

88. J.S. Rowlinson
Proc. Roy. Soc., Series A, 219, 405 (1953)

89. R.O. Neff and D.A. Mcquarrie
J. Phys. Chem. 79, 1022 (1975)

90. A. Münster
Classical Thermodynamics, Chapters VI and VII, N.Y.
(1970)

91. K.E. Bett, J.S. Rowlinson and G. Saville
Thermodynamics for Chemical Engineers, Athlone Press
(1975)

92. J.W. Leach
A.I.Ch.E. Jnl. 14, 568 (1968)

93. T.W. Leland, Rowlinson and Sather
Trans. Far. Soc. 64, 1447 (1968)

94. J.S. Rowlinson and I.D. Watson
Chem. Engg. Sci. 24, 1565 (1969)

95. A.J. Vennix and R. Kobayashi
A.I.Ch.E. Jnl. 15, 930 (1969)

96. M.J.D. Powell
Computer Jnl. 7, 303 (1965)

97. E. Hala, Pick, Fried and Vilm
Vapor Liquid Equilibrium (1966)

98. D.S. Tsiklis
Handbook of Techniques in High Pressure Research and
Engineering, N.Y. (1968)

99. B.L. Rogers and J.M. Prausnitz
I. and E.C. Fundam. 9, 174 (1970)

100. Culberson and Mcketta
J. Petrol. Tech. 3, 223 (1961)

101. G.C. Kennedy et al
Am. J. Sci. 262, 1055 (1964)

102. W.B. Streett
Cryogenics 5, 27 (1965)

103. J.J. Mcketta et al
J. Petr. Technology 2, 1 (1950)

104. R.G. Reynolds
Ph.D. Thesis, Univ. of London (1964)

105. B. Juren
Unpublished work

106. A. Michels et al
Physica 27, 886 (1961)

107. L.R. Roberts and J.J. Mcketta
A.I.Ch.E. Jnl. 7, 173 (1961)

108. B.F. Dodge and A.K. Dunbar
J. Am. Chem. Soc. 49, 591 (1927)

109. W.B. Streett and A.L. Erickson
Phys. Earth Planatory Interiors, 5, 357 (1972)

110. G.M. Schneider
Experimental Thermodynamics, Volume 2, Chapter 16,
Part 2 (1975) edited by B. Vodar

111. H. Lentz
Rev. Sci. Instruments 40, 371 (1969)

112. F.I. Stalkup and R. Kobayashi
A.I.Ch.E. Jnl. 9, 121 (1963)

113. P.W. Bridgeman
The Physics of High Pressures, London (1958)

114. a) K.E. Bett and R.G. Reynolds
J.Sc. Instruments 42, 642 (1965)

    b) Goodfellow and H.M. Webber
    Chemistry and Industry 5, 127 (1972)

115. K.E. Bett and B. Juren
     Paper presented at the Symposium "Physical Properties
     of Liquids and Gases for Plant and Process Design",
     Glasgow (1968)

116. Sage and Lacey
     J. Ch. Engg. Data $\underline{1}$, 29 (1956)

117. G.M. Schneider et al
     Ber. Bunsenges. Phys. Chem. $\underline{81}$ (10), 1093 (1977)

118. C.L. Young
     Unpublished results

119. C.P. Hicks and C.L. Young
     Chemical Reviews $\underline{75}$, 119 (1975)

120. C.L. Young et al
     Trans. Far. Soc. II $\underline{73}$, 613, 618 (1977)